

Phased Array Antennas for mmWave Frequency Spectrum for 5G communication



A THESIS SUBMITTED IN PARTIAL FULFILLMENT OF THE
REQUIREMENTS FOR THE DEGREE OF BACHELOR OF
SCIENCE IN ELECTRICAL & ELECTRONIC ENGINEERING

Summer 2018

Submitted By

Shahriar Mohammad Real (14221006)

Rifat Rahman Turjo (15121015)

Fabliha Fatema Sobhan (15121040)

Nabila Ashraf (15121028)

Supervised By

Dr. Hasanuzzaman Sagor

Assistant Professor

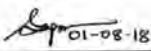
Department of Electrical and Electronic Engineering,

BRAC UNIVERSITY

ACCEPTANCE

The undersigned certify that he has read and recommend for acceptance, a thesis entitled "Phased Array Antennas for mmWave Frequency Spectrum for 5G communication" in partial fulfilment of the requirements of the degree of Bachelor of Science Electrical and Electronic Engineering.

Supervisor:

A handwritten signature in black ink, appearing to read 'Sagor', is written over a horizontal line. To the right of the signature, the date '01-08-18' is written.

Dr. Md. Hasanuzzaman Sagor

Assistant Professor

Department of Electrical and Electronic Engineering,

BRAC UNIVERSITY

Email: hasan.sagor@bracu.ac.bd

DECLARATION

We, hereby declare that this thesis work titled “Phased Array Antennas for mmWave Frequency Spectrum for 5G communication” is solely our own work. The work has not been presented elsewhere for assessment. It contains no material which has been accepted for the award of any other degree or diploma at any university or equivalent institution. The materials used from sources have been properly acknowledged and referred.

Shahriar Mohammad Real

Rifat Rahman Turjo

Fabliha Fatema Sobhan

Nabila Ashraf

ACKNOWLEDGEMENT

This paper is the work of Shahriar Mohammad Real, Rifat Rahman Turjo, Fabliha Fatema Sobhan and Nabila Ashraf, students of Electrical and Electronics Engineering (EEE) Department of BRAC University. The paper has been prepared as an effort to compile the knowledge of our years of study in the University and produce a final thesis paper, which addresses the Phased Array Antennas for mmWave Frequency Spectrum for 5G communication.

To begin with, we would like to express our sincere and earnest gratitude to Almighty Allah (S.W.T) for helping us successfully complete our undergraduate thesis in Electrical and Electronics Engineering.

We would like to express our sincere gratefulness and gratitude to our advisor Dr. Md. Hasanuzzaman Sagor for his undivided support, immense knowledge and guidance. He was extremely supportive and helped us in every step of our thesis work. He was also extremely inspirational and motivating. Without his supervision, instruction and feedback we could never complete our work. The authors would also like to thank the Electrical and Electronics Engineering (EEE) Department, School of Engineering and Computer Science, BRAC University, for providing us with the necessary facilities.

ABSTRACT

We are currently analyzing and simulating an array of antenna with changing phases. Conventional antennas (such as parabolic reflectors) are difficult to move either in azimuth or in elevation, and require more time as they are controlled by servo motors and actuators. On the contrary, the phased array antenna utilizes electronic means to rotate the beam in desired direction. To move or rotate the beam in desired direction, phase of transmitting elements in the array are varied by a device known as phase shifter. Our research mainly focuses on obtaining results in showing that creating an array of antenna and steering the beam in a particular direction is much more efficient in comparison to the conventional method. Moreover, creating an array of antennas can help us to increase the gain compared to a single antenna and we can also move the beam in our desired direction without any mechanical movement of the antenna. Additionally, we worked to change the design of our microstrip patch array element and fruitfully created a key shaped antenna that gives substantially better performance than the original array.

Table of Contents

CHAPTER 1	1
1.1 ANTENNA OVERVIEW	1
1.2 TYPES OF ANTENNA	2
1.2.1 WIRE ANTENNA	2
1.2.2 TRAVELLING WAVE ANTENNA	4
1.2.3 REFLECTOR ANTENNA	6
1.2.4 APERTURE ANTENNAS	7
1.2.5 MICROSTRIP ANTENNA	9
1.2.6 ARRAY ANTENNA	10
1.3 ANTENNA PARAMETERS	11
1.3.1 RADIATION PATTERN	11
1.3.2 ANTENN GAIN	16
1.3.3 DIRECTIVITY	18
1.3.4 S PARAMETER	19
1.3.5 ANTENNA EFFICIENCY	21
1.3.6 BANDWIDTH	22
1.3.7 INPUT IMPEDANCE	23
CHAPTER 2	26
2.1 INTRODUCTION	26
2.2 CHALLENGES OF mmWave	26
2.3 RESEARCH ADVANCES	27
2.4 DESIGN METHODOLOGY	28
2.5 APPLICATIONS	28
CHAPTER 3	30
3.1 GENERAL OVERVIEW	30
3.1.1 ADVANTAGES AND DISADVANTAGES	31
3.1.2 APPLICATIONS	32
3.1.3 DIFFERENT TYPES OF MICROSTRIP PATCH	33
3.2 FEEDING METHODS	33
3.3 BASIC CONFIGURATION	36
3.3.1 METHODS OF ANALYSIS	36
3.3.2 RECTANGULAR PATCH ANTENNA PARAMETERS	37

3.3.1 CHARGE AND CURRENT DISTRIBUTION.....	39
CHAPTER 4.....	41
4.1 SELECTION OF SUBSTRATE MATERIAL	41
4.1.1 SURFACE WAVE EXCITATION	41
4.1.2 DIELECTRIC CONSTANT	43
4.1.3 LOSS TANGENT.....	43
4.2 DIFFERENT DIELECTRIC SUBSTRATES.....	44
4.2.1 RT- DUROID 5880.....	44
4.2.2 ARLON AD-270.....	45
4.2.3 FR4 GLASS EPOXY.....	45
4.3 SLOT ANTENNAS.....	45
CHAPTER 5.....	47
5.1 GENERAL OVERVIEW.....	47
5.1.1 ADVANTAGES OF PHASED ARRAYS	47
5.1.2 THEORY OF PHASED ARRAYS.....	48
5.2 DIRECTIVITY OF ANTENNA ARRAYS.....	48
5.3 ARRAY FACTOR.....	50
5.4 RADIATION PATTERN OF ANTENNA ARRAYS.....	51
5.4.1 RADIATION PATTERN OF PLANAR ARRAYS	53
5.5 GRATING LOBES VERSUS ELEMENTAL SPACING.....	55
5.6 GRATING LOBES VERSUS ELEMENTAL SPACING.....	57
CHAPTER 6.....	59
6.1 INTRODUCTION	59
6.2 TYPES OF PHASE SHIFTERS	60
6.3 TOPOLOGIES FOR IMPLEMENTING PHASE SHIFTERS.....	63
6.3.1 HIGH- PASS/ LOW- PASS.....	63
6.3.2 LOADED LINE PHASE SHIFTERS.....	65
6.3.3 SWITCHED LINE PHASE SHIFTERS.....	66
6.3.4 REFLECTION- TYPE PHASE SHIFTERS.....	67
6.4 PHASE SHIFTERS PARAMETERS	68
6.4.1 PHASE ERROR.....	68
6.4.2 INSERTION LOSS.....	68
6.4.3 TRANSIENT RESPONSE	69
6.4.4 AMPLITUDE VARIATION	69
CHAPTER 7.....	70

7.1 INTRODUCTION	70
7.1.1 APPLICATIONS OF BEAM STERING.....	70
7.2 MECHANICAL VERSUS ELECTRONIC BEAM STEERING	71
7.2.1 MECHANICAL BEAM STEERING	71
7.2.2 ELECTRONIC BEAM STEERING	72
7.2 CRITERIONS FOR BEAM STEERING	73
7.3 OTHER TECHNIQUES OF BEAM STEERING	75
CHAPTER 8	76
8.1 RESULTS FROM SIMULATION	76
8.1.1 SINGLE KEY ANTENNA.....	76
8.1.2 SINGLE MICROSTRIP ANTENNA	79
8.1.3 COMPARISON BETWEEN SINGLE MICROSTRIP AND KEY ANTENNA	81
8.2 ARRAY SIMULATION.....	82
8.2.1 MICROSTRIP ANTENNA ARRAY	82
8.2.1 KEY ANTENNA ARRAY	87
8.2.1 COMPARISON BETWEEN ARRAY PARAMETERS	91
8.3 COMPARISION OF DIFFERENT SUBSTRATES	94
8.3.1 ROGERS RT 5880.....	94
8.3.2 ARLON AD 270	95
8.3.3 COMPARISON BETWEEN RESULTS	97
8.4 COMPARAING RESULTS OF DIFFERENT ELEMENTAL SPACING.....	98
8.4.1 ANTENNA ARRAY WITH 0.6λ ELEMENTAL SPACING	98
8.4.2 ANTENNA ARRAY WITH 0.7λ ELEMENTAL SPACING	100
8.4.3 ANTENNA ARRAY WITH 0.8λ ELEMENTAL SPACING	102
8.4.4 ANTENNA ARRAY WITH 1λ ELEMENTAL SPACING	104
8.4.5 COMPARISON BETWEEN RESULT VALUES	105
8.5 ARRAY BEAMSTEERING.....	107
CHAPTER 9	114
9.1 FUTURE SCOPE.....	114
9.2 CONCLUSION.....	114
References.....	116

List of Figures

Figure 1: Antenna as a transition device.....	1
Figure 2: Dipole Antenna.....	3
Figure 3a: Rectangular loop antenna.....	4
Figure 3b: Circular loop Antenna.....	4
Figure: 4 Helical Antenna.....	5
Figure: 5 Yagi Uda Antenna.....	5
Figure: 6 Parabolic Antenna (a) Parabolic Right Cylinder (b) Paraboloid.....	6
Figure 7: Corner Reflector (a) Front View (b) Top View.....	7
Figure: 8 (a) Rectangular Waveguide Horns (b) Pyramidal (c) Sectoral H Plane (d) Diagonal.....	8
Figure: 9 Different slot shapes.....	9
Figure: 10 Microstrip (a)Rectangular Patch (b) Circular Patch.....	10
Figure: 11 Microstrip Antenna Array.....	10
Figure: 12 Coordinate system for antenna analysis.....	11
Figure: 13 (a)Elevation Angle Theta (b) Azimuth Angle Phi.....	12
Figure: 14 Radiation Pattern in 3d plane.....	12
Figure: 15 Radiation Pattern consisting of main lobes and side lobes.....	13
Figure: 16 Pictorial representations of the three regions surrounding an antenna.....	14
Figure: 17 Typical changes of antenna amplitude pattern shape over the three fields.....	16
Figure: 18 Radiation Pattern in Azimuth and Elevation plane.....	17
Figure: 19 S11 (return loss) for the 20 GHz rectangular patch antenna.....	21

Figure: 20 Reflection, conduction and dielectric losses in an antenna.....	22
Figure: 21 Circuit model for low frequency.....	24
Figure: 22 Circuit model for high frequency.....	24
Figure 23: (a)A simple Microstrip Patch Antenna (b) Side view.....	30
Figure: 24 Different shapes of the Microstrip Patch	33
Figure: 25 Feeding Methods for Microstrip Antennas using (a) coaxial feed, (b) microstrip-line inset feed, (c) proximity-coupled feed, and (d) aperture-coupled feed.....	34
Figure: 26 Patch antenna with a quarter-wavelength matching section.....	36
Figure: 27 Physical and effective lengths of rectangular microstrip patch.....	38
Figure: 28 Charge distribution and Current density of a Rectangular Patch.....	39
Figure 29: Equivalent Current density	40
Figure: 30 (a) Shaped Slot Microstrip Antenna (b) T Shaped Slot Microstrip Antenna (c) U shaped Slot Microstrip Antenna (d) Circular slot key shaped microstrip Antenna.....	46
Figure 31: Array and Co-ordinate systems.....	49
Figure 32: Basic Linear Array Configuration.....	52
Figure: 33 Linear phased array antenna.....	53
Figure 34: Planar Array Configuration.....	54
Figure 35: Grating-lobe formation.....	57
Figure 36: A generalized two port phase shifter.....	59
Figure 37: Schematic for High-pass/Low-pass Pi and T model.....	64
Figure 38: T-model High-Pass/Low-Pass Phase Shifter.....	64
Figure 39: Pi-model High-Pass/Low-Pass Phase Shifter.....	65
Figure 40: Loaded-line Phase Shifters.....	65
Figure 41: Switched-line Phase Shifters.....	67

Figure 42: Reflection-type Phase Shifters.....	67
Figure 43: Beam Steering system using phase shifters.....	72
Figure 44: Key shaped Antenna.....	76
Figure 45: S Parameters for microstrip key antenna at 60 GHz.....	77
Figure 46: Polar plot of key antenna.....	78
Figure 47: 3d Farfield directivity pattern of key antenna.....	78
Figure 48: Microstrip antenna.....	79
Figure 49: S Parameters for microstrip antenna at 60 GHz.....	80
Figure 50: Polar plot of microstrip antenna.....	80
Figure 51: 3d Farfield directivity pattern of microstrip antenna.....	81
Figure 52: S parameter comparison for single antenna	81
Figure 53: Polar Plot comparing single element antenna.....	82
Figure 54: A 2x2 microstrip antenna array operating at 60 GHz.....	83
Figure 55: The antenna feeding point.....	84
Figure 56: Reference Impedance.....	84
Figure 57: S Parameters for 2x2 microstrip antenna array at 60 GHz.....	85
Figure 58: Voltage standing wave Ratio.....	85
Figure 59: Directivity of a 2x2 microstrip array antenna.....	85
Figure 60: Gain of Directivity of a 2x2 microstrip array antenna.....	86
Figure 61: Radiation Efficiency of a 2x2 microstrip array antenna.....	86
Figure 62: Polar Plot of microstrip antenna array.....	87
Figure 63: A 2x2 microstrip key antenna array operating at 60 GHz	87
Figure 64: The antenna feeding point.....	88
Figure 65: Reference Impedance.....	89
Figure 66: S Parameters for 2x2 microstrip key antenna array at 60 GHz.....	89
Figure 67: Voltage standing wave Ratio.....	89

Figure 68: Directivity of a 2x2 microstrip array antenna.....	90
Figure 69: Gain of Directivity of a 2x2 microstrip array antenna.....	90
Figure 70: Radiation Efficiency of a 2x2 microstrip array antenna.....	91
Figure 71: Polar plot of key antenna array.....	91
Figure 72: S parameter comparison for antenna arrays.....	92
Figure 73: Polar plot comparison of antenna array.....	93
Figure 74: 3d Farfield directivity pattern for RT 5880.....	94
Figure 75: S Parameters for Rogers RT 5880.....	94
Figure 76: Polar plot for RT 5880.....	95
Figure 77: 3d Farfield directivity pattern for AD 270.....	95
Figure 78: S parameters for AD 270.....	96
Figure 79: Polar Plot of AD 270.....	96
Figure 80: S parameter comparison for different Substrates.....	97
Figure 81: Key Antenna array with 0.6λ Elemental Spacing.....	98
Figure 82: S parameter for 0.6λ elemental spacing.....	99
Figure 83: Polar plot for 0.6λ elemental spacing.....	99
Figure 84: 3d Farfield directivity pattern for 0.6λ elemental spacing Parameters.....	100
Figure 85: S parameter for 0.7λ elemental spacing.....	101
Figure 86: Polar plot for 0.7λ elemental spacing.....	101
Figure:87 3d Farfield directive pattern for 0.7λ elemental spacing Parameters.....	102
Figure 88: S parameter for 0.8λ elemental spacing.....	102
Figure: 89 Polar plot for 0.8λ elemental spacing.....	103
Figure :90 3d Farfield directivity pattern for 0.8λ elemental spacing.....	103
Figure 91: S parameter for 1λ elemental spacing.....	104
Figure: 92 Polar plot for 1λ elemental spacing.....	104
Fig:93 3d Farfield directivity pattern for 1λ elemental spacing.....	105

Figure 94: Polar Plot of arrays at different elemental spacing.....	106
Figure 95: Key shaped antenna of 16 elements steered at 30 degrees.....	107
Figure 96: Farfield plot of a 2x2 key antenna with 16 patches steered at 30 degrees.....	107
Figure 97: Key shaped antenna of 16 elements steered at 45 degrees.....	108
Figure 98: Farfield plot of a 2x2 key antenna with 16 patches steered at 45 degrees.....	108
Figure 99: Key shaped antenna of 16 elements steered at 60 degrees.....	109
Figure 100: Farfield plot of a 2x2 key antenna with 16 patches steered at 60 degrees.....	109
Figure 101: Key shaped antenna of 16 elements steered at 75 degrees.....	110
Figure 102: Farfield plot of a 2x2 key antenna with 16 patches steered at 75 degrees.....	111
Figure 103: Key shaped antenna of 16 elements steered at 90 degrees.....	111
Figure 104: Farfield plot of a 2x2 key antenna with 16 patches steered at 90 degrees.....	112
Figure 105: Beamsteering at different Scan Angles.....	113

List of Tables

Table 1: Comparison of Various Types of Feed Techniques for Microstrip Patch Antennas...	35
Table 2: Key Antenna Parameters.....	76
Table 3: Microstrip Antenna Parameters.....	79
Table 4: Microstrip Antenna Array Parameters.....	83
Table 5: Microstrip Key Antenna Array Parameters.....	88
Table 6: Comparison between Arrays.....	92
Table 7: Comparison between different substrates.....	97
Table 8: Comparison between Different element spacing.....	105
Table 9: Beamsteering vs Directivity comparison.....	112

CHAPTER 1

Antenna Overview and Basics

1.1 ANTENNA OVERVIEW

An antenna is a metallic structure that radiates or receives radio electromagnetic waves. An antenna is often known as the transitional device between a guiding device and free space as shown in figure 1. The transmission line or the guiding device may take the shape of the coaxial line or a wave guide and can be used to transmit the electromagnetic energy from the transmitting source to the antenna or from the antenna to the receiver. The oscillating current applied to the antenna by the transmitter during transmission creates an oscillating electric and magnetic field around the antenna. During reception the opposite occurs. The oscillating electric and magnetic field of the radio waves exert a force on the electrons of the antenna, causing movement of the electrons and thus producing oscillating current.

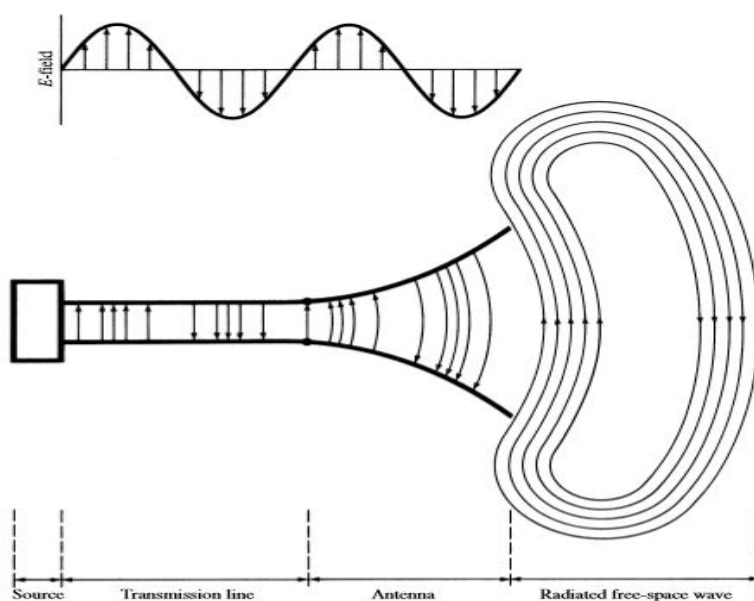


Figure 1: Antenna as a transition device [6]

Along with transmitting and receiving energy, an antenna is also used to concentrate radiation energy in a particular direction while suppressing it in others (directional) or it can even transmit and receive in all directions (omnidirectional). The first antennas were built by German physicist Heinrich Hertz in 1888. It was one of his experimental work to prove the existence of electromagnetic waves that James Clerk Maxwell predicted [1]. Over the last 60 years antenna technology has played a major role in communication revolution. A good antenna design can improve the overall performance of the system. Antenna is the most essential component in wireless communication. They are used in radio broadcasting, broadcast television, communication receivers, mobile phones, radars and satellite communication. Thus antennas are the most vital element in the field of communication.

1.2 TYPES OF ANTENNA

1.2.1 WIRE ANTENNA

Wire antennas are the some of the oldest, simplest and most cost effective antennas. They have many versatile applications and are thus used in automobiles, airplanes, houses, ships, spaceships and many more. Wire antennas are of various shapes such as straight wire (dipole), loop and helix. Loop antennas does not necessarily need to be circular, it can be of any shape-rectangle, square, ellipse and many more.

1.2.1a Dipole Antenna

Dipole antennas are one of the most simple, important and commonly used types of RF antenna. In [2] Poole provided a description about the structure of the dipole antenna. The dipole antenna consists of two conductive elements such as metal rods that are divided in the centre and an insulator is used to separate the two segments of the rod. The rods are joined to a coaxial cable at the end. The split between the radiating elements at the centre allows the feeder to apply radio frequency voltage.

Half wave dipole antennas are by far the most widely used antennas. The total length of the antenna is equal to half of the wavelength that the antenna is to generate. Dipole can be shorter or longer than half the wavelength, but this ratio provides the best efficiency. Ambresh et al in [3] showed that a typical gain for dipole antenna is 2dB and the bandwidth is generally around 10%.

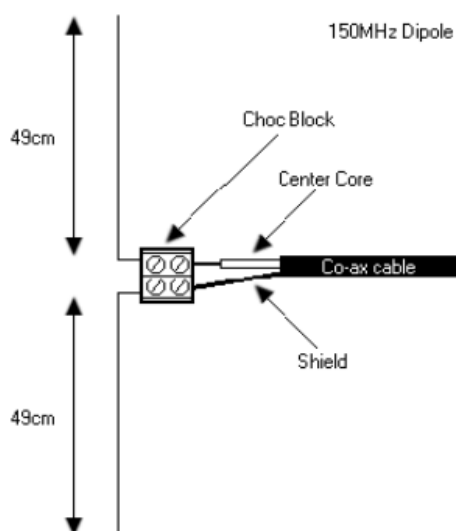


Figure 2: Dipole Antenna [6]

1.2.1b Loop Antenna

The loop antenna mainly consists of a conductor that is bent into different shapes like circular, square, elliptical and many more. The impedance of these antennas are difficult to match since they have low radiation resistance and high reactance. [4] They are very useful as receivers. They can be used at low frequencies instead of dipole antennas which becomes very large. In [3] Ambresh et al stated that the efficiency of small loop antenna is not good, however a high signal to noise ratio compensates for it. The core of the loop antenna can be filled with ferrite to enhance its performance. A typical gain for loop antenna is from -2dB to 3dB and a bandwidth of around 10%. The following figure shows a circular and a rectangular loop antenna:



Figure: 3a Rectangular loop Antenna [3]



Figure: 3b Circular loop Antenna [3]

1.2.2 TRAVELLING WAVE ANTENNA

Travelling wave are a group of antennas that use travelling wave on a guiding structure as the main radiating mechanism. In travelling wave antenna, the travelling wave of electromagnetic oscillations propagates along its geometric axis. They are made with either discrete radiators placed along the axis at a certain distance from each other or they are made of continuous radiators that stretch out in the direction of the axis. Since travelling wave antennas are non-resonant they have a wider bandwidth than resonant antennas. Few common types of travelling antennas are Yagi Uda, helical and spiral antennas.

Helical Antenna

In [4] the basic construction of a helical antenna has been clearly explained. This type of antenna consists of a single conductor wound into a helical shape. The helical antenna is usually mounted over a ground plane while the feed line is connected between the ground plane and the bottom of the helix. The current and the phase constantly vary along the helical antenna since it is a travelling wave. They are circularly polarised. The helical antennas operating in normal mode are used in mobile radios and broadcasting antennas. The ones that are operating in axial mode are used in satellite communication.

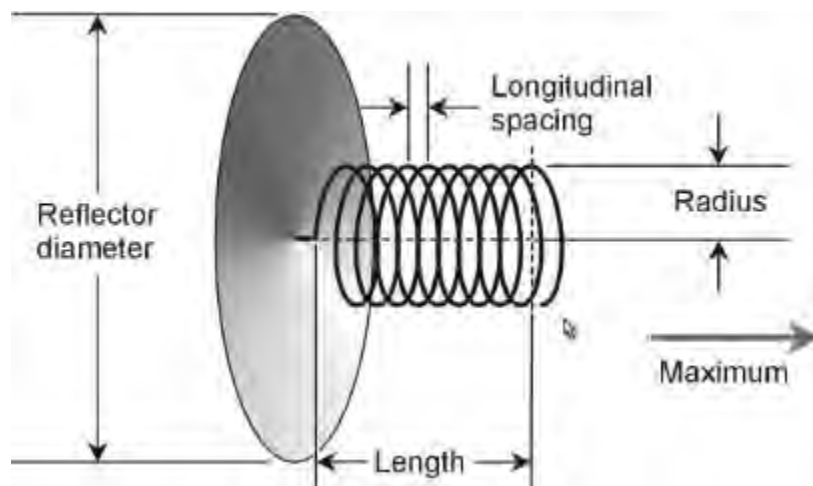


Figure: 4 Helical Antenna [4]

Yagi Uda Antenna

This antenna was first invented in Japan by Shintaro Uda. His work which was published in Japanese was later translated into English by Yagi as mentioned by Poole in [2]. This antenna is simple and easy to construct. The Yagi antenna consists of three elements-driven element, reflector and director. Power is applied in the driven element while director elements are placed at the back of the driven element in the direction of maximum sensitivity. They generally have a high gain typically greater than 10dB. The Yagi Uda antennas typically operate in the HF to UHF bands (3MHz to 3GHz) [4]. They are directional which enables interference levels to be minimised for receiving and transmitting. However, they have a small bandwidth.

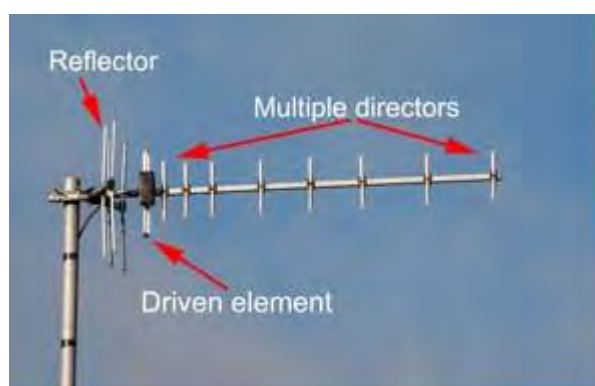


Figure: 5 Yagi Uda Antenna [2]

1.2.3 REFLECTOR ANTENNA

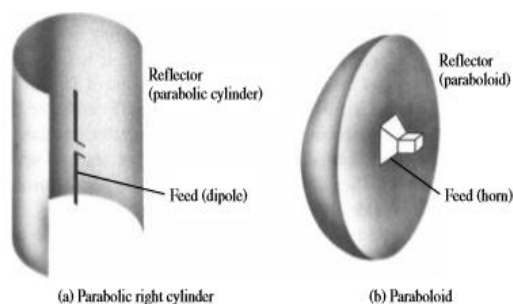
There was a need of sophisticated antennas to communicate over greater distance in order to transmit and receive signals. A very common type of antenna for such application is the reflector antennas. These are high gain antennas that are usually needed for long distance radio communication, satellite communications, high resolution radars, radio astronomy and many more. They are most widely used high gain antennas. They can easily achieve gains of 30dB for microwave and higher frequencies. Some of the common types of reflector antennas include corner reflector and parabolic reflector.

1.2.3a Parabolic Reflector

Basic construction of this type of antenna consists of a metal parabolic reflector. In [5] Straw et al described the construction of the parabolic reflector antenna. There is a small feed antenna suspended in front of the reflector at its focus. The reflector which is usually made of a metallic surface is bent into a paraboloid. During transmission the radio frequency current is supplied through transmission line cable to feed antenna while during reception the radio waves are focused to the point at the feed antenna which converts it to electrical current that travels through the transmission line to the receiver. These antennas typically have very high gain (30-40 dB) and low polarisation with a reasonable bandwidth [4]. These parabolic reflector antennas also known as dish antennas have wide range of application in radio and wireless applications.



Figure: 6 Parabolic Antenna [6]



(a) Parabolic Right Cylinder (b) Paraboloid

1.2.3b Corner Reflector

The geometrical shape of the reflectors are often adjusted to increase the directivity of an antenna. One such arrangement is accomplished in such a way that the two plane reflectors are aligned in a way to form a corner. These corner reflector antennas generally have a moderate gain (10-15 dB) [4]. In [6] Balanis highlighted a unique feature of corner reflectors. Corner reflectors have a rare feature which is that if the reflector is used as a passive target it will return the signal exactly in the same direction as it is received when its included angle is 90° . Because of this unique property many military ships and vehicles are designed with minimum sharp corners to reduce their detection by enemy radar. Other than this they are also mostly used in UHF television antennas and point-to-point communication links and data links for wireless WANs.

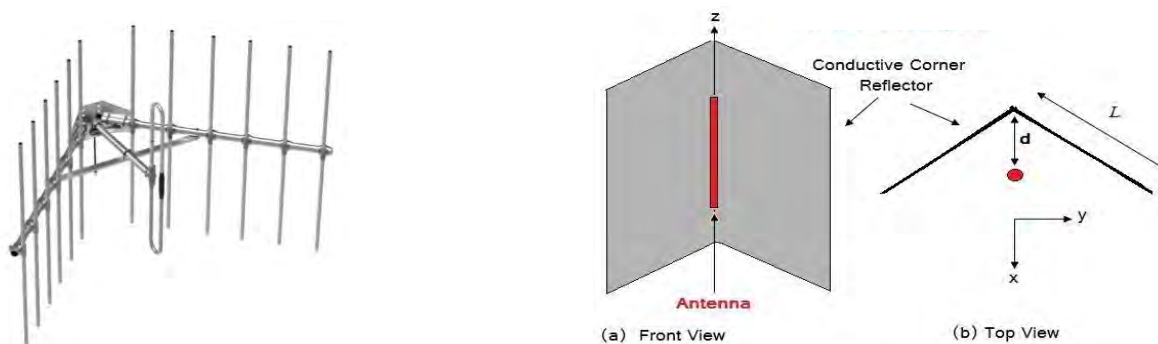


Figure: 7 Corner Reflector (a) Front View (b) Top View [4]

1.2.4 APERTURE ANTENNAS

Aperture antennas are mainly made with dielectric and metal walls mostly with ridges. Feedpins or waveguide ports are used as excitations. Aperture antennas are more popular because of the increasing demand for sophisticated antennas and utilisation of higher frequencies. These antennas are very useful for aircraft and spacecraft applications. Most common types of aperture antennas are horn antennas and slot antennas.

1.2.4a Horn antennas

Horn antennas are very popular at UHF (300 MHz- 3GHz) and higher frequencies. They usually have directional radiation pattern and high antenna gain which can range up to 25dB in some cases, while in most cases its usually from 10-20dB. The gain of the antenna often increases as the frequency operation increases [4]. They have a wide impedance bandwidth. Horn antennas can have several shapes depending on their function. Figure. Ambresh et al in [3] talked about how the pyramidal horn is used to maximise gain since the antenna is flared on both H plane and E plane, giving the antenna a fixed directivity. B and c are special cases of pyramidal horn, however in this case only E or H plane is flared and thus maximised.

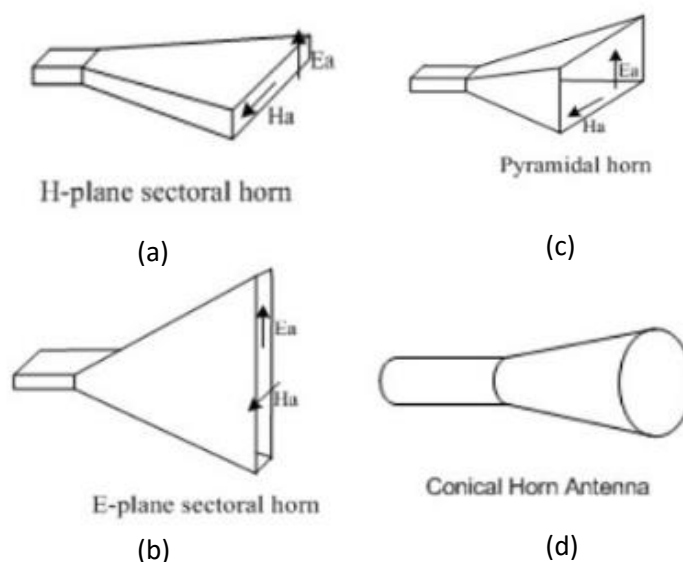


Figure: 8 (a) Rectangular Waveguide Horns (b)Pyramidal
(c)Sectoral H Plane (d) Diagonal [3]

1.2.4b Slot Antenna

These are antennas are made by simply cutting slots or cut on the surface on which they are mounted. They are mostly used in frequencies between 300Hz and 24GHz. They have roughly omnidirectional radiation pattern. Voltage source is applied across the short end of the slot antenna which induces an E field distribution within the slot and current that travel around the edges of the slot, thus contributing to radiation. The polarisation of the slot antenna is linear. The shape, size of the slots can be altered to tune performance. [4]

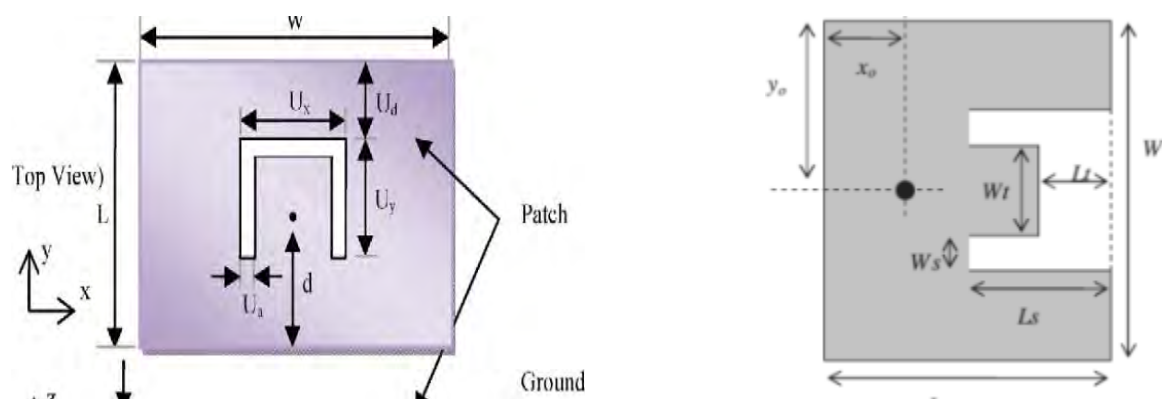


Figure: 9 Different slot shapes [68]

1.2.5 MICROSTRIP ANTENNA

Microstrip antennas are one of the most popular and widely used printed antennas. They are also referred to as patch antenna and have low cost, low profile and are easy to fabricate. Basic construction of the microstrip patch antenna includes a radiating patch on top of a dielectric substrate that has a ground plane beneath it. The microstrip antennas with good desirable performance have thicker substrate whose dielectric constant is lower for better efficiency. The microstrip patch antenna has different feeding techniques. Microstrip line, coaxial probe, aperture coupling and proximity coupling are the ones that are more commonly used. Microstrip antenna patches can be of different shapes- rectangular, circular, planar, etc. Major disadvantages of microstrip patch antenna are their low efficiency, low power, high Q, poor polarisation, spurious feed radiation and narrow frequency bandwidth as discussed by Balanis in [6]. In high performance aircrafts, space crafts and satellites where size, cost, weight, performance and ease of installation are major factors, these low profile microstrip antennas can be used.

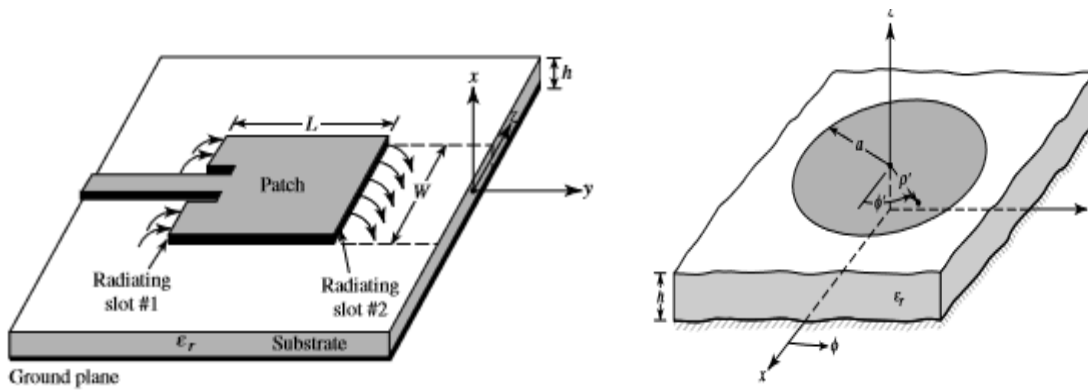


Figure: 10 Microstrip (a) Rectangular Patch (b) Circular Patch [6]

1.2.6 ARRAY ANTENNA

An array antenna is a set of many antennas that are connected together and it is supposed to work as a single antenna. Individual antennas that are called elements are connected to transmitter or receiver by feedline. This feedline feeds power to each of the elements in an array. Many applications need radiation characteristics that may not be achieved by single element. The arrangement of the array must be such that radiation from each of the element adds up to give maximum radiation in a particular direction. It increases the overall gain and cancel out interference from a particular set of directions.[4]

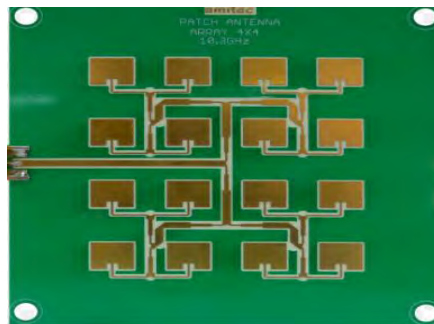


Figure: 11 Microstrip Antenna Array [4]

1.3 ANTENNA PARAMETERS

1.3.1 RADIATION PATTERN

A radiation pattern aka an antenna pattern can be described as the variation of the power radiated by an antenna as a function of the direction away from the antenna. Radiation properties typically consist of flux density, radiation intensity, field strength, directivity, phase or polarization. It is usually defined in the far field region and represented by means of a function of directional coordinates. In most cases we are mainly focused on the two- or three dimensional spatial distribution of radiated energy as a function of the observer's position along a path or surface of constant radius. In the figure below we can see a 3D representation of a set of coordinates for antenna radiation pattern. [4, 6]

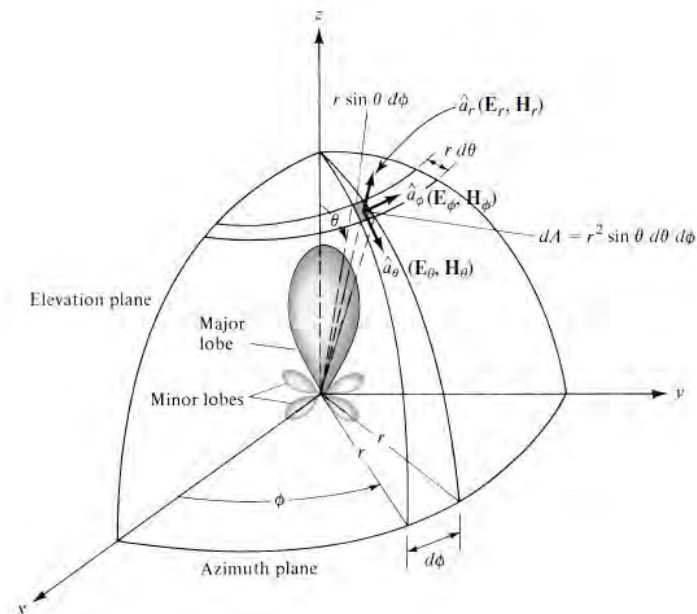


Figure: 12 Coordinate system for antenna analysis [6]

Although for the sake of simplicity we normally represent radiation patterns by plotting them in the 2-D plane as can be seen from the figures below [4]. Standard spherical coordinates are used, where Θ is the angle measured off the z -axis, and Φ is the angle measured counter clockwise off the x -axis.

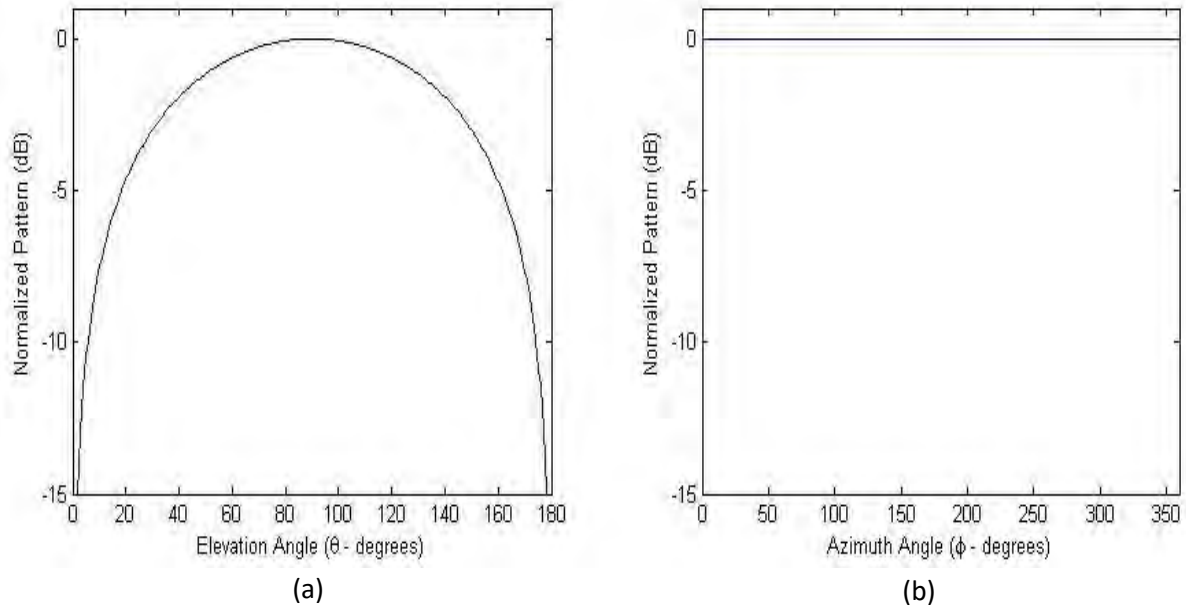


Figure: 13 (a) Elevation Angle Theta (b) Azimuth Angle Phi [4]

From the above figure on the left we can see that radiation pattern is at a maximum at broadside to the antenna or 90 degrees of the z-axis minimum at 0 and 180 degrees. On the right what we observe is the azimuthal plot. It is a function of the azimuthal angle for a fixed polar angle (90 degrees off the z-axis in this case) and appears constant as the radiation pattern is symmetrical around the z-axis (Look to 3D plot below).

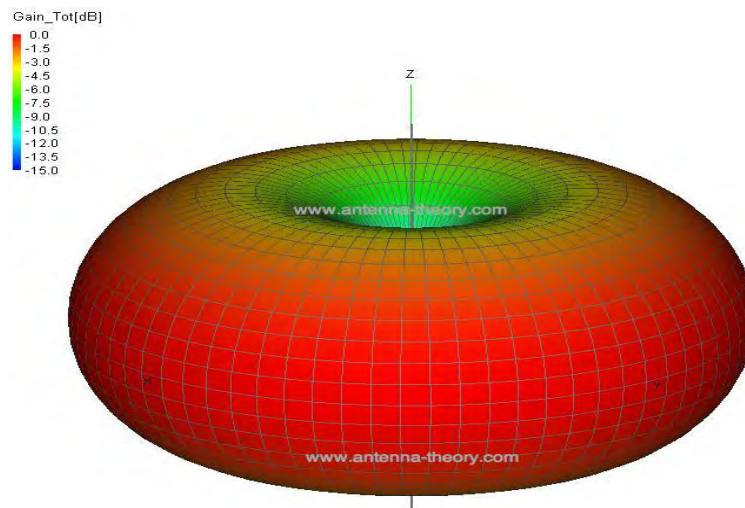


Figure: 14 Radiation Pattern in 3D plane [4]

Mainly when it comes to antenna radiation patterns we are tend to draw our attention to two aspects, field and power pattern. A field pattern describes a plot of the magnitude of the electric or magnetic field as a function of the angular space while a power pattern refers to a plot of the

square of the magnitude of the electric or magnetic field as a function of the angular space. We normally represent power patterns on the logarithmic scale (in decibels dB) as it can consist of even the parts of the pattern such as the side lobes which will be discussed below. [6]

When it comes to antenna radiation patterns we often classify the individual parts as lobes and within these lobes there are subclasses such as major lobes, minor lobes, side and back lobes. Major lobes are defined as the radiation lobe that contains the direction of maximum radiation and in the following figure it is the lobe pointing in the $\theta=0$ direction or z axis. On the other hand, a minor lobe can be any lobe except the major lobe whilst a side lobe is a radiation lobe that is not in the direction of the intended lobe and finally a back lobe is one that is 180 out of phase with the direction of the beam of the antenna. Minor lobes are considered as signs of radiation in undesirable directions and side lobes are the largest of them and ought to be minimized. Side lobes of -20dB or smaller are usually not desirable for most applications. [6]

Coming to the last important bit about antenna radiation we have the half-power beamwidth (HPBW) and null beamwidth. HPBW is defined as is the angular separation in which the magnitude of the radiation pattern decrease by 50% (or -3 dB) from the peak of the main beam. Null Beamwidth is referred to as such the angular separation from which the magnitude of the radiation pattern decreases to zero (negative infinity dB) away from the main beam.

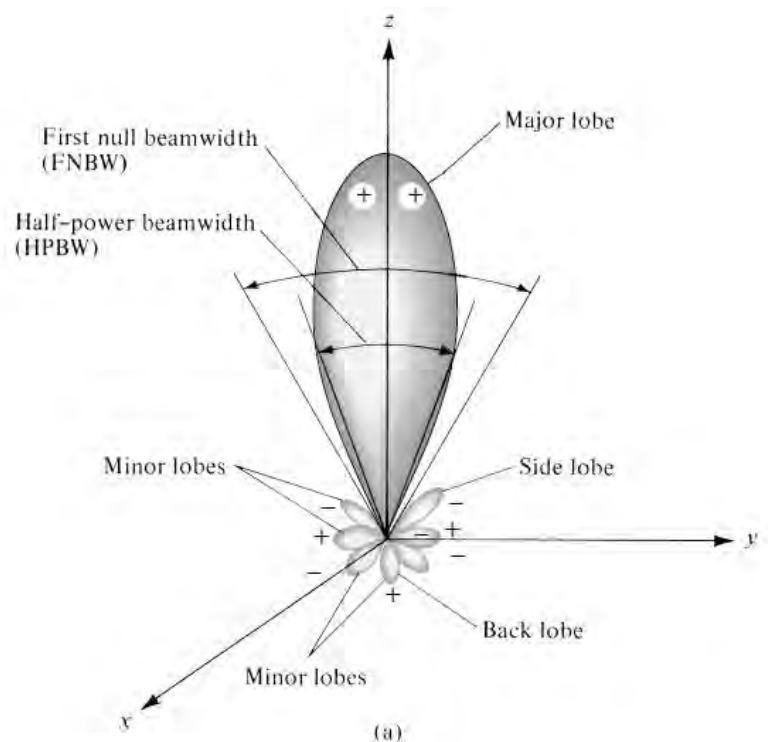


Figure: 15 Radiation Pattern consisting of main lobes and side lobes [6]

FIELD PATTERN

The distribution of radiated field strength around an antenna is a function of both the distance from the antenna itself and the angular co-ordinates. In simple words, it is the region of electromagnetic field around a transmitting antenna. Since it is crucial for us to learn the radiation pattern of an antenna we need to be first familiarized with the nature of the field regions encircling the antenna. This region has been sectioned into three regions: Reactive near-field, radiative near-field and lastly the far-field. It is important to learn the field structure within each of these regions. However, it is found that the transition between one fields to the next has no distinctive changes but instead is quite imperceptible, and there are no distinguishing changes between them [6, 7]

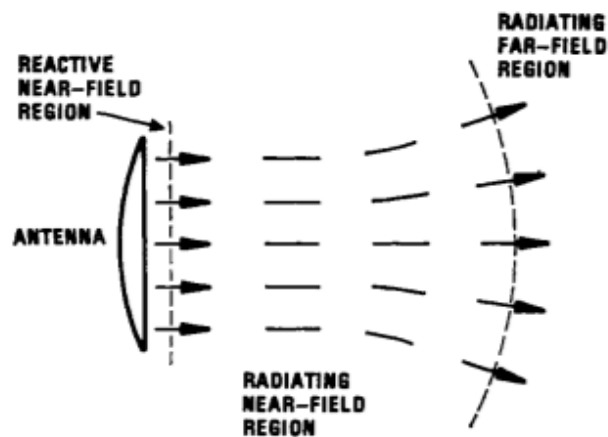


Figure: 16 Pictorial representation of the three regions surrounding an antenna [7]

Reactive Near-Field Region

The region closest to the antenna is defined as the reactive near-field region. Since it is in the closest vicinity of the antenna, both a reactive component and radiative component exist here. But the reactive field prevails in this region since the strength of the reactive component deteriorates very quickly as we move farther away from the antenna. This basically entails that the H-fields and E-fields have a phase difference of 90 degrees between them. The boundary of this region is known to be,

$$R < 0.62 \sqrt{\frac{D^3}{\lambda}}$$

Where, R is the distance from the antenna surface; λ represents the wavelength and D represents the largest dimension of the antenna. However, for radiators like short dipoles this boundary is known to exist at $\lambda/2\pi$ distance from the antenna surface. [4, 6]

Radiative Near-Field (Fresnel) Region

The reactive component seemed to predominate in the previous region. But as we exceed the boundary of the reactive near field region and enter into the radiative near-field region it is the radiation component that starts to dominate and not so much the reactive component. This region may also be referred to as Fresnel region. In this region between the near and far fields, the angular field distribution varies with distance from the antenna surface. The radiation pattern in this region changes substantially with distance. This region is known to exist between,

$$0.62\sqrt{\frac{D^3}{\lambda}} < R < \frac{2D^2}{\lambda}$$

This measurement is based on a maximum phase error of $\pi/8$. A significant thing to note here is that if D , which is the maximum dimension is not substantial enough compared to the wavelength this region may possibly not exist. [4, 6]

Radiative Far-Field (Fraunhofer) Region

The far-field region, also referred to as Fraunhofer region is the most important of the three sub-division. This is because most antenna are used for connecting long distance, so far field region would be the best region to study, as this is where the most antennas function. As the name suggest this is the region furthest away from the antenna, and only in this region is where the angular field distribution is basically independent of the distance from the antenna. And the field components are actually transverse. Even as we move away from the antenna the shape of the radiation pattern is not affected at all. This is where the electric and magnetic field are orthogonal to each other and the direction of propagation is that of plane waves. The inner boundary of this region is given by,

$$R > \frac{2D^2}{\lambda}$$

The outer boundary of this region extends to infinity. However, for a few particular antennae, take for instance multi-beam reflector antenna, they are not indifferent to phase variation over their apertures. The inner boundary mentioned above are not acceptable for them. Instead the region is set to start from $|\gamma| D^2/\pi$, where γ is the propagation constant of the medium. [4, 6]

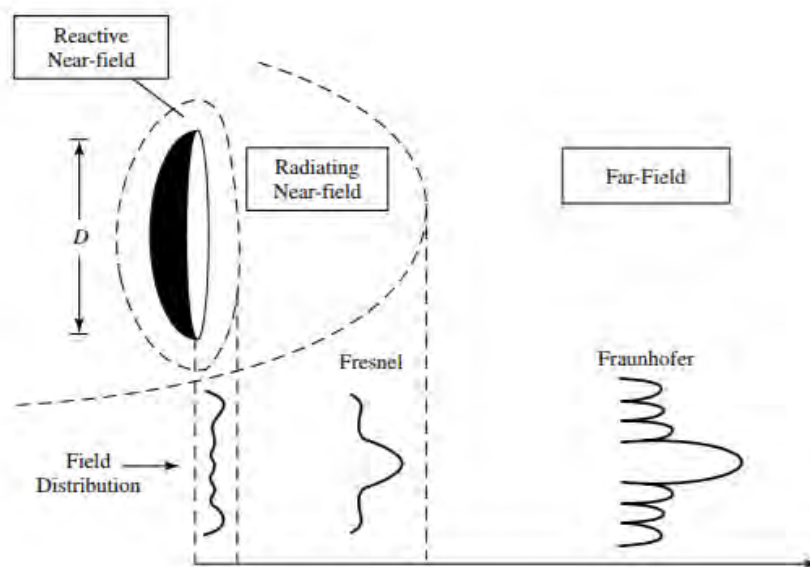


Figure: 17 Typical changes of antenna amplitude pattern shape over the three fields [6]

The amplitude pattern of the antenna varies over the three regions as it can be seen in the picture above. This occurs due to difference in the fields. It can be observed that closest to the antenna the pattern is more uniform and spread out, with little changes. But as we progress into the Fresnel region the pattern is seen to smoothen and lobes get formed. And then lastly in the Fraunhofer region the pattern becomes distinguished, consisting of a major lobe and few minor lobes.

1.3.2 ANTENN GAIN

The term antenna gain is known as a measure of the quantity of power transmitted in the

direction of the peak radiation in respect to an isotropic source. For instance if we had a transmitting antenna with 3dB gain it indicates that the power received far from the antenna will be 3 dB higher (twice as much) when compared to what we might see when receiving from a lossless isotropic antenna with the same input power. Likewise, a receiving antenna with a 3dB in a specific direction implies that it would receive 3dB more power if compared to a lossless isotropic antenna. Antenna Gain (G) can be related to directivity (D) and antenna efficiency by the following

$$G = \eta_{rad} \cdot D$$

Where, G =Gain of the Antenna

η_{rad} = Radiation efficiency,

D =Directivity

The gain on an antenna is proportional to its electrical size. For instance a large dish antennas can have gains as high as 40dB or more though this is not often the case. Similarly, it can also be extremely low such as for short dipole antennas but in theory is never less than 0dB but it's possible that due to low efficiency its peak maybe of a lower value. Antenna gain can also be measured as a function of an angle which is technically a plot of the radiation pattern where the units are measured in antenna gain as shown in the figure below. [4]

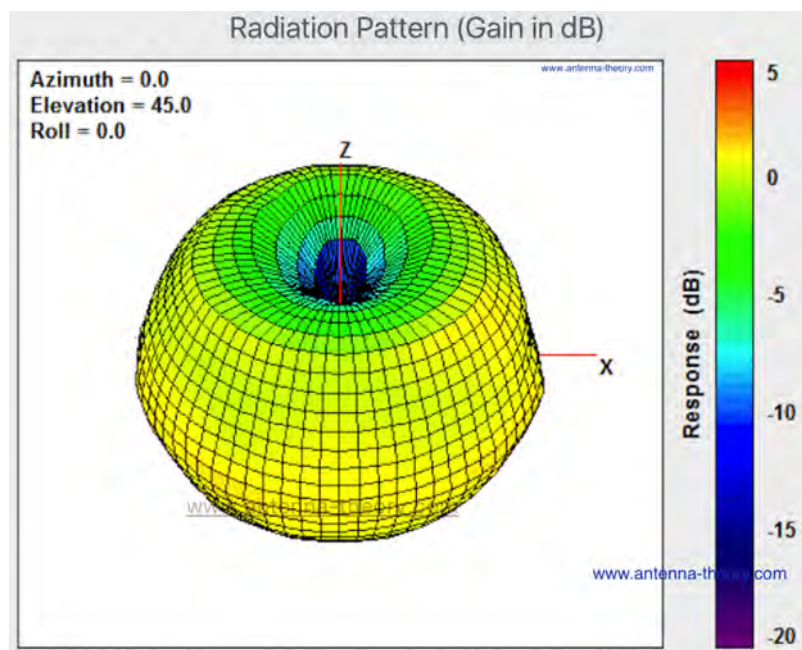


Figure: 18 Radiation Pattern in Azimuth and Elevation plane [4]

1.3.3 DIRECTIVITY

Directivity is one of the other vital parameters of any antenna and is essentially a measurement of its radiation pattern's direction. Directivity of an antenna defined as the ratio of the radiation intensity in a given direction from the antenna to the radiation intensity averaged over all directions where the average radiation intensity is equal to the total power radiated by the antenna divided by 4π . We assume that direction of maximum radiation intensity is implied if no direction is specified. An antenna that radiates equally in all directions would have effectively zero directionality, and the directivity of this type of antenna would be 1 (or 0 dB).

The expression associated with this definition can be seen below

$$D = \frac{U}{U_0} = \frac{4\pi U}{Prad}$$

If direction is unspecified we may take the direction of maximum radiation intensity as

$$D_{max} = D_0 = \frac{U|_{max}}{U_0} = \frac{U_{max}}{U_0} = \frac{4\pi U_{max}}{Prad}$$

Where,

D = directivity (dimensionless)

D0 = maximum directivity (dimensionless)

U = radiation intensity (W/unit solid angle)

Umax = maximum radiation intensity (W/unit solid angle)

U0 = radiation intensity of isotropic source (W/unit solid angle)

Prad = total radiated power (W)

When it comes to antennas with orthogonal polarization components the partial directivity of an antenna for a given polarization in a given direction as can be referred to as the part of the radiation intensity corresponding to a given polarization divided by the total radiation intensity averaged over all directions. In addition we may define the total directivity as the sum of the

partial directivities for any two orthogonal polarizations. If we are dealing with spherical coordinate system the total maximum directivity D_0 may be expressed as

$$D_{\theta} = \frac{4\pi U_{\theta}}{(P_{\text{rad}})_{\theta} + (P_{\text{rad}})_{\phi}}$$

$$D_{\phi} = \frac{4\pi U_{\phi}}{(P_{\text{rad}})_{\theta} + (P_{\text{rad}})_{\phi}}$$

U_{θ} = radiation intensity in a given direction contained in θ field component

U_{ϕ} = radiation intensity in a given direction contained in ϕ field component

$(P_{\text{rad}})_{\theta}$ = radiated power in all directions contained in θ field component

$(P_{\text{rad}})_{\phi}$ = radiated power in all directions contained in ϕ field component

The general expression for directivity and maximum directivity can now be written as

$$D(\theta, \phi) = 4\pi \frac{F(\theta, \phi)}{\int_0^{2\pi} \int_0^{\pi} F(\theta, \phi) \sin \theta d\theta d\phi}$$

$$D_0 = 4\pi \frac{F(\theta, \phi)|_{\text{max}}}{\int_0^{2\pi} \int_0^{\pi} F(\theta, \phi) \sin \theta d\theta d\phi}$$

1.3.4 S PARAMETER

S parameter is one of the key parameter that helps us to evaluate the overall performance of the antenna. This parameter basically defines the relation between the input and output port in a system. For instance, in a two port system, incidentally name port 1 and 2, the power transmitted from port 2 to 1 will be characterized by S12. Similarly, S21 represents the power

transmitted from port 1 to 2. Whereas, S11 and S22 would be the reflected power that the port 1 and 2 are trying to transmit, respectively. [4]

When it comes to the subject of antennas, S11 is the most used parameter compared to S12 or S21. It essentially signifies the amount of power that is basically reflected from the antenna. Therefore, it can also be represented using Reflection coefficient, denoted by Γ or Return loss. This loss of power that is returned may occur due to some kind of discontinuity usually due to mismatch between two impedances in the transmission line. Return loss is usually expressed in decibels as given below, [4, 8]

$$RL_{dB} = 10 \log_{10} \frac{P_i}{P_r}$$

Where P_i denotes the incident power and P_r denotes the reflected power. Similarly, the relation between return loss and reflection coefficient is given by the following,

$$\Gamma = \frac{Z_L - Z_S}{Z_L + Z_S}$$

$$RL_{dB} = -10 \log |\Gamma|^2 = -20 \log |\Gamma|$$

Return loss commonly gives a negative decibel value. A more negative return loss indicates more loss. This entails that there is good impedance match, and less power is reflected back to the source. [8] For a 0 dB return loss it suggests that all the power has been reflected back and none has been radiated by the antenna. Whereas, a -10 dB return loss indicates that for 3 dB incident power -7 dB that has been reflected while the rest has been either radiated or absorbed by the antenna. But in most cases, the power is commonly radiated.

S-parameters are normally defined for a particular frequency and system impedance, and varies as a function of frequency. Therefore, it is possible to determine the bandwidth of an antenna from its S-parameter. [4]

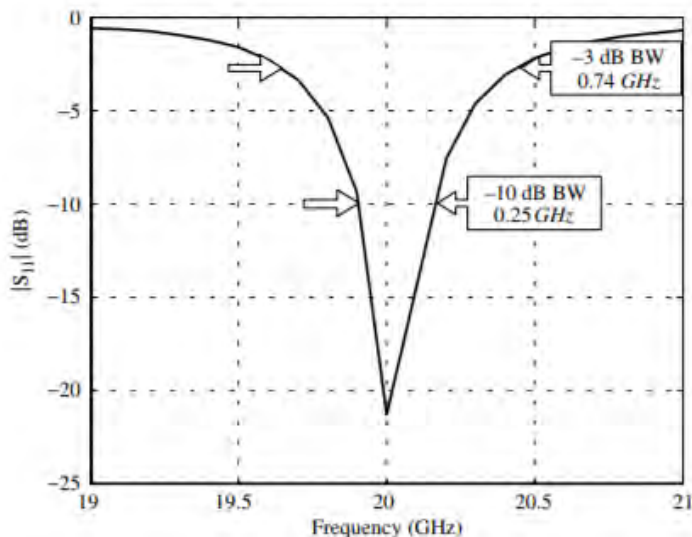


Figure: 19 S₁₁ (return loss) for the 20 GHz rectangular patch antenna [6]

1.3.5 ANTENNA EFFICIENCY

Antenna efficiency, which is another very important parameter for antenna can be expressed as the radiation efficiency. It is defined as the ratio of the power delivered to the antenna to the power that is actually radiated by the antenna. A very high efficiency indicates that most of the power that was incident at the antenna's input was successfully radiated. Whereas an inefficient antenna means a significant amount of power was lost. These losses may occur due to I^2R losses (conduction and dielectric). [4]. The radiation efficiency of an antenna is given by the equation below. It can be expressed as a ratio, percentage or even in decibels and is frequency dependent. According to the reciprocal property of the antenna, no matter if the antenna is being used a receiver or transmitter, its radiated efficiency will remain unchanged.

$$\epsilon_R = \frac{P_{radiated}}{P_{input}}$$

$$\epsilon_R = \epsilon_c \cdot \epsilon_d$$

It is practically impossible for the antenna efficiency to be 100% but dish antennas, horn antennas, or half-wavelength dipoles have virtually no lossy materials around them so they come very close to it.

However, the overall radiation efficiency of the antenna is slightly different to the radiation efficiency. This is because it also takes into account the loss due to reflected power caused by the mismatch of impedance in the transmission line.

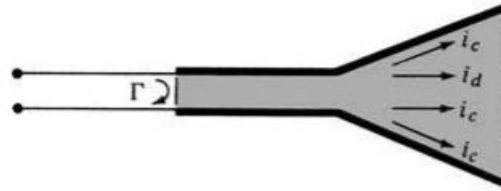


Figure: 20 Reflection, conduction and dielectric losses in an antenna [6]

It can be given by,

$$e_0 = e_r e_c e_d$$

Where,

e_0 = Total efficiency

e_r = Reflection (mismatch) efficiency

e_c = Conduction efficiency

e_d = Dielectric efficiency [6]

1.3.6 BANDWIDTH

One of the core deciding parameter to choose the type of antenna for an application is bandwidth. It refers to the range of frequency where the antenna can productively provide or receive energy. One other way to look at is the frequency range on either side of the center frequency within which the other parameters of the antenna such as gain, radiation efficiency, impedance etc. are adequate. For broadband and narrowband antennas, the bandwidth is denoted as a ratio and percentage, respectively. These values are crucial for determining which operation the antenna is most suitable for since most of the characteristics are not even remotely affected by the frequency in the same manner, so bandwidth has no other distinctive characterization.

$$BW = F_H / F_L$$

$$BW = 100 \times \frac{F_H - F_L}{F_C}$$

Where,

F_H = Higher frequency

F_L = Lower frequency

It is possible to find the bandwidth of an antenna from its S-parameter, i.e. return loss (dB) versus frequency plot. Where the return loss value is the lowest will be the center frequency of the antenna. While, the range frequencies where the return loss is lower than -10 dB is the bandwidth.

It is possible to modify the acceptable frequency range of a narrowband antenna if the required changes are made either to the actual dimensions of the antenna or the coupling networks like transformers or both as the frequency varies.

1.3.7 INPUT IMPEDANCE

The impedance of the antenna calculates the value of the voltage divided by the current at the antenna input. The impedance of the antenna can either be a real value or a complex number. A real value indicates that the antenna is resonant. If it is expressed in complex form, then the real part of the impedance will signify the power that is either radiated or absorbed whereas the imaginary part implies the power stored in the near fields of the antenna i.e. the power that has not been radiated. The impedance of the antenna with no load attached is given by,

$$Z_A = R_A + jX_A$$

The input impedance is function of frequency. As a result, the antenna is connected to the rest of the transmission line and equipment only within the bandwidth. The value of the antenna is influenced by quite a few factors which include geometry, method of excitation, and its nearness to surrounding objects. Due to such composite geometries, not all antennas have been investigated analytically but instead experimentally.

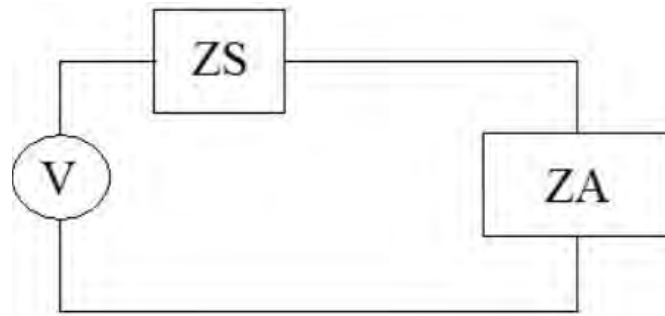


Figure: 21 Circuit model for low frequency [4]

For low frequency antennas, the transmission line can be ignored as its length is small compared to the wavelength at that frequency. For the circuit model shown above, Z_s represents the source impedance and Z_A the antenna impedance. Therefore, the power delivered to the antenna is given by,

$$P_A = \frac{V^2 \cdot Z_A}{(Z_A + Z_S)^2}$$

The magnitude of Z_A cannot be very small compared to Z_s because in that case no power shall be delivered to the antenna. Same thing occurs if Z_A is too large compared to Z_s , and as a result the antenna would be unable to transmit or receive energy. Therefore, to ensure maximum power is transferred Z_A has to be equal to the complex conjugate of Z_s . This is one of the essential design parameter of an antenna and it may be a rigorous job to do it right.

Whereas, at high frequency the magnitude of the wavelength reduces. As a result, the length of the transmission line can no longer be considered negligible compared to the wavelength.

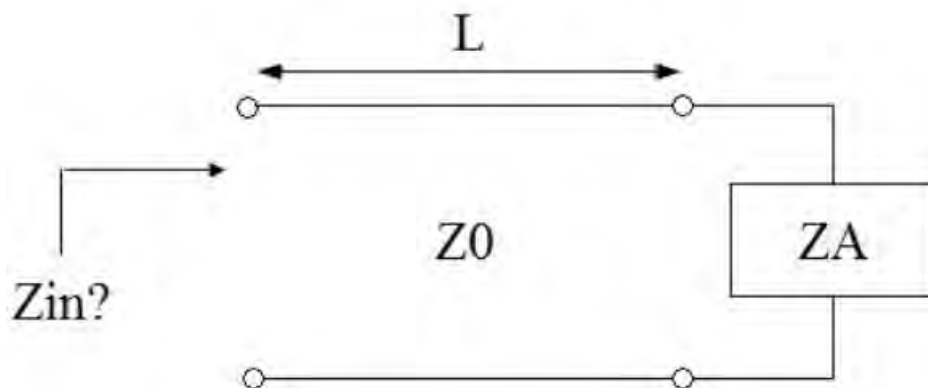


Figure: 22 Circuit model for high frequency [4]

The transmission line now makes it challenging for delivering the power to the antenna as it transforms its impedance, unless it is properly matched to the antenna. In the circuit model above, if L signifies the length of the transmission line and Z_0 its impedance than the input impedance is given by,

$$Z_{in} = Z_0 \frac{ZA + jZ_0 \cdot \tan\left(\frac{2\pi f}{c} L\right)}{Z_0 + jZA \cdot \tan\left(\frac{2\pi f}{c} L\right)}$$

As it is mentioned above, it is important to know that if the transmission line impedance matches with that of the antenna then Z_{in} will no longer be affected by the transmission line length. This reduces the complications as Z_{in} can now be matched properly to the source impedance in order for the power to be delivered to the antenna. As a result, impedance mismatch can now be evaded which would have otherwise reflected the power back to the generator.

CHAPTER 2

Literature Review

2.1 INTRODUCTION

One of the major reasons that is viewed as the key pioneer to pushing 5G network into our current commercial reality is the demand for more radio spectrum. In order to achieve this increased spectrum we must dive into the realm of millimeter wave spectrums-the radio spectrum that 6GHz and above [9]. Though it may enable us to reach a much wider range of operating frequencies the downside is that we must tackle the challenges of the ineffectiveness of signals that are travelling through physical obstruction like buildings and other objects. However, overcoming this shortcoming is the of utmost importance of one the key advances of 5G networks that is phased antenna arrays whose purpose lies in electronically steering radio waves in our desired direction [10]. In this section we will take a close look at the different kinds of antenna arrays, the design challenges, research advances, design methodology and applications from the different publications, journals and other sources that we have used during our research that has led to the advancements of the work in our thesis.

2.2 CHALLENGES OF mmWave

When we step in the era of technology for 5G communication, specifically mm wave antenna arrays there are a few hurdles and difficulties that lie along the way. To begin with, two of the key motivators to dive into mmWave communication research are as follows [11, 12]. One being that to bolster up the service rate provided by heterogeneous networks at rates of Gb/s such as uncompressed video whilst the other is the prospect of possible mmWave communication in outdoors lie within our grasp due to the die to rapid development of hardware such as high gain element antennas, CMOS technology with good reliability etc. The difficulties comes in play when we consider that the free-space path loss is increased by 3dB

with twice the transmission frequency therefore sophisticated antenna designs are required in order to overcome the severe attenuation [13]. In addition to that we also need to take note that for mmWave communications between base station and access points they both will require to be in line of sight range as surrounding obstacles may dampen the performance drastically given that these wavelength of mmWave bands are extremely short and is an existing problem for high gain antennas operating at mmWave frequencies [14, 15]. The author in [14] has stated that in order to overcome such shortcoming previously mentioned we require a proper beam forming scheme; a vital aspect for all 5G technology and that must be applied for mmWave applications. Lastly, for operating the higher of frequency band size of antenna become smaller and become a many challenges for fabrication as was stated in [16]. All of these factors from free-space path loss to performance reduction due to obstacles and mmWave antenna design difficulties were some of the major challenges when it came to designing mmWave antenna array systems.

2.3 RESEARCH ADVANCES

Phased array antennas become much smaller and thinner as a result of today's state of the art MMIC technology. The frequency of phased array antennas have been reported reaching W-band [17] as well as the Ka-band [18] with the focus being those mainly on the radar applications and the next generation (5G) mobile communications where as ours would be intended for vehicular tracking. Over the last decade, many researches have been conducted to create low cost solutions for phased array communications such as the virtual phase shifter array dedicated to receive Ku-band satellite broadcasting TV signals containing 256 elements and the T/R module cost is less than \$20 per channel [19]. Up until now researchers have mostly been interested in developing mmWave antenna operating at 28 GHz as it is considered as one of the prospective bands for mm-Wave 5G smartphone applications [20]. In contrast, we aim to use our antenna array at an operating frequency of 60GHz after reading about the advancements made to phased array antenna design optimization that are discussed in [21]. In [21] the author outlines a method to determine the 3D antenna array pattern of the 60 GHz antenna array with the use of packet measurements and without disassembling the device or bypassing the antenna while integrated within an 802.11ad modem. With all of the information, advancements and knowledge previously mentioned and many other researchers' work that

will be discussed in the following sections we conducted our design simulation and testing of our phased array antennas.

2.4 DESIGN METHODOLOGY

In the beginning of our research for designing an antenna array we looked to [22] work which consisted of design of a 1X4 microstrip array antenna operating at 6.3GHz for C-band communication satellite application. Although our final design of the antenna differs largely from theirs given that we operate at a frequency ten times larger coupled with the fact we created a 2x2 microstrip planar array. However, the work mentioned in [22] has laid some of the groundwork for us and where our work initially started. For instance, we came to learn that the for antenna systems with beam steering capabilities are mostly composed of mechanical [23], electronical [24] and hybrid [25] beamshaping system and a phased array system such as ours will be using steering the beam by electronical means. Moving forward to the actual type of antenna design we had opted to design our base model for a microstrip patch antenna given their great development, both as single radiators and in array configurations as stated by [26]. Furthermore, it was also stated in [26] some of their limitations, such as low gain and low power handling capabilities, can be overcome by making use of array configurations which was perfectly matched the goals and objectives of our thesis. Lastly we have also utilized slot antenna arrays due to their planar structures, low cost, and easy feeding methods have been intensively which have been extensively studied in [27, 28, and 29]. After referring to all of these different books, papers and authors we began carried on with our design of the antenna array and made changes and improvements to our work along the way.

2.5 APPLICATIONS

Along the way of researching and studying about phased antenna array we came across many of their uses in unique and practical applications. One of the most interesting ones where the utilization of phased array for a beam steering fabric based parasitic antenna array is introduced for operation at around 4.4 GHz as demonstrated in [30]. As more space is available on different parts of the clothing or uniform of a person which can be used to host an array the wearable antenna array creates new opportunities for high-gain beam steering array antennas [31, 32,

33]. Their results have shown that utilized using conductive and nonconductive fabrics, conductive epoxy, and PIN diode switches to achieve 6.8-8.5 dBi gain and beam steering along three different directions. However there are some drawbacks with trying to utilize the wearable antenna array in high frequencies mainly being that it has been found that the shadowing from the user plays the major role in the performance of the mobile terminal antenna [34, 35]. Another very promising and often highly prioritized use of mmWave antenna array is the aforementioned 5G communications particularly for base stations such as the one mentioned in [36] where a phased-array antenna is designed to have a bandwidth of 3.4-3.8 GHz using a bow tie shaped antenna and achieving a -10dB reflection coefficient with elevation scan angles from -45 to +45 degrees and all azimuthal angles. They have used bow shaped antenna for its large impedance bandwidth and semi-infinite space for feed lines and electronics behind the antenna. Lastly one of the more unique applications that we have found so far consists of a circular phased antenna array has been constructed on the finger ring for 5G IoT applications operating at 28GHz [37] where they verified the antenna array in free space and in a user hand phantom for on three fingers. Their results showed a high coverage efficiency of 70% for 7dBi gain in free space however when user effects are introduced to the simulation setup a drop of 20% has been recorded nonetheless they maintained the same coverage efficiency curve shape for all three applications. After having seen all the various types and applications of antenna arrays we have decided to work on our 2x2 Microstrip 'key shaped' antenna array intended for the purpose of vehicle tracking at 60GHz as it is a relatively lightly touched concept at such high mmWave frequencies with vast potential and user application.

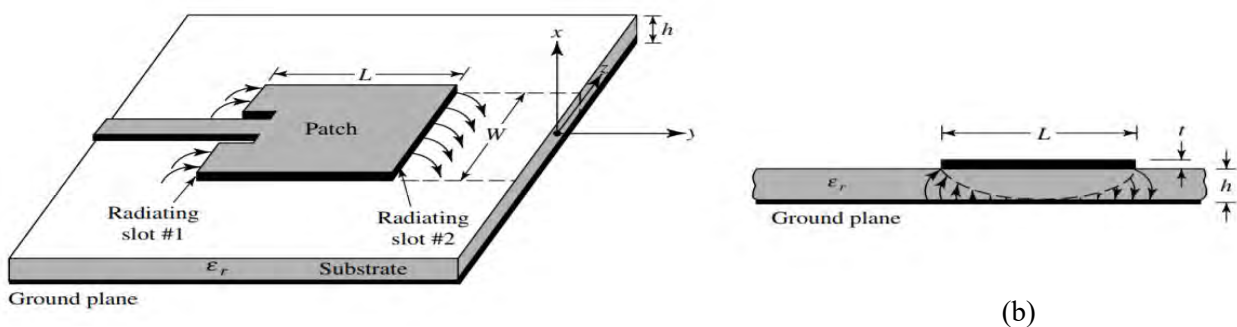
CHAPTER 3

Microstrip Patch Antenna

3.1 GENERAL OVERVIEW

Microstrip antenna, also commonly referred to as patch antennas have garnered a lot of use in the microwave frequency region due to being simple and easily printable on circuit board (PCB). It has now become an established type of antenna especially desirable when low profile radiators are in requirement. Since they are well matched with the printed circuit technology they are easy and cheap to fabricate both as single elements and arrays. They can be easily conformed to both planar and nonplanar surfaces and are mechanically strong and sturdy when attached to rigid surface. They are also adaptable when it comes to resonant frequency, polarization, pattern, and impedance when different patch shape and modes are selected. [6, 38]

A typical microstrip antenna is made from a patch of metal on top of a grounded substrate constructed using highly conductive metal. [4] The patch can be of any geometrical shape but rectangular and circular are the most common ones. The microstrip patch is designed such that its pattern maximum is perpendicular to the patch (broadside radiator). The patch and the ground are separated with a dielectric substrate. There are various different substrate materials to choose from with dielectric constant (ϵ_r) varying from 2.2 to 12. The effect of different substrate materials and thickness and their influence on the overall performance of the antenna will be explained later in the chapter. [6]



(a) Figure 23: (a) A simple Microstrip Patch Antenna (b) Side view [6]

As shown in the figure 1 above, the patch is of length L and width W . In case of rectangular patches, the length is generally $\lambda_0/3 < L < \lambda_0/2$ (where, λ_0 is the free-space wavelength). The thickness of the patch is also very small, $t \ll \lambda_0$. It is mounted on top of a substrate of thickness, h ($0.03\lambda_0 \leq h \leq 0.05\lambda_0$) and permittivity ϵ_r . [6]

3.1.1 ADVANTAGES AND DISADVANTAGES

Microstrip antennas have a wide range of benefits when paralleled to conventional microwave antennas. Therefore, they are coveted for many applications with frequencies ranging from ~ 100 MHz to ~ 100 GHz. Some widely recognized advantages and disadvantages of microstrip patch antenna are listed below. However, it is important to note that these are very much dependent on the mode of application. [39,40]

Advantages:

- It has thin profile.
- It is very light weight and has low volume.
- It is easy to fabricate, and is low in cost so can be produced in large quantities.
- It can be easily conformed to surfaces.
- It is supposedly inexpensive.
- It can be integrated into microwave integrated circuits.
- It can be used to readily create simple arrays.
- Both dual frequency and dual polarization antennas can be easily made.
- They support both, linear and circular polarization with simple feed.
- No cavity backing is required.
- Feed lines and matching networks can be fabricated simultaneously with the antenna structure.

Disadvantages:

- It has low efficiency.

- It has extraneous radiation from feeds, junctions and surface waves.
- It has narrow bandwidth and tolerance problems.
- It has low power handling capacity.
- It requires quality substrate and good temperature tolerance.
- Complex feed systems are required for high performance arrays.
- It is difficult to achieve polarization purity.
- Large ohmic loss in the feed structure of arrays.
- Most microstrip antennas radiate into half space.
- It is Difficult to achieve polarization purity.

3.1.2 APPLICATIONS

As it can be seen before, microstrip antennas do have some disadvantages. But their advantages greatly surpass the limitations. Primarily, it was military systems that widely used the application of these antennas in implementations stretching from missiles, rockets and aircrafts to satellites. However, presently their uses are growing more and more especially in the commercial sector as a result of their low cost and fabrication technology. Over time, due to progress of research and findings and improved usage they can possibly replace conventional antennas in most application. Some prominent uses of microstrip antennas are listed below.[39]

- Feed elements in complex and intricate antennas.
- Satellite communication, direct broadcast services (DBS).
- Doppler and radars of other kind.
- Radio Altimeters.
- Command and control system.
- Missiles and Telemetry
- Satellite navigation receivers
- Mobile radio (pagers, telephones etc)
- Biomedical radiators and intruder alarms
- Remote sensing and environmental instrumentation.

3.1.3 DIFFERENT TYPES OF MICROSTRIP PATCH

The geometric shape of the patch can be altered into many forms in order to optimize the performance of the antenna. Typically, the patches are cut out to be square, rectangular, thin strip (dipole), circular, elliptical, triangular or any other pattern. Being the easiest to analyze and manufacture as well as having desirable radiation characteristics square, rectangular, dipole (strip), and circular are the ones that are mostly used. [6]

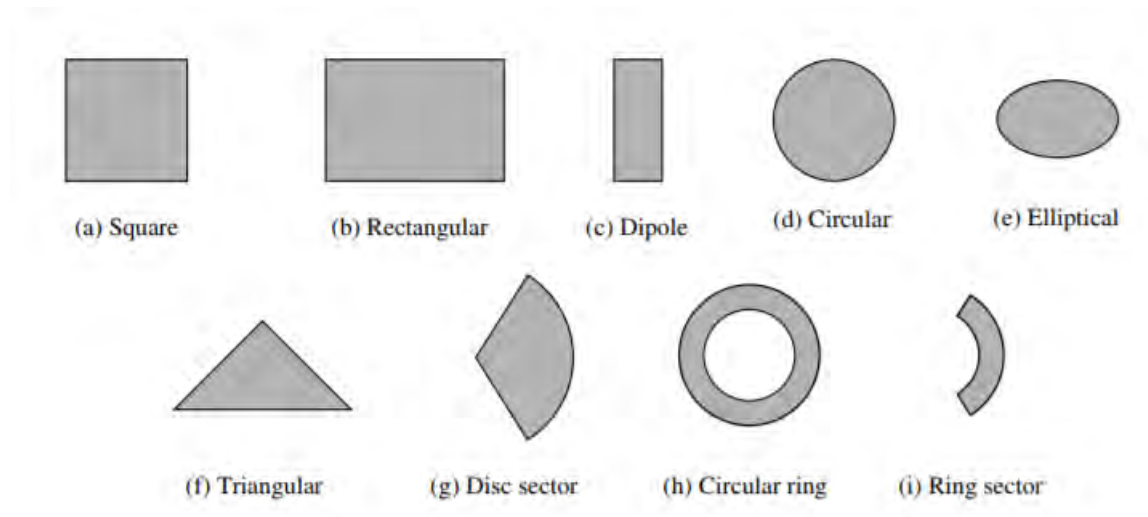


Figure: 24 Different shapes of the Microstrip Patch [6]

3.2 FEEDING METHODS

Microstrip patch antennas can be fed using many different feeding techniques. This process of feeding can be classified in to two categories:

- **Contacting:** In this assembly the RF power is fed directly into the radiating patch with the help of a connecting element such as microstrip line.
- **Non-contacting:** This structure allows the power to be transformed from the strip line to the patch by means of electromagnetic field coupling. [41]

Some of the most well-known feeding techniques are microstrip line, coaxial probe, aperture coupling, and proximity coupling. Different applications use different feeding techniques based on their requirements. One of the most popular feeding technique is the coaxial-line feed. Here, the inner conductor and the outer conductor of the coax is attached to the patch and ground

plane, respectively. It has the advantage of being easy to fabricate and simply matched by adjusting the position of the inset feed. However, it is more challenging in terms of modelling and has narrow bandwidth. Also having a narrow bandwidth, next is the aperture coupling which comprises two layers of substrate set apart by the ground plane. In order to allow independent optimization, the bottom substrate has a microstrip feed line whose energy is coupled to the patch via a slot in the ground plane. This method may not be the easiest to fabricate but is moderately easy to model. On the other hand, proximity coupling may be difficult to fabricate but it has the widest bandwidth and is also easy to model. This feeding technique basically makes use of two dielectric substrates. It is aligned such that the feed line is between the two substrates whereas the radiation element is placed on top of the upper substrate. And last but not the least, is the feed line method. It is basically a piece of conducting strip, smaller than the patch in terms of width. It has the advantage of being easy to fabricate, match and model. [6,38,41]

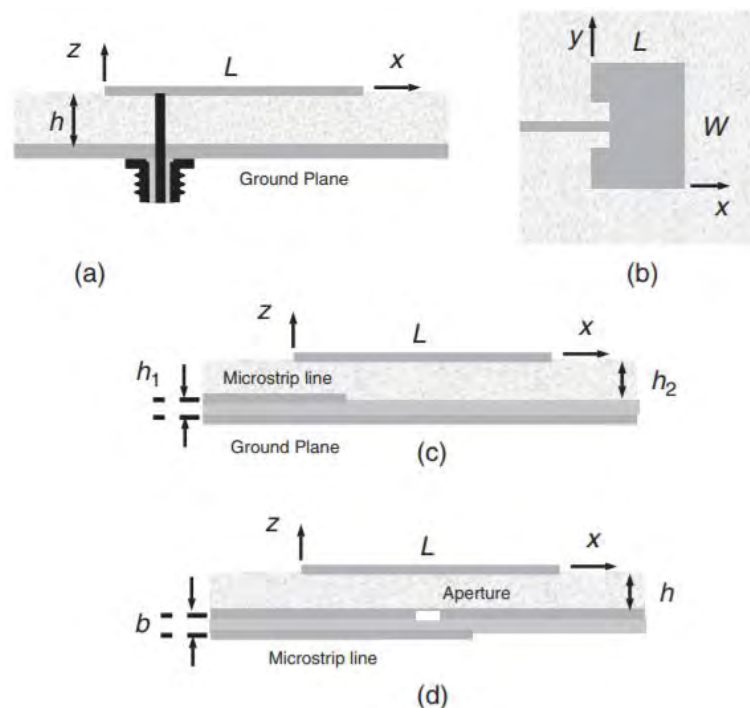


Figure: 25 Feeding Methods for Microstrip Antennas using (a) coaxial feed, (b) microstrip line inset feed, (c) proximity-coupled feed, and (d) aperture-coupled feed [38]

Table 1: Comparison of Various Types of Feed Techniques for Microstrip Patch Antennas
[39]

Characteristics	Co-axial probe feed	Microstrip line feed	Proximity coupled	Aperture coupled
Configuration	Non-planar	Co-planar	Planar	Planar
Spurious feed radiation	More	More	More	More
Polarization purity	Poor	Poor	Poor	Excellent
Ease of fabrication	Soldering and drilling required	Easy	Alignments required	Alignments required
Reliability	Poor due to soldering	Better	Good	Good
Impedance matching	Easy	Easy	Easy	Easy
Bandwidth (achieved with impedance matching)	2-5%	2-5%	13%	21%

For our thesis purpose we have used inset feeding technique with a quarter wave transformer feeding network. Since the typical feed line method produces a high input impedance the inset feeding technique is introduced. The current is supposed to be high in magnitude toward the center of the patch. As a result, the input impedance ($Z=V/I$) can be lowered if the feed line is brought near to the center.

The reduced input impedance is given as,

$$Z_{in}(R) = \cos^2\left(\frac{\pi R}{L}\right)Z_{in}(0)$$

Where R is the distance into the patch where the line is fed, L is the length of the patch and $Z_{in}(0)$ is the input impedance if the feed line was attached at the edge of the patch. [4]

The quarter wave transformer feeding network helps to match the impedance as well as reduce the energy which gets reflected back when the transmission line is attached to the load. It basically uses a different characteristic impedance with a length one-quarter of the guided-wavelength in order to match the line to the load.

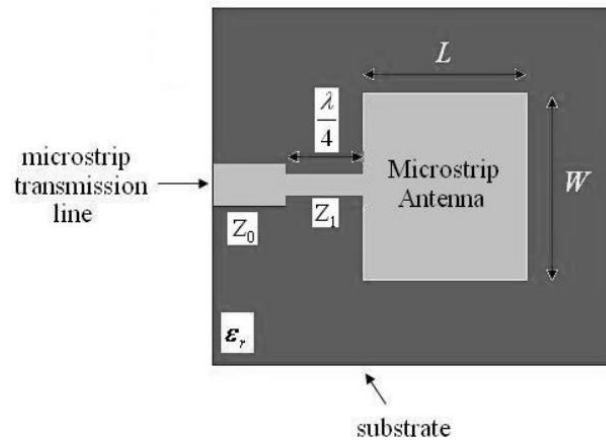


Figure: 26 Patch antenna with a quarter-wavelength matching section [4]

In order to match the input impedance (Z_{in}) to the transmission line (Z_0) the following equation can be used where, Z_A is the impedance of the antenna. [4]

$$Z_{in} = Z_0 = \frac{Z_1^2}{Z_A}$$

3.3 BASIC CONFIGURATION

3.3.1 METHODS OF ANALYSIS

Microstrip patch antenna have various methods of analysis but the most popular ones are transmission-line model, cavity model and full wave model. The transmission is known for being very easy and provide adequate physical insight. It can be used to calculate the parameters associated with microstrip patch antenna. However, the downfall to this model is that it does not provide much accuracy and it is very challenging to model coupling with this. It also has limited versatility. On the other hand, while the cavity model does provide more accuracy it is very complex. Although it has been known to be used successfully, similar to the

transmission line model it difficult to model coupling but gives good physical insight. Lastly the full wave method is the most accurate and can be used to treat single elements, finite as well as infinite arrays, stacked arrays etc. But it has the disadvantage of being the most complex and does not provide much physical insight [6].

3.3.2 RECTANGULAR PATCH ANTENNA PARAMETERS

The parameters of a rectangular patch antenna are what controls the properties of the antenna. These parameters include the length L, width W, permittivity and frequency.

Due to the finite length and width of the patch, the electric field at the edges of the patch experiences the fringing effect. Electrically, the patch of the microstrip antenna looks bigger than its physical measurements due to this fringing effect. The amount of fringing is influenced by the patch dimensions and substrate height. It is essentially function of the ratio of the length of the patch to the height of the substrate (L/h) and the dielectric constant of the substrate. For microstrip patch antenna this L/h ratio is supposed to be much greater than 1 which effectively reduces the fringing effect. However, it cannot be ignored since it affects the resonant frequency of the antenna.

An effective dielectric constant, ϵ_{reff} is established to account for the fringing and wave propagation, since the waves travel in both the air and substrate. The value of ϵ_{reff} ranges from 1 to the actual dielectric constant of the material (ϵ_r). If the value of the dielectric constant is much greater than one ϵ_{reff} would be very close to ϵ_r . ϵ_{reff} is a function of frequency; it remains constant for low values of frequency. At moderate frequencies it rises monotonically until it reaches the actual ϵ_r value at very high frequency. For $W/h > 1$, the effective dielectric constant ϵ_{reff} is given by the following expression,

$$\epsilon_{\text{reff}} = \frac{\epsilon_r + 1}{2} + \frac{\epsilon_r - 1}{2} \left[1 + 12 \frac{h}{W} \right]^{-1/2}$$

Also due to the fringing effect, the length of the patch gets extended on both side by ΔL as demonstrated in the figure below. An approximation of ΔL is given by,

$$\frac{\Delta L}{h} = 0.412 \frac{(\epsilon_{\text{reff}} + 0.3) \left(\frac{W}{h} + 0.264 \right)}{(\epsilon_{\text{reff}} - 0.258) \left(\frac{W}{h} + 0.8 \right)}$$

Since the extension occurs on both side the effective length is now calculated by,

$$L_{\text{eff}} = L + 2\Delta L$$

The actual length of the patch can then be calculated from the following,

$$L = \frac{1}{2f_r \sqrt{\epsilon_{\text{reff}}} \sqrt{\mu_0 \epsilon_0}} - 2\Delta L$$

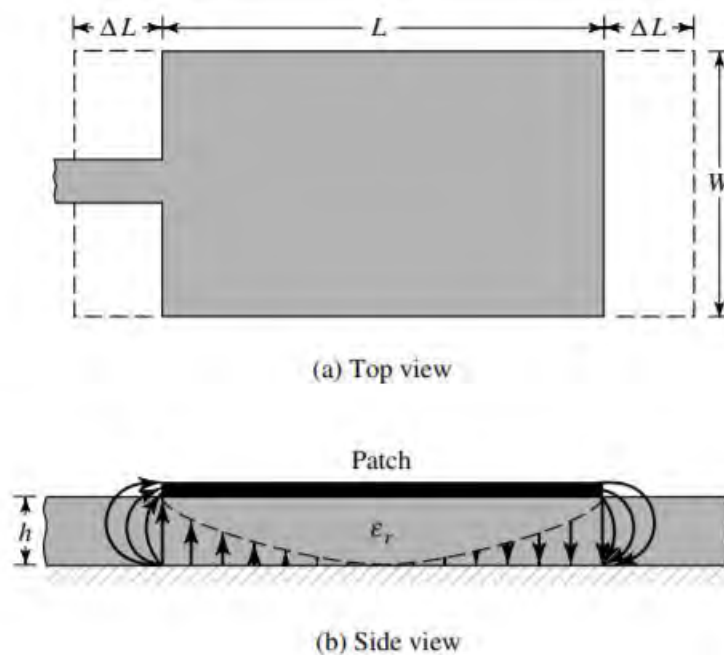


Figure: 27 Physical and effective lengths of rectangular microstrip patch [6]

Correspondingly, for efficient radiation, the width is given by the formula below. Here, v_0 represents the speed of light.

$$W = \frac{1}{2f_r \sqrt{\mu_0 \epsilon_0}} \sqrt{\frac{2}{\epsilon_r + 1}} = \frac{v_0}{2f_r} \sqrt{\frac{2}{\epsilon_r + 1}}$$

And lastly, a simple yet somewhat accurate formula for calculate resonant frequency is given by,

$$f_0 = \frac{c}{2(L+2\Delta L)\sqrt{\epsilon_r}}$$

Here the speed of light is denoted by c. [6]

3.3.1 CHARGE AND CURRENT DISTRIBUTION

The field distribution between the patch and the ground could possibly be used in order to determine the radiation of a microstrip antenna. Then again, the surface current distribution on the patch can also be used to define the radiation.

If the patch of the microstrip antenna is energized by supposedly connecting it to a microwave source, then this results in a charge distribution on the upper and lower surfaces of the patch and on the surface of the ground plane. This is shown in the figure below.

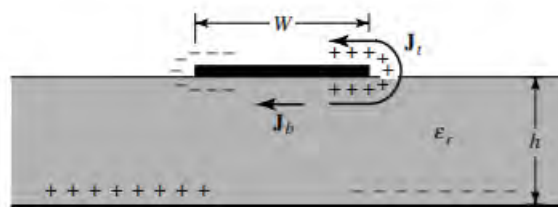


Figure: 28 Charge distribution and Current density of a Rectangular Patch [6]

The positive and negative charge distribution occurs because the patch is approximately half wave long at the dominant mode. Owing to the repulsive forces occurring between like charges, the charges that are positioned at the bottom of the patch push some of the charges to the top. Consequently, the current densities J_b and J_t are generated at both the bottom and top surfaces of the patch. However, the attractive forces between the charges is superior to the repulsive forces since the W/h ratio is pretty small. This results in most of the charge concentration and current flow to remain below the patch. Nonetheless, a small quantity of current does flow around the edges to the top surface and hence creates a weak magnetic field tangential to the edges.

Nevertheless, the patch can be demonstrated as a cavity with electric walls at the top and bottom surface and magnetic walls at the surrounding edges. This is only possible if a few simple approximations can be made such as, the tangential magnetic field mentioned before is zero due to being very weak. Although this stands to be certified for substrates with high dielectric constant. Another assumption to be made is that the field variations along the height is fairly constant and the electric field appears to be normal to the patch surface. Only TM modes are allowed in this cavity.

The four surrounding walls signify four slots which allows radiation to take place. These slots are represented by the equivalent current densities J_s and M_s , corresponding to the magnetic field, H_a and electric field E_a . For very thin substrates J_t at the top is much smaller than J_b at the bottom. So J_t and then similarly J_s are set to zero. Therefore, the only non-zero current density left is M_s at the periphery of the patch. As a result, the radiation from the patch can be recognized as four ribbons of magnetic current radiating in free space as shown in diagram below. [39]

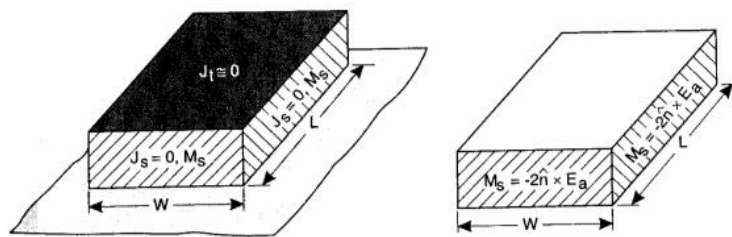


Figure 29: Equivalent Current density [39]

CHAPTER 4

Different Substrate Materials and Slot Antennas

4.1 SELECTION OF SUBSTRATE MATERIAL

Substrate is the base on which the antenna is fabricated. The substrate of the microstrip antenna is mainly needed for mechanical support and also affects the electrical performance of the microstrip antenna. So selection of the correct substrate material is crucial for the best results. Thus the first step in designing an antenna is to choose the right substrate material keeping the following factors into consideration[42]:

Criteria for selecting the right substrate material:

- Surface wave excitation
- Dispersion of the dielectric constant and loss tangent of the substrate
- Copper loss
- Anisotropy of the substrate
- Effects of temperature, humidity and aging
- Mechanical requirement such as conformability, machinability, solder-ability, weight, elasticity etc.
- Cost

4.1.1 SURFACE WAVE EXCITATION

Surface waves are generally excited when the relative permittivity ϵ_r of a substrate is greater than 1. The surface waves initiate in the substrate at an angle Θ which generally lies between $\pi/2$ and $\sin^{-1}(1/\sqrt{\epsilon_r})$. These surface waves hit the ground plane at the angle Θ and undergoes reflection. From here they strike the dielectric-air interface where they undergo total internal reflection and in this way they continue to travel in a zigzag pathway until they finally reach the boundaries of the microstrip structure. Here some of the waves are reflected back

while some are diffracted by the edges leading to end fire radiation. However on the way if the surface waves come across any other antenna it may lead to undesired coupling between array elements, affecting the performance of the array.

Surface waves are TM and TE modes of the substrate. The phase velocity of the surface waves is mainly dependent on the dielectric constant and the height of the substrate. The lowest order TM mode, TM₀ has no cut off frequency. However the cut off frequencies of the higher order modes TM_n and TE_n are given below:

$$f_c = nc/[4h(\sqrt{\epsilon_r}-1)]$$

Where c is the speed of light and h is the height of substrate. The cut-off frequencies for the TE_n modes are given by n=1, 3, 5 ... and the cut-off frequencies for the TM_n modes are given by n=0,2,4,6...

For TE_n mode:

$$\pi c(n) = c/f_c(n),$$

Therefore,

$$h/\pi c(n) = n/(4\sqrt{\epsilon_r}-1)$$

From this equation we can find out $\pi c(n)$ and therefore the corresponding frequency at which the TE_n mode will be excited for substrates of different height. However the height of the substrate should be chosen in such a way that the ratio of h/π_0 is well below $h/\pi c(n)$ where π_0 is free space wavelength at operating frequency.

$$h \leq c/(4f_u\sqrt{\epsilon_r}-1)$$

Where, f_u is the highest frequency in the band of operation

The value of h also has to be practical, something that is commercially available. Another practical formula for h is:

$$h \leq 0.3c/(2\pi f_u\sqrt{\epsilon_r})$$

Here h should be chosen as high as possible also keeping the limit in mind in order to achieve maximum efficiency[42].

4.1.2 DIELECTRIC CONSTANT

Dielectric constant is a measure of the permittivity of materials.

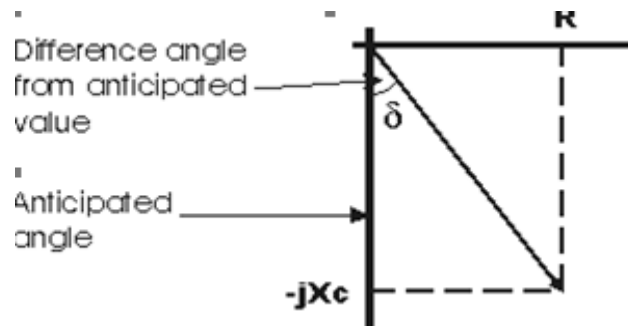
$$\text{Dielectric constant} = E/E_0$$

Where, E_0 is the permittivity of free space 8.854×10^{-12} F/m

There are many materials with dielectric constant usually in the range between $2.2 \leq E_r \leq 12$ that can be used for the substrate of the microstrip antenna. However the substrates should be chosen in a way such that it has a dielectric constant value that gives the most desirable antenna performance. A thicker substrate will not only give strong mechanical support but is also more desirable because it has lower dielectric constant. A low dielectric value of E_r will increase the fringing field at the edges of the patch thus improving the radiated power. Along with better radiation power, it will also improve the efficiency and provide larger bandwidth. However a thicker substrate with low dielectric constant value will increase the weight, dielectric loss, surface wave loss and extraneous radiation. On the other hand even though thin substrates with higher dielectric constant will reduce the size, weight and dielectric loss, these are achieved at the expense of reduced efficiency and bandwidth. Therefore while designing an antenna, standard practice requires a compromise between bandwidth and efficiency [42].

4.1.3 LOSS TANGENT

The dissipation factor also known as the loss tangent ($\tan \delta$) is the tendency of the dielectric materials to absorb some of the energy when signal is applied. It is the tangent of the difference of the phase angle between capacitor voltage and capacitor current with respect to the theoretical 90 degree value anticipated. This difference is caused due to the dielectric losses inside the capacitor[43].



Loss tangent plays a crucial role in antenna designing because it has a considerable effect on the gain and electrical performance of the antenna. A high loss tangent means the dielectric material is absorbing more energy thus increasing the dielectric losses and reducing the gain of the antenna. Other than reducing the gain it also increases the bandwidth of the microstrip antenna. Therefore increase in loss tangent degrades the performance of the antenna [43].

4.2 DIFFERENT DIELECTRIC SUBSTRATES

Properties of a few different substrate materials that were used to see how the performance of the antenna was affected is given below. A comparison of the difference in the radiation pattern is shown in another chapter.

4.2.1 RT- DUROID 5880

RT-Duroid 5880 is a PTFE (polytetrafluoroethylene) compound strengthened with Glass Microfibers. Due to the randomly oriented microfiber RT-Duroid has a uniformly distributed dielectric constant of 2.2. This extremely low value for dielectric constant efficiently lessens any losses related to it, as a result making it perfectly apt for designing micro strip antennas. Apart from that, this material is isotropic and very easy to work with during the fabrication process. It also tends to have a low moisture reabsorption and exceptional chemical resistance. The RT Duroid substrate has a low loss tangent of 0.0004 and presents high tensile strength. It has a dissipation factor of 0.0012. It also exhibits a volume resistivity of 2×10^7 Mohm.cm and surface resistivity of 3×10^7 Mohm[45,47].

4.2.2 ARLON AD-270

Arlon AD 270 is one of the lower cost substrates under the Arlon's AD series. This collection consists of PTFE (polytetrafluoroethylene) complex compound that has been toughened with woven fiberglass. As a result, the resultant materials comprise both the reduced electrical loss properties of a PTFE material as well as the worth of lower-cost and more affordable fibre glasses suitable for commercial purpose for high volume use. Having a suitably low dielectric constant of 2.7 allows for effectively reduced losses. Apart from that it exhibits high stability over a variable range of frequency making it a good choice for RF applications. AD 270 has a dissipation factor of 0.0023 and thermal conductivity of 0.235 W/mK. Apart from that, the material has a water absorption of 0.07%. The volume and surface resistivity of the materials are 1.2×10^9 Mohm.cm and 4.5×10^7 Mohm respectively[46].

4.2.3 FR4 GLASS EPOXY

FR4 is composite material made from reinforcing woven fiberglass with an epoxy resin. The epoxy gives the material its flame resistive characteristics it is well known for. The FR in FR4 stands for "Flame Retardant". This thermoset plastic shows very low water absorption making giving it its excellent insulating properties. Its mechanical and insulating properties are renowned for being retentive in all considerable conditions. Apart from that FR4 material also show high stability with very little shrinking and high tensile and electrical strength. FR4 Glass Epoxy have dielectric value of 4.36 and therefore exhibit enhanced loss properties. The dissipation factor of this material is 0.017. The loss tangent of this material is 0.013. The volume resistivity of the material is 8×10^7 Mohm.cm and its surface resistivity is 2×10^5 Mohm[44,47].

4.3 SLOT ANTENNAS

We introduce the concept of slots in our micro strip antenna in an attempt to improve our overall performance of our antenna array versus a normal array. They are normally used for frequencies ranging from 300 MHz to 25 GHz or higher and are largely popular for their nearly omnidirectional radiation pattern and obtaining a significantly large bandwidth. The slot size, shape and what is behind its (the cavity) offer design variables that can be used to tune

performance. Slot antennas are an about $\lambda/2$ elongated slot, cut in a conductive plate and excited in the centre. We have conducted several experiments and simulations of various shaped slot antennas like the ones below but unfortunately they could not provide adequate results showing noticeable improvement over our normal rectangular microstrip and had eventually reached a final design (the key antenna) that meets all of our required needs when used in our antenna array [4,6].

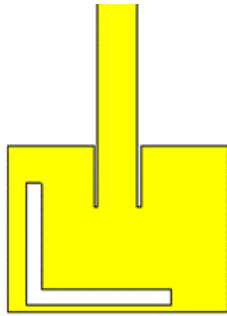


Figure: 30(a) Shaped Slot Microstrip Antenna

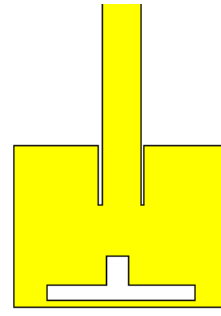


Figure: 30 (b) T Shaped Slot Microstrip Antenna

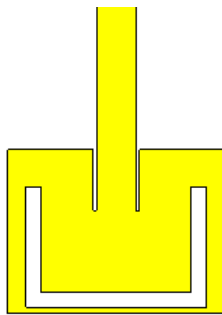


Figure: 30 (c) U Shaped Slot Microstrip Antenna

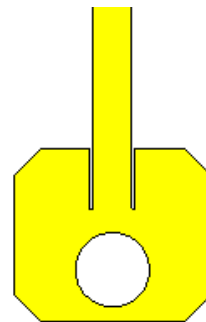


Figure: 30 (d) Circular slot key shaped microstrip Antenna

CHAPTER 5

Phased Array Antenna

5.1 GENERAL OVERVIEW

Phased array antennas are composed of mainly groups of individual radiating elements. They are distributed and oriented in either linear or two-dimensional spatial configuration whose amplitude and phase excitations of each element can be individually controlled resulting in producing a radiated beam of any desired shape in space. By adjusting the phase of the excitation signals at the individual elements we are able to electronically control the position of the beam. Therefore involvement of mechanical motion unnecessary in the scanning process while the antenna aperture remains unchanged and thus it is referred to scanning without inertia [38, 48, 50].

5.1.1 ADVANTAGES OF PHASED ARRAYS

A key feature to be noted about phased arrays is that its capability of rapid and accurate beams scanning in microseconds permits the system to multitask whether it be interlaced in time or simultaneously. For instance, an electronically steered array radar would be able to track a large number of targets and illuminate some of them with radio frequency energy for the purpose of guiding missiles towards them. The above mentioned radar system can also perform hemispherical searches paired with automated target selection and hand-over to tracking. Alongside that it can also be utilized in communications systems, directing high gain beams towards transmitters and receivers in the distance while allowing for complete flexibility. Search and track rates may be adjusted to meet the particular within the limitations set by the total use of time. The antenna beamwidth may be changed electronically by sacrificing gain for greater coverage of areas by means of phase spoiling. Electronically controlled phased-array antennas can give the flexibility needed to perform all the various functions in a way best suited to the specific task at hand. The functions can be programmed rapidly and accurately with digital beam steering techniques[38].

5.1.2 THEORY OF PHASED ARRAYS

To begin our discussion of phased arrays let us take a look at the most simplest configuration: an array of isotropic elements equally spaced along a line. What we will observe is that by taking a look at this simple linear array we will be equipped with the knowledge to understand the framework of more complex array theory. For instance, one may design a two-dimensional array by utilizing the interconnection of linear arrays. In order to make matters less complex we will be taking a few assumptions in consideration namely[38].

- The far-field region of the antenna which is defined by ranges of R that must satisfy

$$R \geq \frac{2L^2}{\lambda}$$

Where L is the largest dimension of the antenna and λ is the operating wavelength of interest. In this region the antenna pattern is insensitive to range except for scale factor of $1/R^2$ in power which is usually ignored.

- We will be using the reciprocity theorem to a great extent to justify the array far-field Analysis from either the transmission or the receiving viewpoint for convenience. The theorem dictates that the pattern of both transmission and reception will be the same so long as no nonreciprocal devices come into play and if such devices exist one may use pattern analysis to neglect their presence.
- For simplicity, interest will be restricted to the responses of arrays to continuous wave (CW) signals.

5.2 DIRECTIVITY OF ANTENNA ARRAYS

In order to explain the concept of directivity of antenna arrays let us take a look at the following figure. For an antenna that has a power density of $S(\theta, \Phi)$ and consisting of a directional pattern we may define the directivity of the antenna $D(\theta, \Phi)$ so that the power density maybe defined in a specified polarization at some distant spherical surface a distance R_0 as given below,

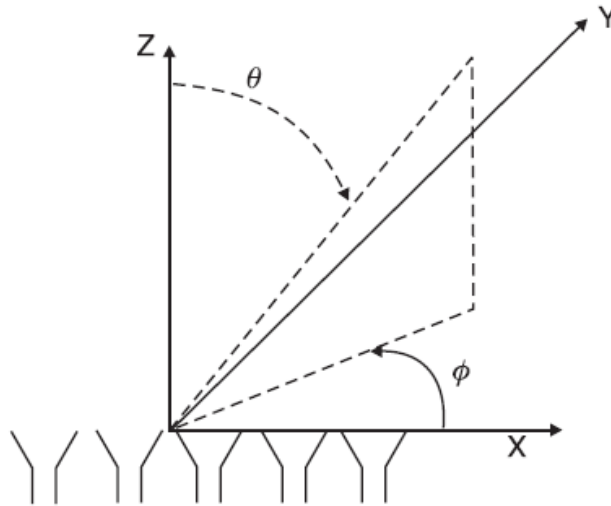


Figure 31: Array and Co-ordinate systems [49]

$$S(\theta, \Phi) = \frac{PradD(\theta, \Phi)}{(4\pi R^2)}$$

So that,

$$D(\theta, \Phi) = \frac{4\pi R^2 S(\theta, \Phi)}{Prad}$$

Or,

$$D(\theta, \Phi) = \frac{4\pi S(\theta, \Phi)}{\int_{\Omega} S(\theta, \Phi) d\Omega}$$

Where the last integral is over the solid angle that includes all of the radiation and is generally referred to as

$$\int_{\Omega} S(\theta, \Phi) d\Omega = \int_0^{2\pi} d\Phi \int_0^{\pi} d\theta S(\theta, \Phi) \sin\theta$$

The expression above is the definition of directivity and implies that the power density used is the total in both polarizations. In the absence of a specified direction (θ, Φ) then the directivity implied is the maximum directivity denoted as,

$$D_0 = \max [D(\theta, \Phi)]$$

Which is a very important parameters for antennas with narrow beamwidth. Directivity is the most important quality of antenna pattern given that it is derived only from the pattern shape. The radiated power is less than the input power P_{in} by an efficiency factor ϵ_L , which accounts for circuit losses, and by the reflected signal power

$$P_{rad} = \epsilon_L P_{in} (1 - |\Gamma|^2)$$

Where Γ is antenna reflection coefficients measured at the feed transmission line and therefore signifies the importance of defining array parameters that relate to that of measurable parameters at the input transmission line [49].

5.3 ARRAY FACTOR

The Array Factor is a function of the positions of the antennas in the array and the weights used. The antenna array's performance may be optimized by tweaking these parameters to achieve desirable properties. For instance, the antenna array can be steered (change the direction of maximum radiation or reception) by changing the weights. The topic will be described in more specific details later but in order to provide a general idea we take a look at the in the following example. Let us consider that N identical elements oriented in the same direction with each radiation pattern given by $R(\theta, \Phi)$ and assume that element i is located at position given by

$$R_i = (x_i, y_i, z_i)$$

Now let's say that the signals from the elements in the antenna array are each multiplied by a complex weight (antenna array element weight) followed by summation to form the phased array output, Y .

Based on the angle of arrival of an incident plane wave, we may observe a varied output of the array. In this manner, the array itself is a spatial filter - it filters incoming signals based on their angle of arrival. The output Y is a function (θ, Φ) , the arrival angle of a wave relative to the

array. In addition because of the concept of reciprocity if the array is transmitting, the radiation pattern will be identical in shape to the receive pattern. Y can be written as:

$$Y = R(\theta, \phi)w_1e^{-j\mathbf{k}\cdot\mathbf{r}_1} + R(\theta, \phi)w_2e^{-j\mathbf{k}\cdot\mathbf{r}_2} + \dots + R(\theta, \phi)w_Ne^{-j\mathbf{k}\cdot\mathbf{r}_N}$$

Where \mathbf{k} is the wave vector of the incident wave. The above equation can be factor simply as:

$$\begin{aligned} Y &= R(\theta, \phi) \sum_{i=1}^N w_i e^{-j\mathbf{k}\cdot\mathbf{r}_i} \\ &= R(\theta, \phi) AF \end{aligned}$$

$$AF = \sum_{i=1}^N w_i e^{-j\mathbf{k}\cdot\mathbf{r}_i}$$

Where AF is the array factor. [4]

5.4 RADIATION PATTERN OF ANTENNA ARRAYS

Let us consider the elementary array (figure:32), consisting of N isotropic elements, equally spaced at a distance d apart. On receive, if a plane wave is incident upon the array from a direction making an angle θ with the array normal, the current in the n th element will be of the form,

$$i'_n = A e^{jnk d \sin\theta}$$

Where, A is a complex constant related to the instantaneous amplitude and phase of the plane wave and k is the wave number:

$$k = \frac{2\pi f}{c} = \frac{2\pi}{\lambda}$$

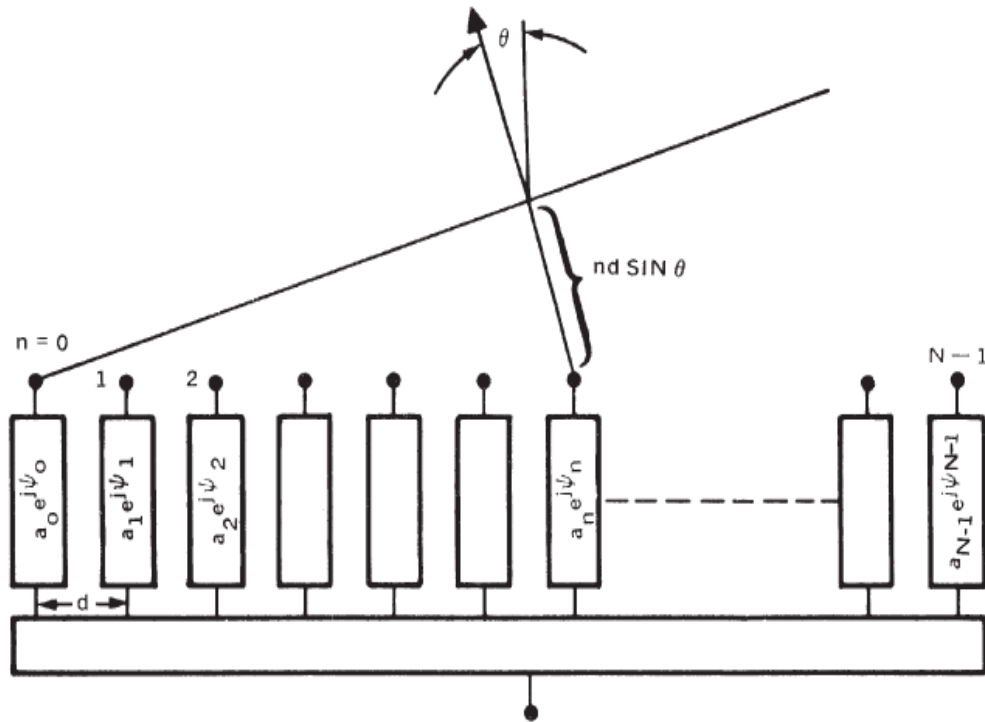


Figure 32: Basic Linear Array Configuration [38]

Where,

f = operating frequency

c = velocity of light

The above equation mentioned in the first assumption shows that the current in the n th element leads that in the $(n + 1)$ th element by a phase shift given by $\Delta y = kd \sin \theta$. This phase shift corresponds to the difference in time of arrival t of the plane wave front of $t = d/c \sin \theta$. If we place a control element behind each radiator, as indicated in Figure (2), with a transfer coefficient for the n th element given by,

$$\frac{i''_n}{i'_n} = a_n e^{j\psi_n}$$

Where, a_n and ψ_n are the real current gain and phase shift of the control element, respectively, the summing network produces an output,

$$|E_a(\theta)| = \sum_{n=0}^{N-1} a_n e^{j(\psi_n + nkd \sin \theta)}$$

The constant A in i_n is now neglected. This relationship gives the response of the array of Figure 32 to a signal arriving from a direction q in terms of the set a_n 's and Ψ_n 's. The set of coefficient is usually called the array amplitude taper, while the Ψ_n 's are called the phase taper. The expression of above is called the array factor. To combine the received signals from all the radiators in phase to produce a maximum response in the scan direction of q_0 , the Ψ_n 's must have the form,

$$\psi_n = -nkd \sin \theta_0$$

This expression shows that the required phase taper across the array aperture is a linear taper (constant phase differential between adjacent radiators). On transmit, when the phases of the control elements such as phasers are set to the phase taper of above, the signals radiated from all the elements will add up in phase to produce a main beam in the direction of q_0 . Hence, the array factor of E_a is the same for both transmit and receive. Substituting the above equation into its predecessor, we have for the array factor [38]

$$E_a(\theta) = \sum_{n=0}^{N-1} a_n e^{jnk d (\sin \theta - \sin \theta_0)}$$

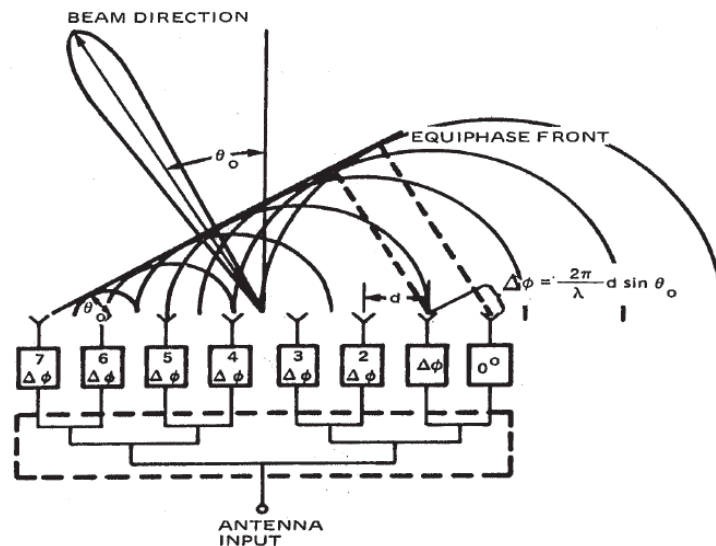


Figure: 33 Linear phased array antenna [38]

5.4.1 RADIATION PATTERN OF PLANAR ARRAYS

A planar array of radiating elements is used when it is necessary to perform beam scanning in two angular dimensions. When it comes to a spherical coordinate system, coordinates θ and Φ

the beam position as shown in the figure below which also displays the element lattice layout in the planar array. For a rectangular lattice, the m th element is located at $x_m=md_x$ and $y_n=nd_y$. By requirement of that the $(m+n)$ be even one can define the element locations [38].

If we were to sum the vector contribution of each element in the array at every point in space the array factor of a two dimensional array may be calculated. We can write the array factor in direct terms of cosines $\cos\alpha_x$ and $\cos\alpha_y$ of the spherical coordinate system as follows:

$$E_a(\cos\alpha_x, \cos\alpha_y) = \sum_m \sum_n i_{mn} e^{jk(md_x \cos\alpha_x + nd_y \cos\alpha_y)}$$

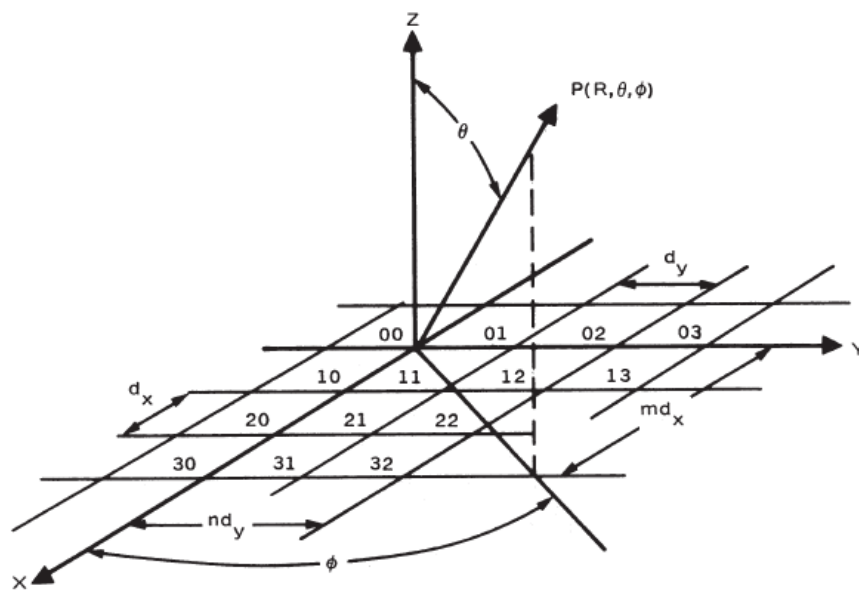


Figure 34: Planar Array Configuration [38]

Where,

$$\cos\alpha_x = \sin\theta\cos\Phi$$

$$\cos\alpha_y = \sin\theta\sin\Phi$$

For a uniformly illuminated ($i_{mn}=1$) rectangular array, we have

$$E_a(\cos\alpha_x, \cos\alpha_y) = \sum_{m=-(M-1)/2}^{(M-1)/2} e^{jkmd_x \cos\alpha_x} \sum_{n=-(N-1)/2}^{(N-1)/2} e^{jknd_y \cos\alpha_y}$$

Each sum can be evaluated producing a result for a uniformly illuminated linear array

$$E_a(\cos\alpha_x, \cos\alpha_y) = \left[\frac{\sin\left(\pi M \frac{d_x}{\lambda} \cos\alpha_x\right)}{M \sin\left(\pi \frac{d_x}{\lambda} \cos\alpha_x\right)} \right] \left[\frac{\sin\left(\pi N \frac{d_y}{\lambda} \cos\alpha_y\right)}{N \sin\left(\pi \frac{d_y}{\lambda} \cos\alpha_y\right)} \right]$$

We can obtain beam scanning with planar arrays by linear phasing along both array coordinates. Therefore, in order to scan the beam to the angular position corresponding to the directional cosines $\cos\alpha_x$ and $\cos\alpha_y$ we introduce a linear phase taper at each element so that the excitation at the m th element is given by,

$$i_{mn} = a_{mn} e^{j(kmd_x \cos\alpha_{x0} + knd_y \cos\alpha_{y0})}$$

Where,

$Kd_x \cos\alpha_{x0}$ = element to element phase shift in the x direction

$Kd_y \cos\alpha_{y0}$ = element to element phase shift in the y direction

This form of steering phase indicates that the phase of the m th element is the sum of a row phase $m k d_x \cos\alpha_{x0}$ and a column phase $n k d_y \cos\alpha_{y0}$.

The array factor of a rectangular planar array of M by N elements is then given by

$$E_a(\cos\alpha_x, \cos\alpha_y) = \sum_m \sum_n a_{mn} e^{jk[m d_x (\cos\alpha_x - \cos\alpha_{x0}) + n d_y (\cos\alpha_y - \cos\alpha_{y0})]}$$

5.5 GRATING LOBES VERSUS ELEMENTAL SPACING

The array factor of

$$E_a(\theta) = \sum_{n=0}^{N-1} a_n e^{jnk d (\sin\theta - \sin\theta_0)}$$

can also be expressed in terms of the variable $n = \sin\theta$ as follows:

$$E_a(v) = \sum_{n=0}^{N-1} a_n e^{jnkd(v-v_0)}$$

Where the beam direction v_0 is related to the different phase $\Delta\psi = -kdv_0$. We can observe that $E_a(v_0)$ and $E_a(\theta)$ are related by a one-to-one mapping in the region where $|v| < 1$ referred to as the visible real space corresponding to real angles of θ . Alongside that another thing to keep note of is that $E_a(v)$ is a periodic function of v of period [38].

$$\frac{2\pi}{kd} = \frac{1}{d/\lambda} = \frac{\lambda}{d}$$

The equation is in the form of a Fourier series representation, which is readily analyzable and simple to visualize. The maxima of $E_a(v)$ occur whenever the argument of Eq (9) is a multiple of 2π , for instance, $kd(v-v_0) = 2i\pi$ where $i = \dots -2, -1, 0, 1, 2, \dots$ or

$$v_i - v_0 = \frac{i}{d/\lambda}$$

Now if $v_i = v_0$ or $i=0$ the maximum is often referred to as the principal lobe (PL) aka main beam whilst the other maxima is called the grating lobes (GL) from the corresponding phenomena with optical gratings. When it comes to the design of phased antenna array it is of utmost importance that the grating lobes be eliminated within the visible space since these lobes reduce the power in the main beam and thus reduce the antenna gain, and introduce unwanted signals and noise. This means that the element spacing d must be chosen to avoid the grating lobes. Therefore the elemental spacing d must be chosen such as to avoid the grating lobes over the range of v from -1 to $+1$ and as the main beam is scanned to v_0 the nearest grating lobe to the visible space is positioned at $v_i = v_0 - \lambda/d$. The grating lobe will only appear in visible space at the end fire direction of the array when $v_0 \cdot \lambda/d = -1$ or,

$$\frac{d}{\lambda} = \frac{1}{1 + \sin |\theta_0|}$$

Therefore the element spacing required for maximum scan angles θ_{\max} is

$$\frac{d}{\lambda} < \frac{1}{1 + \sin |\theta_{0\max}|}$$

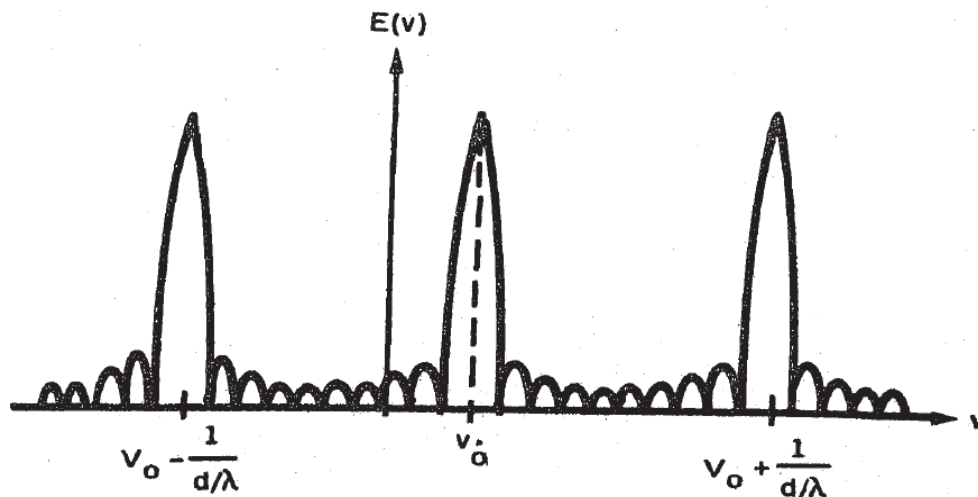


Figure 35: Grating-lobe formation [38]

5.6 GRATING LOBES VERSUS ELEMENTAL SPACING

The selection of an element to be utilized for phased array must be based upon the following considerations [38]:

1. The required area of the element is small enough to fit within the allowable element spacing and lattice without the formation of grating lobes. In general, this limits the element to an area of a little more than $\lambda^2/4$.
2. The Scan Element Pattern of the element provides the appropriate aperture matching over the required scan coverage.
3. The polarization and power handling capability (both peak and average power) meet the system requirements.
4. The physical construction of the element must be able to withstand environmental requirements such as thermal, shock, and vibration requirements.

5. The element must also be inexpensive, reliable, and repeatable from unit to unit since many hundreds or thousands of elements are required in a large phased-array antenna.

CHAPTER 6

Phase Shifters

6.1 INTRODUCTION

Phase shifters are essentially a two port device that are a fundamental component in numerous RF and microwave systems. The basic function of this device is to make changes to the transmission phase angle of the RF signal. In ideal cases, phase shifters produce output signal of equal amplitude to the input signal at all phase states, with little to no attenuation. [51] This indicates only the phase of the signal gets affected by the phase shifters, and no other changes are made between the input and output signals. Phase shifters are used extensively in applications such as satellite communication, phase modulators, microwave measurement systems, phase cancellation, power combining and much more. [38,52] While their areas of use are vast, perhaps their most essential use are for the designing of phased array antenna for radars. In these designs, the phases of each of the elements of the antenna are controlled in order to conform the electromagnetic wave at a specific angle to the array.

The phase delay that is applied between the input and output ports of the device is called insertion phase. The job of the phase shifter is to provide an adjustable insertion phase to the path of the microwave signal without varying the length of the actual path. A generic two port phase shifter is shown in Figure 36.

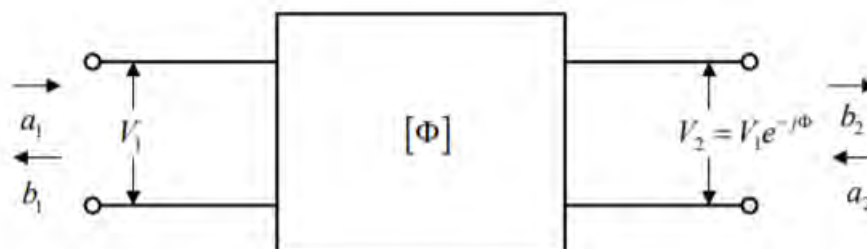


Figure 36: A generalized two port phase shifter [51]

For an ideal phase shifter, no losses would occur. In such case, if the input signal to the device is denoted by V_1 and the insertion phase by Φ , then the signal at the output port represented by V_2 would be equal to $V_1e^{-j\Phi}$. [51]

6.2 TYPES OF PHASE SHIFTERS

Based upon the configuration of the phase shifter selected the phase angle of the input signal is controlled. Different structured phase shifters are classified into different types based on the properties they possess. Some of these classifications are made depending on the method by which they are controlled, i.e. by electrically, magnetically or mechanically. Others are grouped in terms of type of transmission media and the technology of fabrication. A few of these groupings are explained below.

Mechanical Phase Shifters

Mechanical phase shifters are controlled manually. They are appropriate for high power application due to their preferably low insertion losses. They are normally constructed within the transmission line structure. The phase shift is applied with the help of a tuning mechanism such as physically regulating a knob in order to adjust the physical length of the line. Mechanical phase shifters are known to be analog and reciprocal. Their fabrication is painlessly easy and inexpensive due to their simple yet effective design. [51]

Electronic Phase Shifters

Electronic phase shifters fall under the same classification as Mechanical phase shifters i.e. based on their control mechanism. However, unlike mechanical phase shifter these devices are controlled electrically with the help of voltage controlled networks. Although these phase shifters are not as easy to fabricate as their mechanical equivalents they make up for it by working at a much quicker rate as a result of their electrically controlled tuning mechanism. Electronic phase shifters also prove to be comparably more beneficial than the mechanical ones on account of having rapid phase shifting capabilities. [51]

Analog Phase Shifters

In analog phase shifters, the change in phase are controlled through tuning of the voltage level. The phase control in these devices are continuous allowing the phase to be set at any value, which proves to be greatly advantageous to the digital kind. Analog phase shifters happen to have an insertion phase transfer function. As a result, any desirable phase shift can be obtained with the help of the information from the there. However, one thing to be cautious of when handling analog phase shifters is that they are extremely responsive to very slight tuning changes of the input voltage. An apparent advantage of this device is that it has lower cost of parts. [53] Although it may be cheaper, the assembly may be difficult and highly complex. Since the analog phase shifters are not quite receptive to computer interface or any digital controlling system they have to be functioned with the help of appropriate voltage leveling circuitry.

Digital Phase Shifters

These phase shifters are controlled digitally via programming or with the help of a computer interface. Unlike the analog phase shifters, these devices are not continuous instead they have a selected number of allowed states. Therefore, it cannot produce any random value of the insertion phase. 'Phase bits' lead to the production of the discrete phase states. This discretization may lead to quantization errors. The highest order bit starts with 180 degrees, the next being 90 degrees, then 45 degrees and so on. [54] In direct contrast to its analog counterpart, these devices show very little sensitivity to slight deviations in voltage. This means the insertion phase is mostly unresponsive to any faint changes to voltage regulations. One good advantage of this device is that it shows high immunity to noise on control lines. It is also easier to assemble and is not as sensitive as the analog devices. [53]

Reciprocal and Non-Reciprocal Phase Shifters:

Reciprocal phase shifters are not sensitive to direction. They can be used in both directions. Since the phase shift in the direction of transmission and reception is the same no changing of phase states are required. input and output ports are switchable (scattering parameter $S_{21}=S_{12}$, $S_{13}=S_{31}$, etc.)

On the other hand, for non-reciprocal phase shifters switching is required between the transmission and reception since the phase shift is not equal. For practical use, non-reciprocal phase shifters provide random phase and amplitude features. [53]

Active and Passive Phase Shifters:

An important feature of passive phase shifters is that they are lossy, it causes the signal to attenuate while phase shifting. These devices comprise no additional energy source to enhance the input signal; as a result, the power at the output port is smaller or equal to the power inputted at the ports.

On the other hand, complementary to the passive devices, active phase shifters amplify the signal during phase shifting. Additional energy sources somehow add to the magnitude of one or more responses.[53]

Ferrite Phase Shifters:

Ferrite phase shifters' principle of operation depends on the interaction between dipoles in ferrite materials and electromagnetic waves. This interaction can be controlled by modifying the strength of the bias field.

Ferrite phase shifters are dominating the section of phased arrays due to their useful features which includes having fast rise time, a 360-degree phase shift etc. Ferrite phase shifters can be either reciprocal or non-reciprocal.

For ferrite material, the permeability can be varied by changing M , where M represent the magnetization or magnetic moment. As the biasing strength of the magnetic field increases M reaches saturation level, where losses are not as high.

The phase shift is given by,

$$\Delta\phi = 2\pi\sqrt{\epsilon} \left[(\mu'_+)^{1/2} - (\mu'_-)^{1/2} \right] L/\lambda$$

Where μ' denotes the real part of the permeability and ϵ is the dielectric constant of the ferrite. Here L represents the length of the ferrite section.

When the frequency of the magnetic field equals f_m , where $f_m = \gamma H$ ($\gamma = 2.8$ MHz/Oe is the gyromagnetic constant), ferrimagnetic resonance occurs. As a result, the opposite polarized waves get different values of permeability, μ'^+ and μ'^- . [38]

Integrated Circuit Phase Shifters

When compared to Ferrite phase shifters, IC phase shifters have practically better features. Made from semiconductor components, constructed using GaAs, SiGe as well as InP these phase shifters have made exceptional advancement over the years in terms of design, functionality, weight and cost. [38] They have reasonably smaller size and lower power consumption which allows them more prospective opportunities. IC phase shifters can be classified into many categories such as Hybrid IC or MIC, Monolithic Microwave IC phase shifters and the much newer technology based phased shifter using BST and RF MEMS.

6.3 TOPOLOGIES FOR IMPLEMENTING PHASE SHIFTERS

There are various topologies for employing phase shifter such as high-pass/low-pass and all-pass network, loaded line, reflective type, switched transmission line and a few more. Some of these topologies are explained below.

6.3.1 HIGH- PASS/ LOW- PASS

The phase shift in High-pass/Low-pass phase shifters are presented with the help of variable reactance connected in series or shunt across the transmission line. The variable reactance is achieved due to using lumped elements like capacitors and inductors. The high-pass filter structure in π configuration contains of series capacitors and shunt inductors which causes the insertion phase to experience a phase advance. On the other hand, the low pass filter is made up of series inductors and shunt capacitors which allows for a delay in the insertion phase. [55, 56]

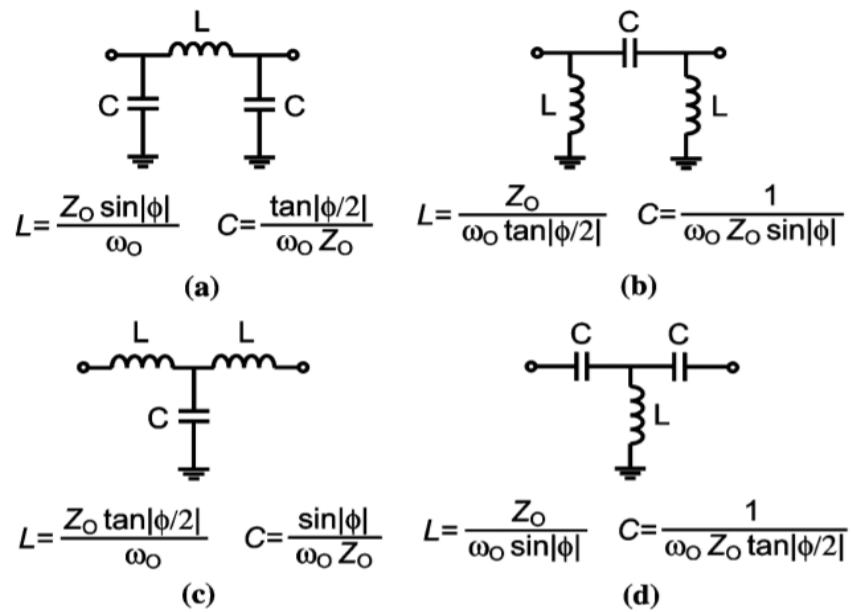


Figure 37: Schematic for High-pass/Low-pass Pi and T model [57]

The phase shift is attained by switching between the filters. These switching can be implemented using either PIN diodes or MESFETs. However, PIN diodes are preferred since they provide easier biasing and have lower cost. [56]

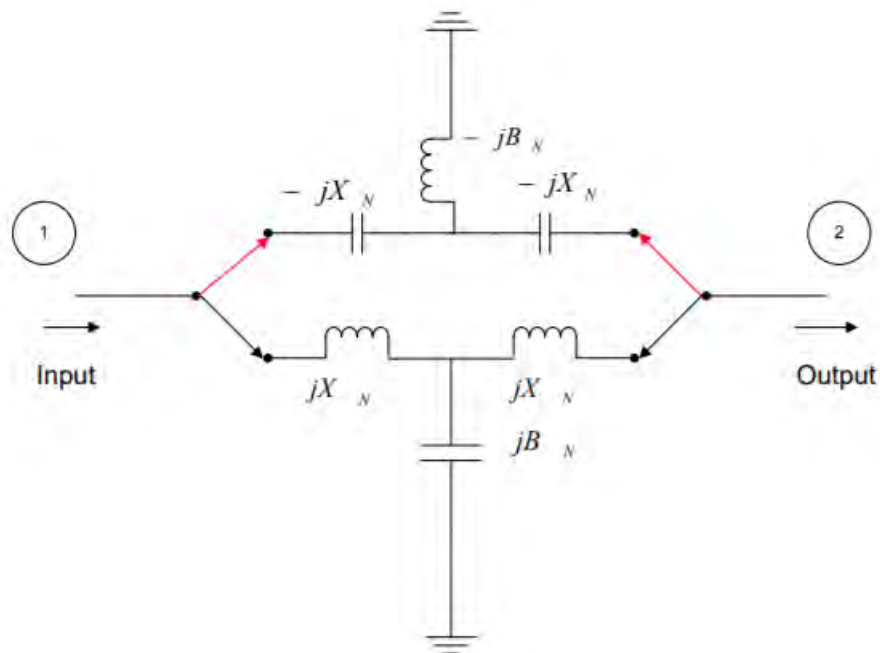


Figure 38: T-model High-Pass/Low-Pass Phase Shifter [55]

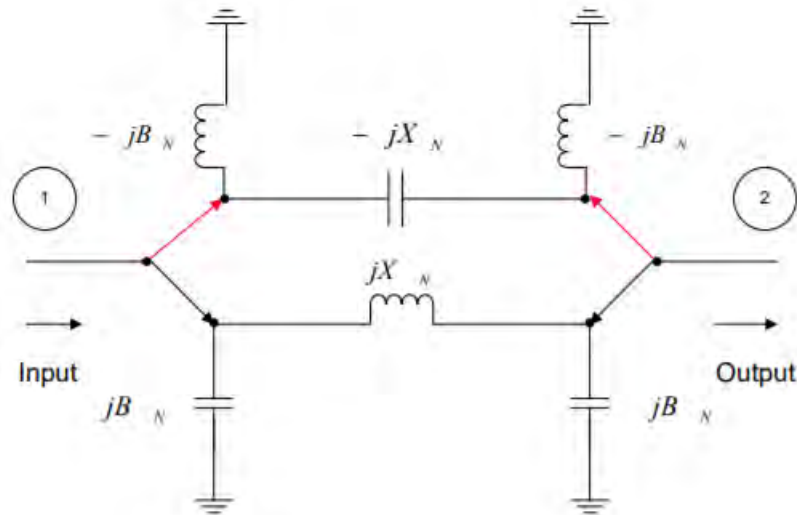


Figure 39: Pi-model High-Pass/Low-Pass Phase Shifter[55]

An advantage of High-Pass/Low-Pass phase shifters is that it provides a compact size and better bandwidth. A compact design is achieved since lumped elements are used in place of delay lines. As a result, they are far more useful than the other phase shifters where there are restrictions in size, like those used in satellites.[53]

6.3.2 LOADED LINE PHASE SHIFTERS

These are another type of phase shifters useful for achieving 22.5° to 45° of phase shift. In these designs, each end of the transmission line is connected to a pair of switchable reactive load.

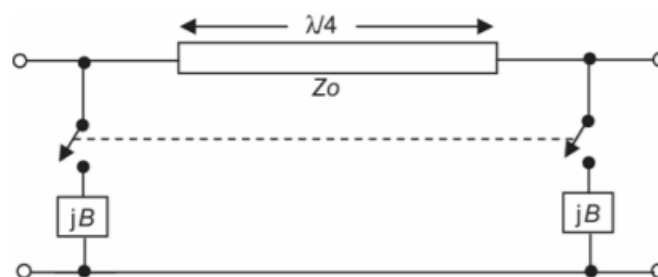


Figure 40: Loaded-line Phase Shifters[38]

The job of the second shunted load is to create a reflection, in order to at least partially cancel the reflection that is created by the first shunted load. These loads are separated with a distance of one-quarter wavelength.

The phase velocity decreases when the reactive load is capacitive and increases when it is inductive. Characteristically, loaded line phase shifters are narrow-banded, with a constant phase shift versus frequency response.

After equating the ABCD matrix of the Figure:40 above with an equivalent section of transmission line with electrical length θ_L radians and characteristic impedance Z Ohms as shown below

$$\begin{pmatrix} 1 & 0 \\ jB & 1 \end{pmatrix} \begin{pmatrix} 0 & jZ_0 \\ j/Z_0 & 0 \end{pmatrix} \begin{pmatrix} 1 & 0 \\ jB & 1 \end{pmatrix} = \begin{pmatrix} \cos(\theta_L) & jZ \sin(\theta_L) \\ j \sin(\theta_L)/Z & \cos(\theta_L) \end{pmatrix}$$

We get,

$$Z = Z_0 / [1 - (BZ_0)^2]^{1/2}$$

$$\theta_L = \cos^{-1}(-BZ_0)$$

However, for lower size maintained circuits the line length is generally in the order of $\lambda/8$ as a result limiting the minimum frequency of operation. [38]

6.3.3 SWITCHED LINE PHASE SHIFTERS

The Switched line phase shifter is essentially a time delay device. SPDT switches allow for switching between transmission lines all with different path lengths. One of the two transmission lines is characterized as the “reference” line, and the other as the “delay” line. The amount of phase shift is mostly dependent on the length of the line used.

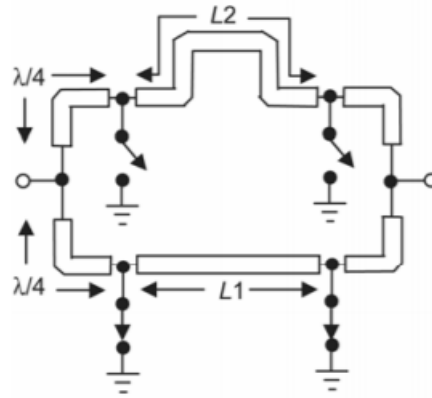


Figure 41: Switched-line Phase Shifters [38]

The difference in phase shift is given by,

$$\Delta\phi \approx \beta (L2 - L1)$$

where β is the propagation constant of the transmission line (here, β equals radian frequency ω divided by the phase velocity, v_p) [38]

6.3.4 REFLECTION- TYPE PHASE SHIFTERS

These phase shifters generally contain two impedance elements, a 3-dB hybrid coupler and a switch. The two impedance elements are connected across the two ports of the hybrid coupler via a single pole, single throw (SPST) switch. [61]

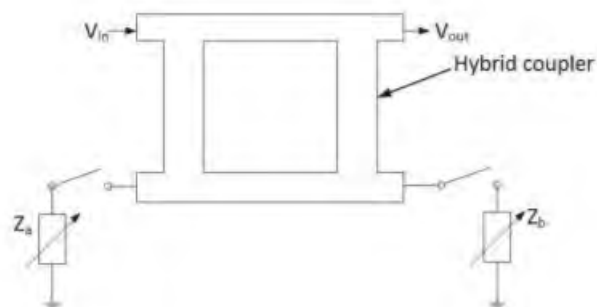


Figure 42: Reflection-type Phase Shifters [61]

6.4 PHASE SHIFTERS PARAMETERS

Parameters like center frequency of operation, bandwidth, insertion loss, VSWR or return loss, transient response, phase shift error, amplitude imbalance, power handling capabilities and size are only some of the criteria for judging the electrical performance of a phase shifter. It is very important to know these requirements for proper selection of the device.

6.4.1 PHASE ERROR

Phase shifters are attached to each element of the array antenna where their job is to shift the phase of the input signal to a specified angle. However, practically there exists error which results in loss of amplitude of the signal.

Assuming the phase errors are distributed uniformly over the range $[-\Delta\phi_{\max}, \Delta\phi_{\max}]$. Then the result amplitude loss due to the phase error is given by

$$L_{\Delta\phi} = \frac{\sin \Delta\phi_{\max}}{\Delta\phi_{\max}} \quad \text{or} \quad L_{\Delta\phi}(\text{dB}) = \left| 20 \log \left| \frac{\sin \Delta\phi_{\max}}{\Delta\phi_{\max}} \right| \right|$$

However, it is to be noted that there is no net phase shift of the real composite signal as a result of the phase error. [38]

6.4.2 INSERTION LOSS

Insertion loss, which is described as the loss of the signal power due to the addition of phase shifters in the transmission line, is ideally supposed to be zero. However practically, that is not the case; nevertheless, it should be kept to a preferably low value. Insertion losses are dependent on bit value, temperature and frequency. The larger is the operating bandwidth the more significant is the variation in insertion losses. Insertion losses also tend to be different for different phase shifters due to production dispersion of mechanical, microwave and magnetic parameters. [60]

If the power transmitted to the load before insertion is given by P_T and the power received by the load after insertion is given by P_R , then the insertion loss is calculated using the following, [58]

$$IL(\text{dB}) = 10 \log_{10} \frac{P_T}{P_R}$$

6.4.3 TRANSIENT RESPONSE

All phase shifters are characterized by their different transient response time or switching speed. As the resultant beam from the antennas are caused to change direction, due to the finite response time of the phase shifters, it causes the beam pattern to evolve.

It is seen that the beam direction can be switched using two modes: parallel or serial. In parallel mode, which is more desirable than the serial, the changes in phase settings are made simultaneously but since different control voltages have to be applied the change in phase do not take effect at the same time. In serial mode, as the name suggests, the settings are altered serially, i.e. one by one indicating a far longer switching time. For both processes, there is a resultant change in direction of the beam but at the stake of having a shape evolution of the pattern. The switching also causes distortion and loss.[59]

6.4.4 AMPLITUDE VARIATION

As it was previously stated that the phase shifters are supposed to produce an output signal that is of equal amplitude to the input signal. But that only occurs idyllically. Since it is practically impossible to provide all the ideal conditions required, there will be some changes in amplitude of the RF signal. This disturbance exists as a function of frequency. Amplitude variation may result in problems in the distribution of amplitude for beam steering.

CHAPTER 7

Beam Steering

7.1 INTRODUCTION

There are many numerous applications that calls for a need to control the direction of signal radiation. For operations at millimeter wave frequencies there are distinctive challenges that arise as a result of the propagation characteristic such as high free space path loss, absorption due to atmospheric gases, objects, rainfall etc. These challenges stand to be much bigger obstacles when long distances are concerned. Which is why it has become imperative that antennas are designed to produce highly directive radiation pattern in order to evade these obstacles and maintain the link with other nodes in a network. This is achieved through beam steering. [61]

Beam steering basically entails veering the beam to the desired direction in order to reduce the power dissipated in unwanted direction while sustaining high gain. In other words, it is all about redirecting the direction of the main lobe of the radiation pattern. It is essential for improving the signal reception in a specific direction. Not only that, it also helps to reduce the level of interference as well as enhance the systems performance. Moreover, it reduces the power used in transmission by focusing the radiation towards a specific direction.

7.1.1 APPLICATIONS OF BEAM STERING

Apart from communication purposes there are a lot other infrastructural applications that require the use of phased array antennas and their ability of beam steering. Some of these countless number of applications include low Earth orbiting communications satellite constellations and collision warning radar. Other space applications counting civilian space applications, comprise synthetic aperture radar and satellite communications. Apart from that,

beam steering is also well known for its illustrious commercial applications which include Intelligent Vehicle Highway System or Automated Highway System and other on-the-move applications, where the beam of the antenna needs to be steered towards the transmitter or receiver. However, one of the most predominant use of beam steering may possibly be military radar and tracking platforms. Other military applications include missile defense, space surveillance and last but not he the least ground-based systems for early warning radar. It may also be used for normal detection and tracking, traffic control smart base station antennas for WLAN and cellular communication. [38]

7.2 MECHANICAL VERSUS ELECTRONIC BEAM STEERING

7.2.1 MECHANICAL BEAM STEERING

Mechanical beam steering involves physically manoeuvring the radiating antenna in a specific direction. Mechanical steering is typically executed by turning the antenna with the help of electric motors. The array antenna which utilizes mechanical rotating antenna elements is known to have greater flexibility in controlling the direction of steering. Not only that, it also allows for beam focusing in the near field region by rotating the antenna elements so that they all point to one direction. Mechanical steering successfully provides constant gain in most beam directions by consequently altering the direction of each individual antenna elements. Recently, MEMS technology have made an appearance in order to apply mechanical steering. A lot of work has been done with this since it allows for improved speed of scanning as well as comparatively low loss of the system. It also permits fabricating mechanical moving antenna at low cost through batch process. However, mechanical steering fails to be effective when deliberating features such as antenna size, weight and weather conditions. They are also susceptible to mechanical failure due to wearing and overworking. There is also limitation to static or very slow changing environments due to constraints in steering speed. To overcome these drawbacks, it is would be an economically smarter choice to use the electronic method of beam steering. [61,62]

7.2.2 ELECTRONIC BEAM STEERING

On the other hand, the electronic method uses the application of phase shifters attached to antenna arrays to redirect the signal radiation without any need for mechanically guiding the antenna. In electronic beam steering, it is possible to electronically alter the phase of the radiating element in order to redirect the beam. As a result, a changed pattern is created without mechanically turning any part.

Electronic beam steering is proficient at steering the beam effectively, with minimum side lobes and adeptly narrow beam widths. It is also beneficial for its high directivity and fast steering due to electronic circuitry. Electronic beam steering has become an attention-grabbing subject in recent years because of the small size, speed, and compatibility with new applications in comparison to mechanical beam steering. The electronic method has many advantages over mechanical steering. Some are listed below: [63]

- Agility
- Accuracy
- Flexibility
- Greater speed due to flexible electrical control of the main beam
- System less prone to wear and tear since no physical movement is involved
- More durable

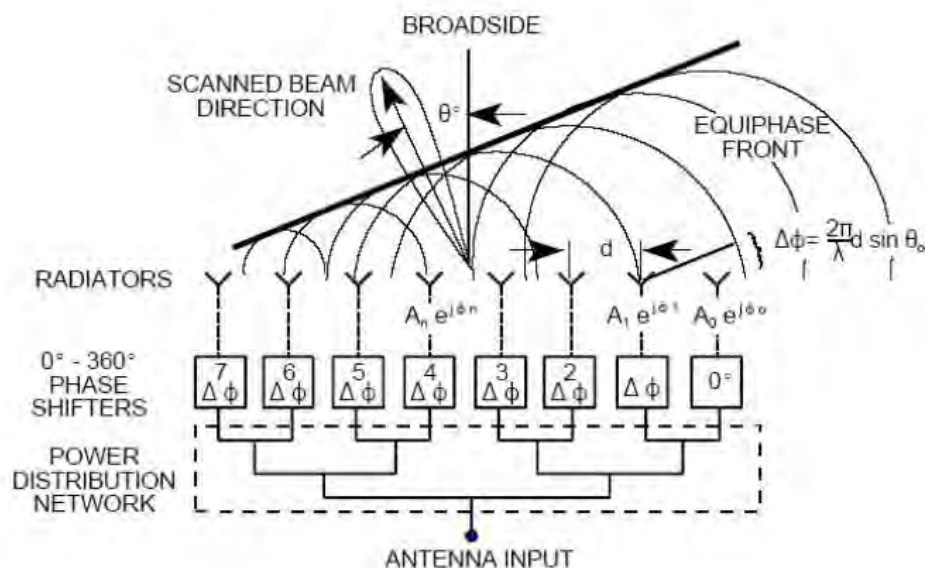


Figure 43: Beam Steering system using phase shifters [38]

Figure 1 above shows a schematic demonstration of beam steering which is achieved using phased array antenna. Let us assume the uniformly spaced linear array is spaced with a distance d as shown in the figure. The wavefront is roughly planar if it is presumed that the array is in the far field of the received signal. Provided that the signal arrives from an angle θ of the antenna boresight, then the wave has to travel an additional distance $d\sin\theta$ to arrive at each successive element. This delay in arrival in terms of phase shift is given by,

$$\Delta\phi = 2\pi f\Delta t = 2\pi d \sin \theta / \lambda$$

In order to steer the array to a desired angle θ_0 we must choose $\Delta\phi_0$ such that $\Delta\phi - \Delta\phi_0 = 0$. Since the phase shift is fixed, λ becomes a fixed λ_0 and $\Delta\phi_0$ is given by the equation below. Here λ_0 is the wavelength the phase shift is based on. For any other wavelength $\Delta\phi - \Delta\phi_0 \neq 0$. [64]

$$\Delta\phi_0 = 2\pi d \sin \theta_0 / \lambda_0$$

As indicated it consists a power distribution network, phase shifters and antenna elements. The job of the power divider is to split the input microwave signal in order to feed each of the radiating element. Next, the phase shifters are positioned former to the radiating elements. The size of the phase shifter is a significant factor here. When phased arrays with few number of elements are created it is not a major concern but when it comes to making huge arrays with a great many elements it puts a constraint on the size. This is especially concerning for two-dimensional phased arrays that are to be steered. Then the size has to be restricted to within the spacing length between the antenna elements. Compactness is also required in order to prevent any influence on the coupling due to parasitic effects. Henceforth, the phase shifters have to be as small as possible to be able to be incorporated into the arrangement. [65]

7.2 CRITERIONS FOR BEAM STEERING

While using phased array antennas a few factors have to be kept in mind in order to optimize the steering for the best results. Some of these factors are listed below: [61]

- Insertion loss
- Steering range
- Steering resolution
- Steering speed
- Complexity
- Size
- Cost

Insertion loss

With losses like free space loss, attenuation due to obstacles and other additional losses already adding up insertion loss from the addition of phase shifters would become a concerning factor. A high insertion loss would considerably worsen the performance of the overall system since a lot of power at the transmission line would be lost. If insertion loss could be kept to a minimum it would ensure better energy conservation. Therefore, phase shifters with considerable low insertion loss should be given preference.

Steering Range

This term refers to the maximum deviation away from the bore sight direction that it is possible to steer. The steering range vastly depends on the radiating element. More specifically, it is the type of antenna that is to be used in the array that affects the performance. Therefore, the literature review of different antenna types and their radiation pattern has to be known.

Steering Resolution

This indicated the step change that can be attained while steering within the range. This can be continuous, predefined or fine. Continuous specifies that all steering angles can be achieved, whereas predefined directs to step resolution greater than 20° . And finally, fine signifies an change of 2° or less. For millimeter wave frequencies a fine steering technique is necessary for maintain the connection between antennas in constantly changing environment. With a limited

steering resolution once the antenna moves away from the predefined steering angle, the connection would be lost.

Steering Speed

This term explains how quick the beam steering can be performed. This term decides the sensitivity of the beam steering and if it is more apt for dynamic or static environment. For on the move applications it is significant to have a high steering speed.

Size

It is basically the size of the system that determines what application is it most appropriate for. Evidently if the system is huge and bulky it cannot be used for communication purposes. Similarly, satellites call for small and light systems.

7.3 OTHER TECHNIQUES OF BEAM STEERING

Phased array is not the only system that is able to perform beam steering. Apart from the mechanical method there are other techniques that were able to successfully steer the radiation pattern in the desired direction. Some of these techniques are listed below: [61]

- Reflectarray
- Parasitic steering
- Integrated lens antennas (ILAs)
- Switched beam antennas
- Traveling wave antennas
- Retrodirective antennas
- Metamaterial Antennas

CHAPTER 8

Simulation and Results

8.1 RESULTS FROM SIMULATION

8.1.1 SINGLE KEY ANTENNA

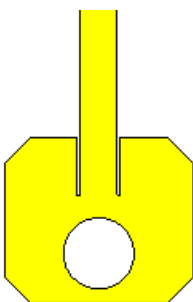


Figure 44: Key shaped Antenna

Driven by the intriguing thoughts of vehicle tracking and application for 5g communication, we have designed a key shaped antenna that can be incorporated inside the key of a car for tracking purposes.

Table 2: Key Antenna Parameters

Parameter	Dimension (in mm)
Substrate Width	2.05
Substrate Length	2.32
Substrate height	0.11
Patch Width	1.52

Patch Length	1.16
Feed Line Width	0.18
Feed Line Length	1.37

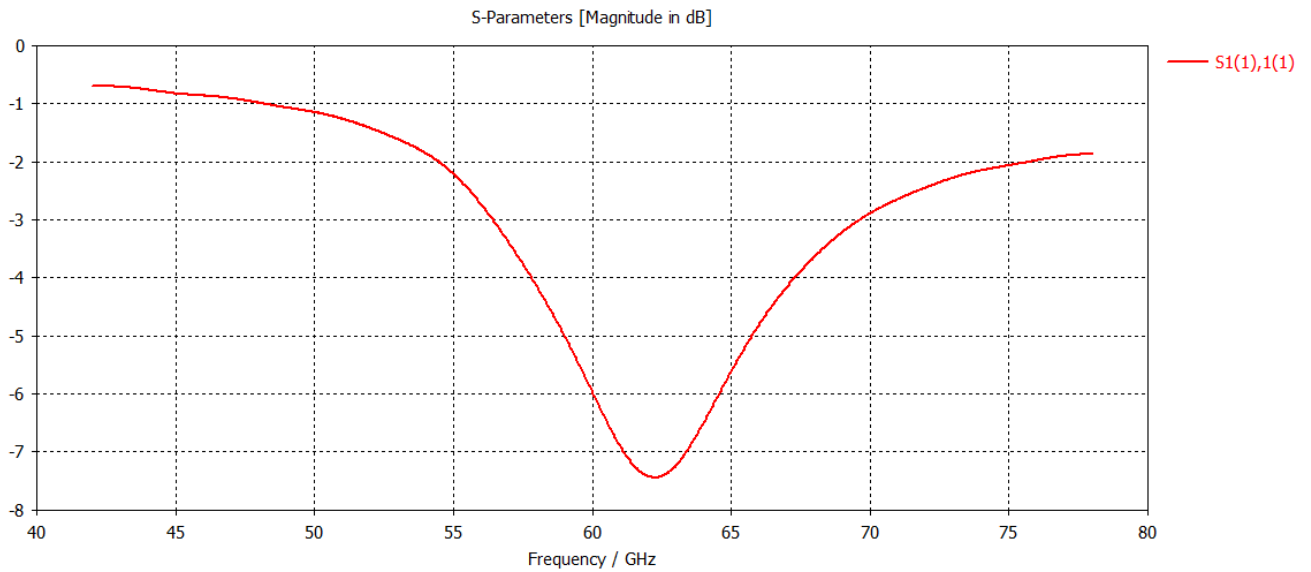


Figure 45 : S Parameters for microstrip key antenna at 60 GHz

Here the S parameter signifies the return loss of the antenna to be at around -6 db at our desired frequency. Our main basic objective was to make the antenna work at 60 GHz. Any S parameter that has a magnitude of more than -10 dB is a very good return loss of that antenna.

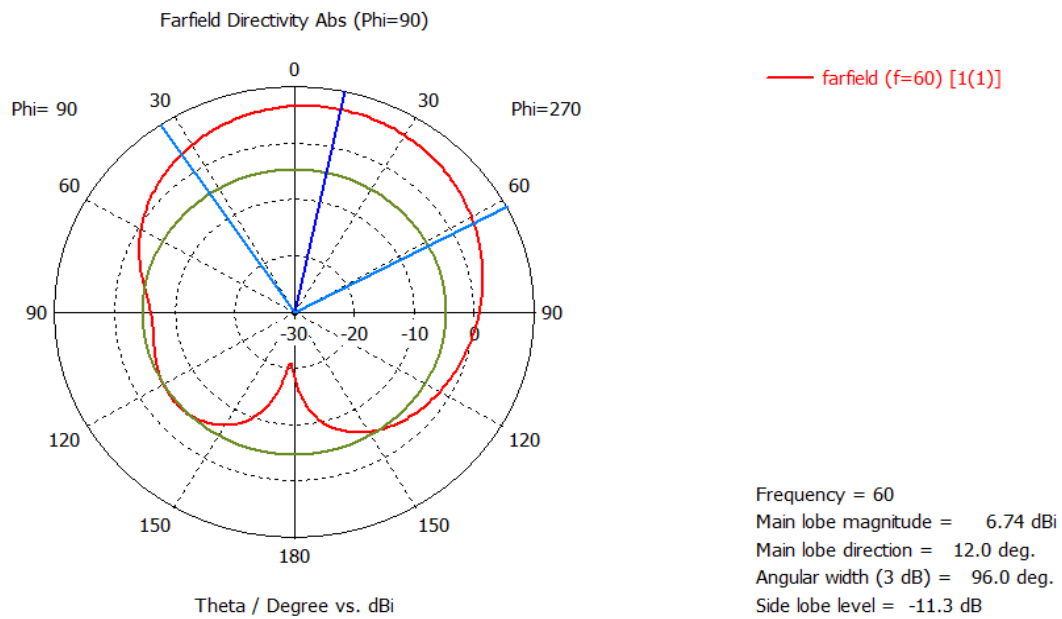


Figure 46: Polar plot of key antenna

From the polar plot of our key antenna we can observe that the main lobe has a magnitude of around 6.74 db. And the side lobe level is considerably good as it attains a value of -11.3 dB.

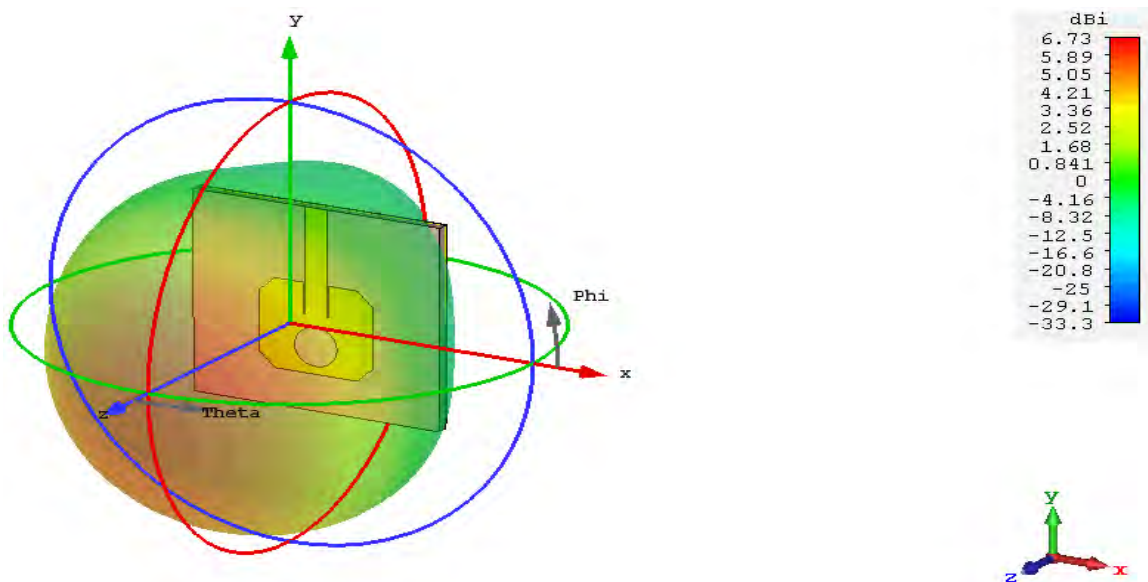


Figure 47: 3D farfield directivity pattern of key antenna

From our key antenna design we were able to yield a directivity of 6.73 db. It is considered to be a very good directive radiation pattern when compared to others.

8.1.2 SINGLE MICROSTRIP ANTENNA

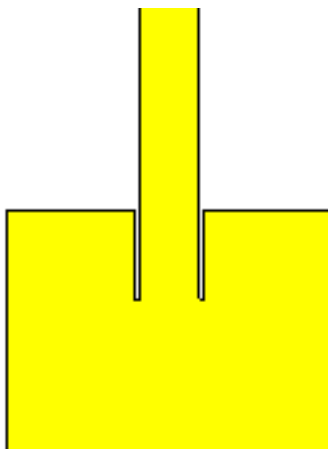


Figure 48: Microstrip antenna

Table 3: Microstrip Antenna Parameters

Parameter	Dimension (in mm)
Substrate Width	2.05
Substrate Length	2.32
Substrate height	0.11
Patch Width	1.52
Patch Length	1.16
Feed Line Width	0.18
Feed Line Length	1.37

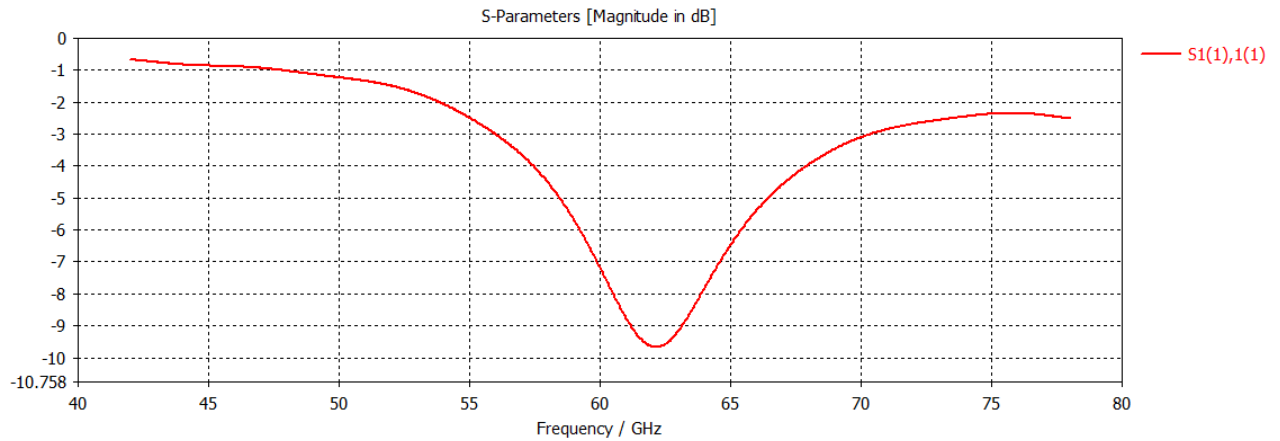


Figure 49: S Parameters for microstrip antenna at 60 GHz

From our observation we can see that the normal microstrip antenna has a return loss of around -7.5 db at the 60 GHz level.

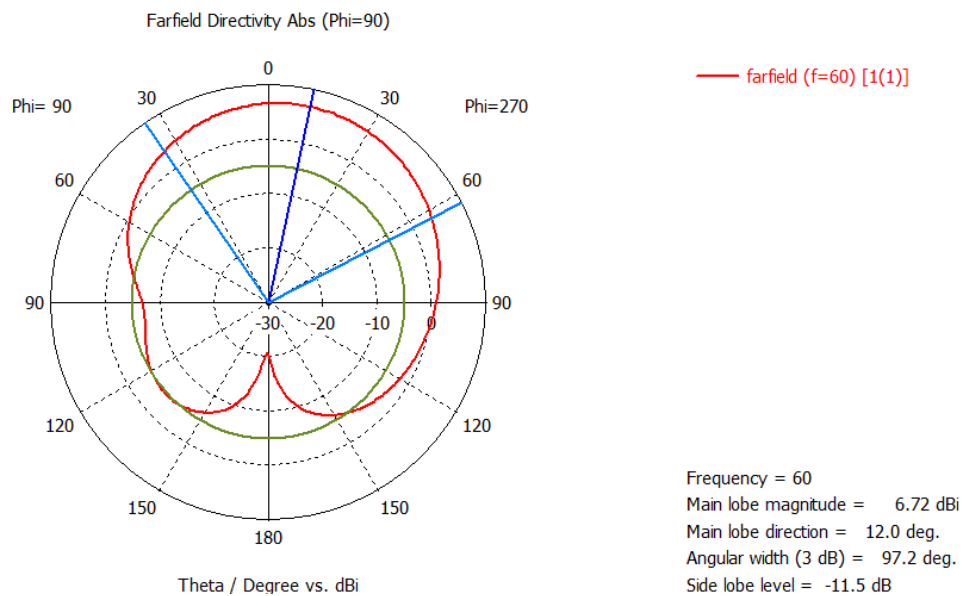


Figure 50: Polar plot of microstrip antenna

From the polar plot of our key antenna we can observe that the main lobe has a magnitude of around 6.72 db. And the side lobe level is considerably good as it attains a value of -11.5 dB.

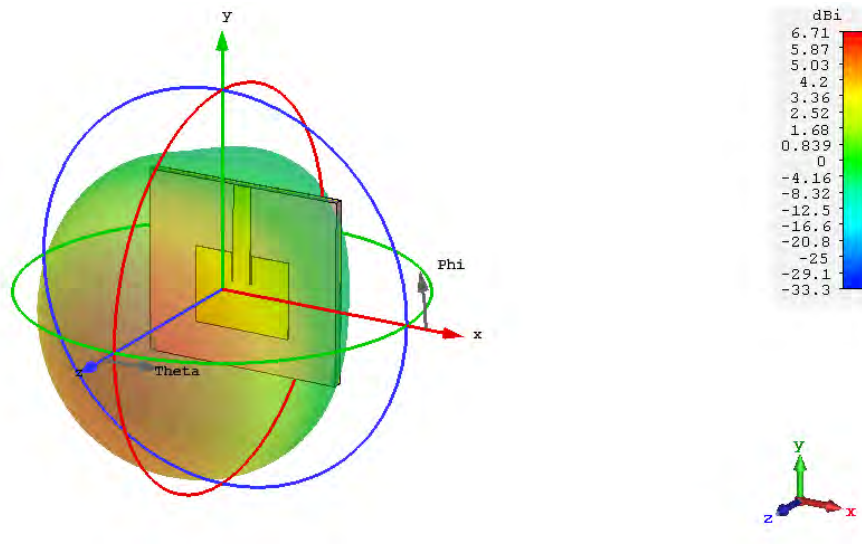


Figure 51: 3d farfield directivity pattern of microstrip antenna

From our key antenna design we were able to yield a directivity of 6.71 db. It is considered to be a very good directive radiation pattern when compared to others.

8.1.3 COMPARISON BETWEEN SINGLE MICROSTRIP AND KEY ANTENNA

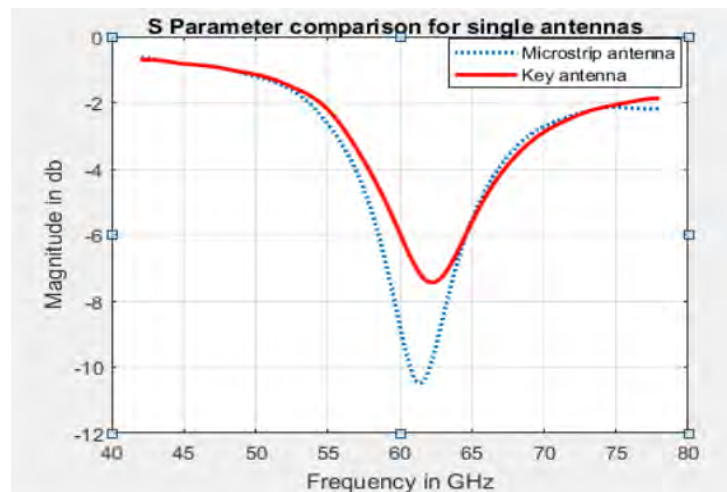


Figure 52: S parameter comparison for single antenna

From the above comparison we can see that the s11 parameter of the normal microstrip yields better results but as we can see in our next simulations that even though it is better for a single

element. When an array is made out of more elements the s parameters of the key antenna increases drastically.

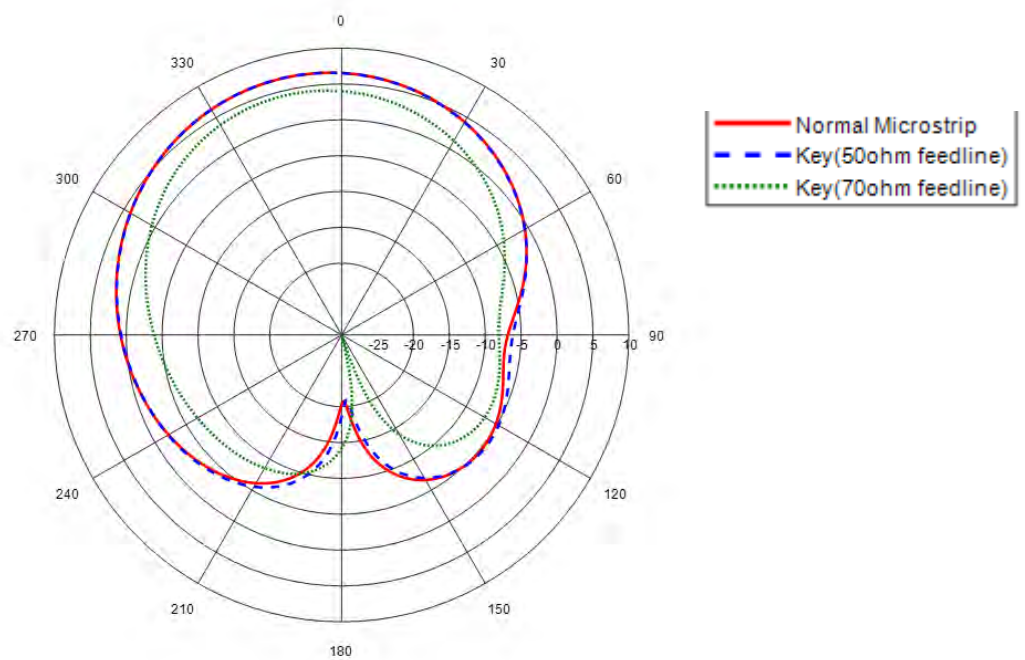


Figure 53: Polar Plot comparing single element antenna

8.2 ARRAY SIMULATION

8.2.1 MICROSTRIP ANTENNA ARRAY

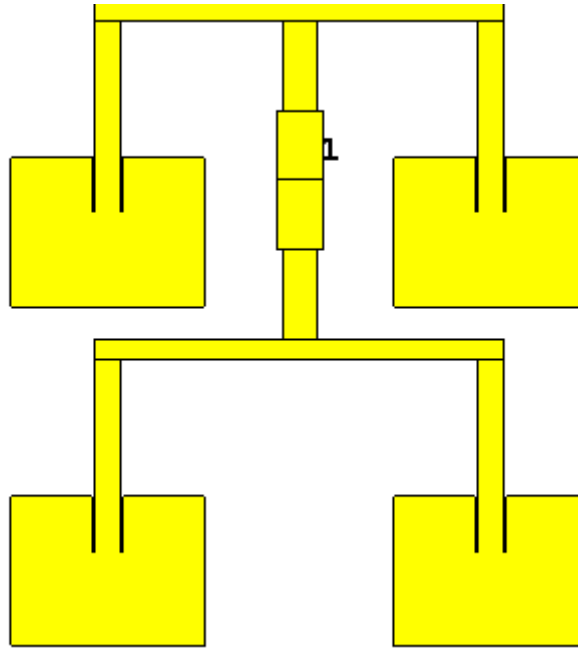


Figure 54: A 2x2 microstrip antenna array operating at 60 GHz

Table 4: Microstrip Antenna Array Parameters

Parameter	Dimension (in mm)
Substrate Width	2.84
Substrate Length	2.2
Substrate height	0.175
Patch Width	1.42
Patch Length	1.10
Feed Line Width	0.18
Feed Line Length	1.37

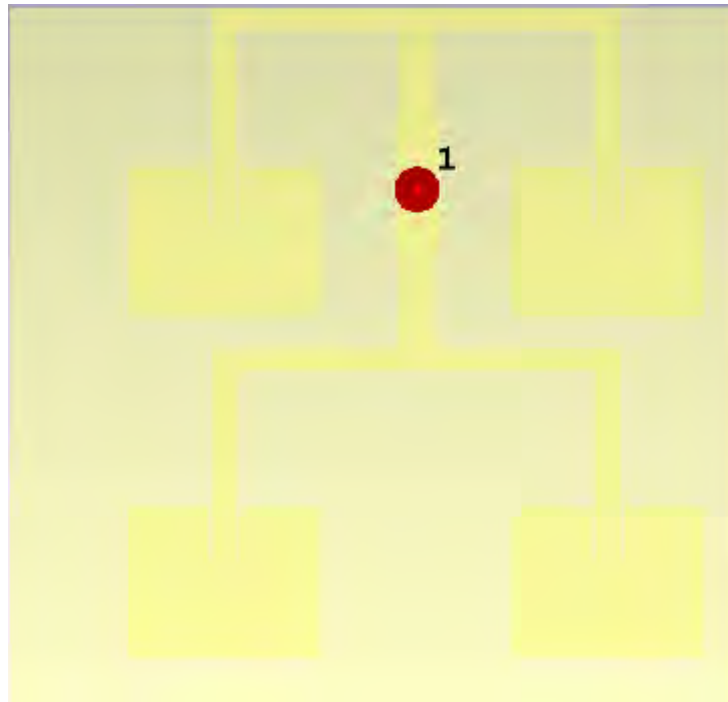


Figure 55: The antenna feeding point

The antenna is feed at the center of the array where the impedance is matched to be 50 ohms for the entire array.

For our simulation we have used a discrete port and the reference impedance results are as follows:

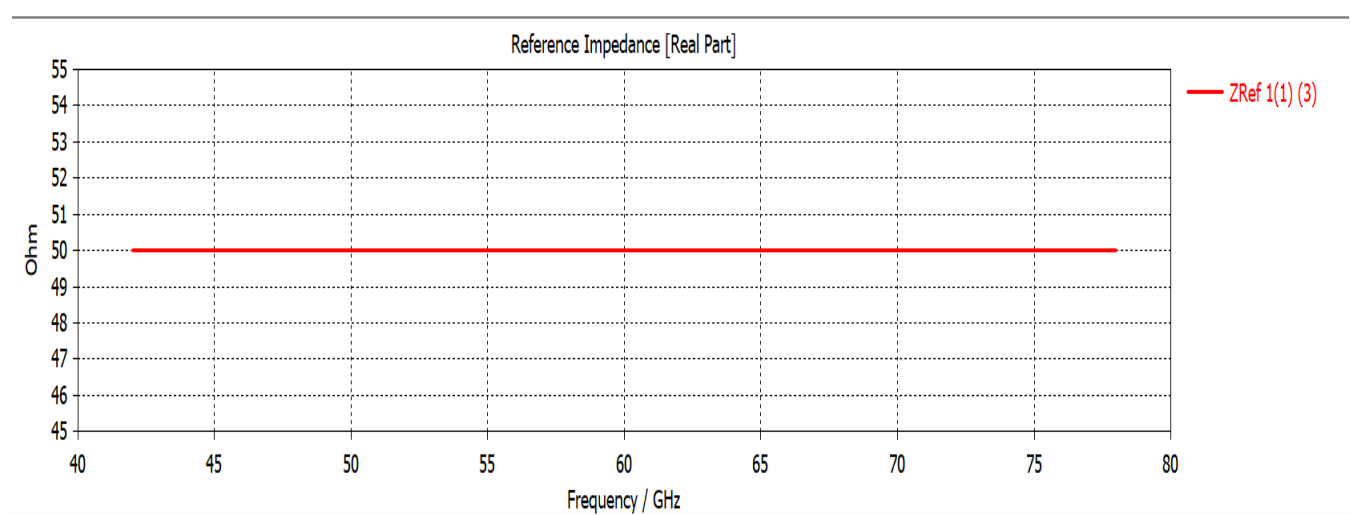


Figure 56: Reference Impedance

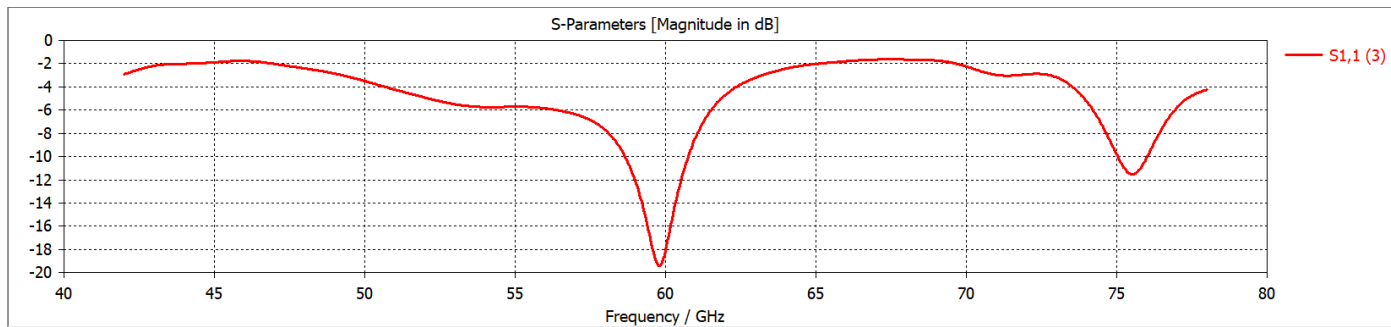


Figure 57: S Parameters for 2x2 microstrip antenna array at 60 GHz

Here the S parameter signifies the return loss of the antenna to be at around -19 dB. Our main basic objective was to make the antenna work at a resonant frequency of around 60 GHz. Any S parameter that has a magnitude of more than -10 dB is a very good return loss of that antenna.

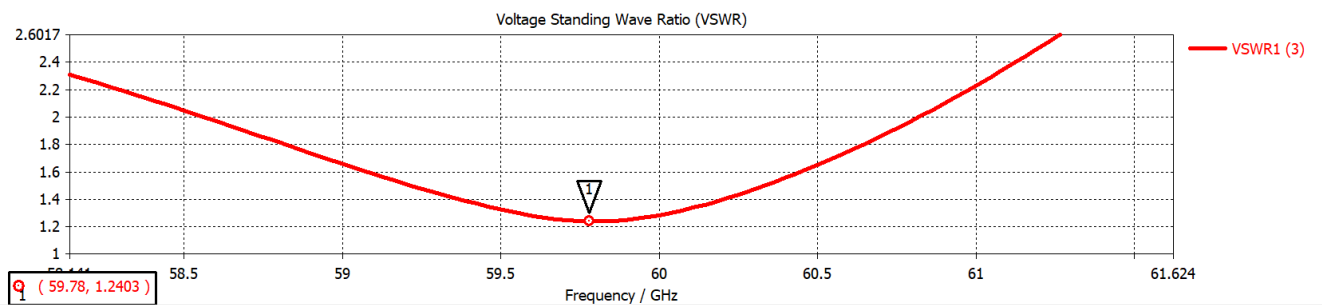


Figure 58: Voltage standing wave Ratio

For the normal microstrip array we have a voltage standing ratio of around 1.2403. VSWR indicates the amount of mismatch between an antenna and the feed line connecting to it. We should always aim to make our VSWR as close to 1 as possible.

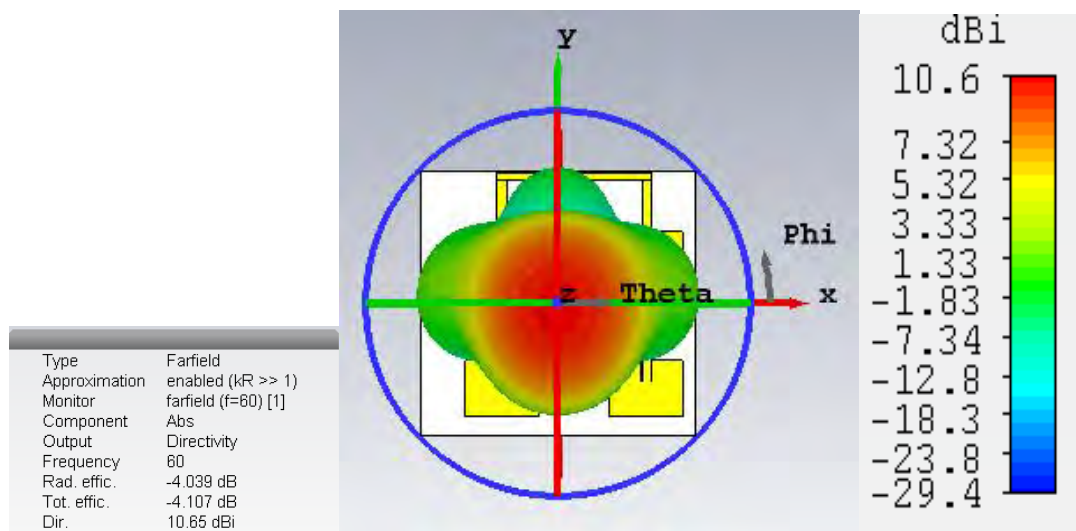


Figure 59: Directivity of a 2x2 microstrip array antenna

Our reference microstrip array antenna has a Directivity of 10.65 dBi. It refers to the fact that how directive our antenna is. An omnidirectional antenna has a directivity of 0 as it radiates equally in all directions.

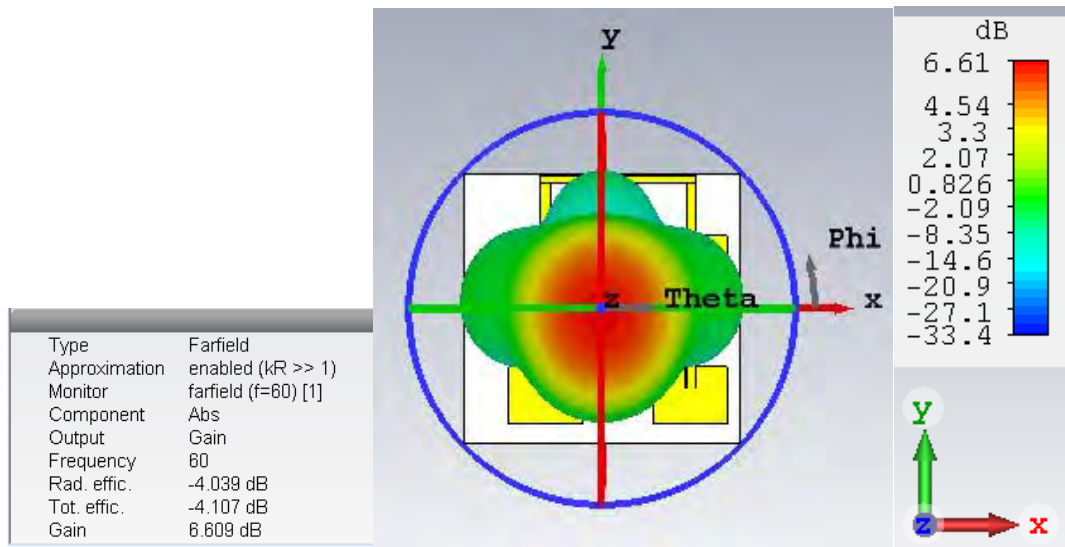


Figure 60: Gain of Directivity of a 2x2 microstrip array antenna

The reference antenna has a gain of 6.609 dB. The higher the gain of the antenna the better.

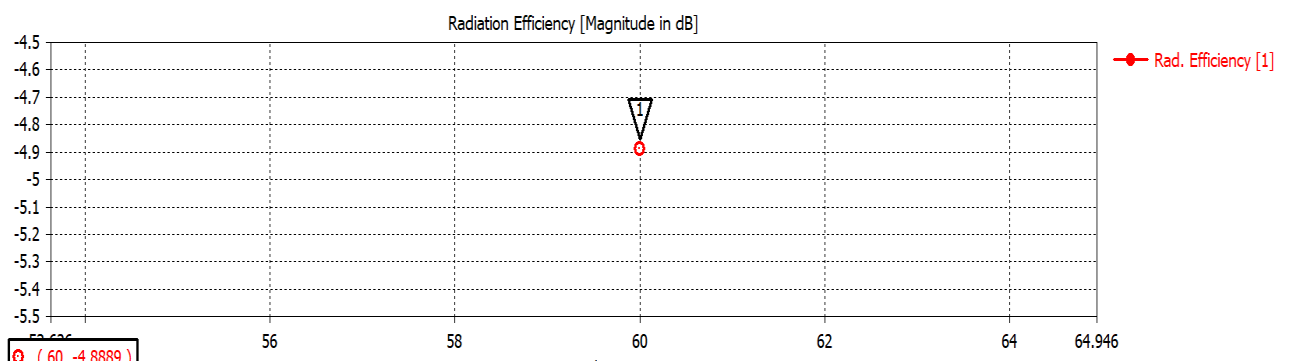


Figure 61: Radiation Efficiency of a 2x2 microstrip array antenna

The radiation efficiency of our reference antenna is -4.8809 dB which corresponds to a percentage of 57%.

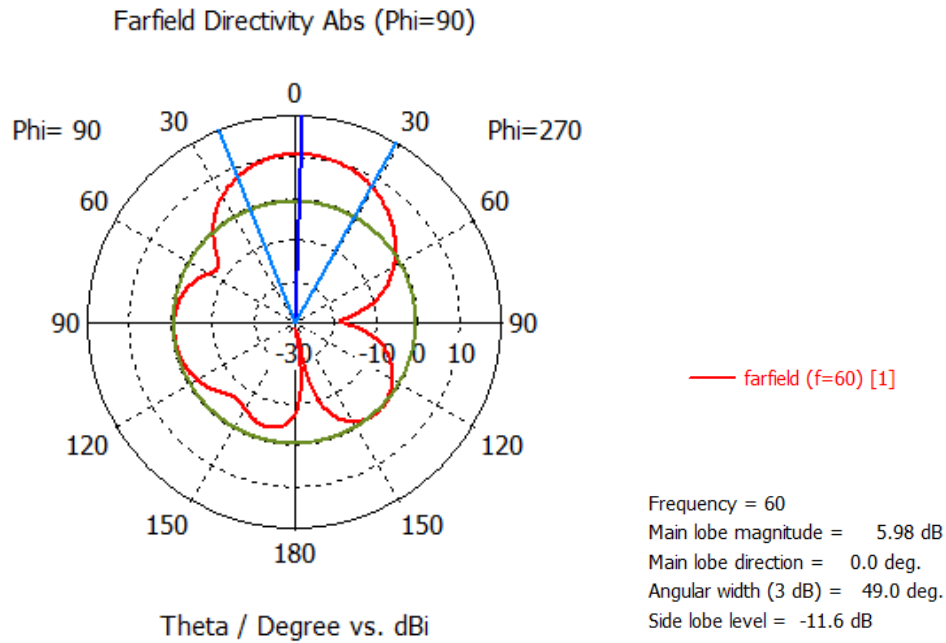


Figure 62: Polar Plot of microstrip antenna array

The microstrip reference model antenna array has a side lobe level of -11.6. A more negative value corresponds to drawing more power away from the main lobe. A side lobe level of below -30 dB is considered unacceptable for most antennas.

8.2.1 KEY ANTENNA ARRAY

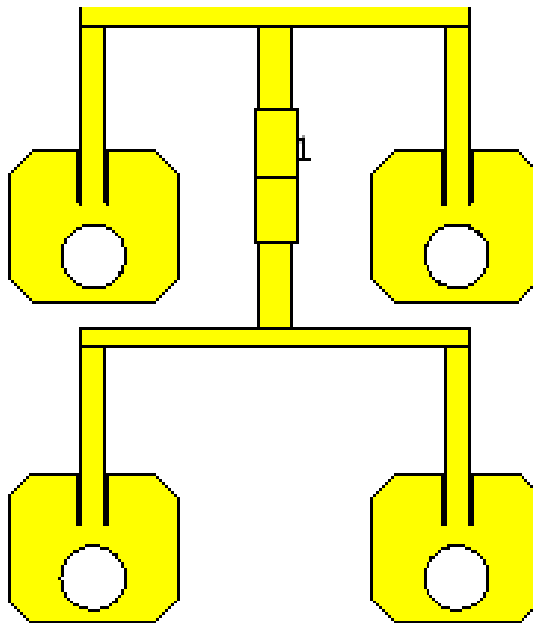


Figure 63: A 2x2 microstrip key antenna array operating at 60 GHz

Table 5: Microstrip Key Antenna Array Parameters

Parameter	Dimension (in mm)
Substrate Width	2.84
Substrate Length	2.2
Substrate height	0.175
Patch Width	1.52
Patch Length	1.16
Feed Line Width	0.18
Feed Line Length	1.37

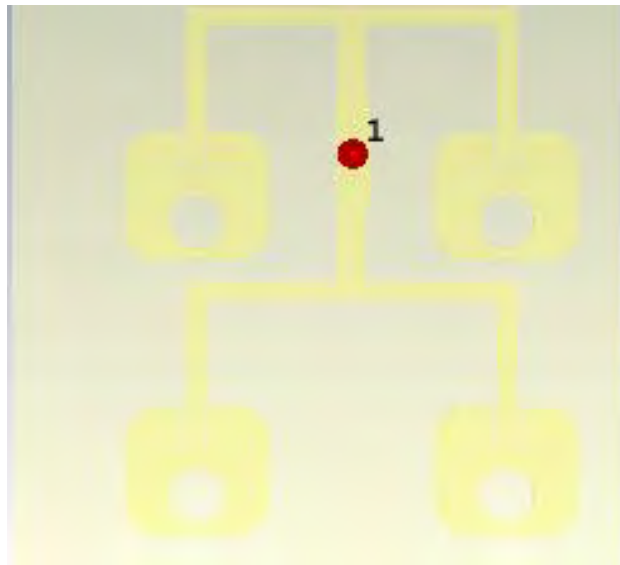


Figure 64: The antenna feeding point

The antenna is feed at the center of the array where the impedance is matched to be 50 ohms for the entire array.

For our simulation we have used a discrete port and the reference impedance results are as follows:

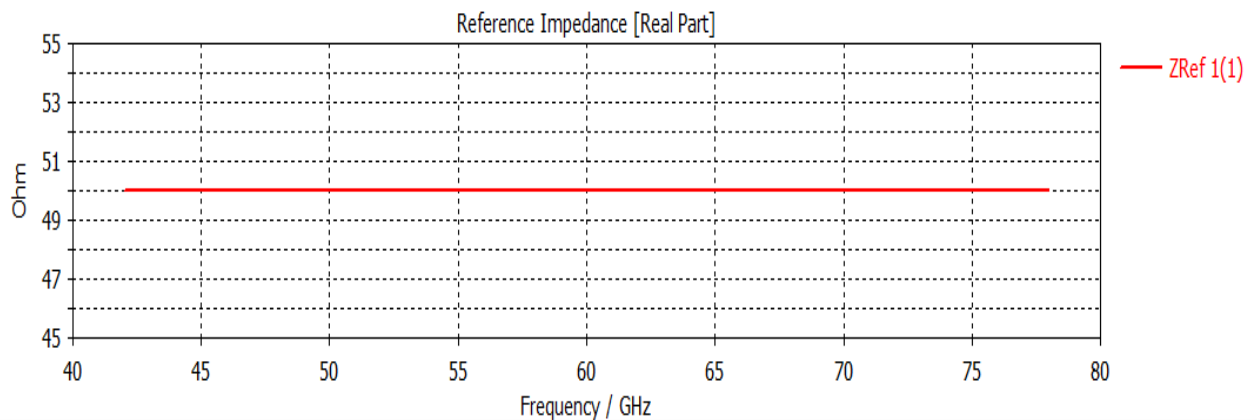


Figure 65: Reference Impedance

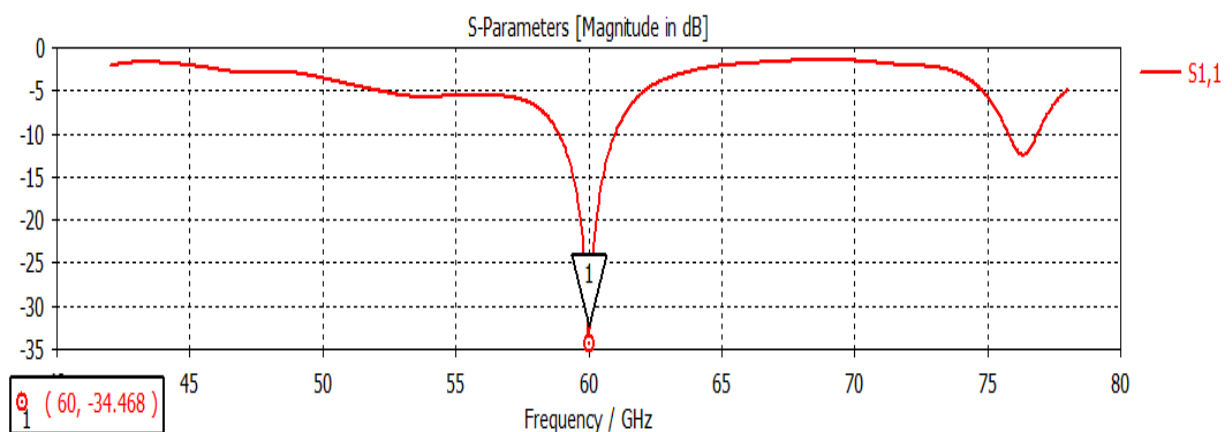


Figure 66: S Parameters for 2x2 microstrip key antenna array at 60 GHz

Here the S parameter signifies the return loss of the antenna to be at around -34.468. Our main basic objective was to make the antenna work at a resonant frequency of around 60 GHz. Any S parameter that has a magnitude of more than -10 dB is a very good return loss of that antenna.

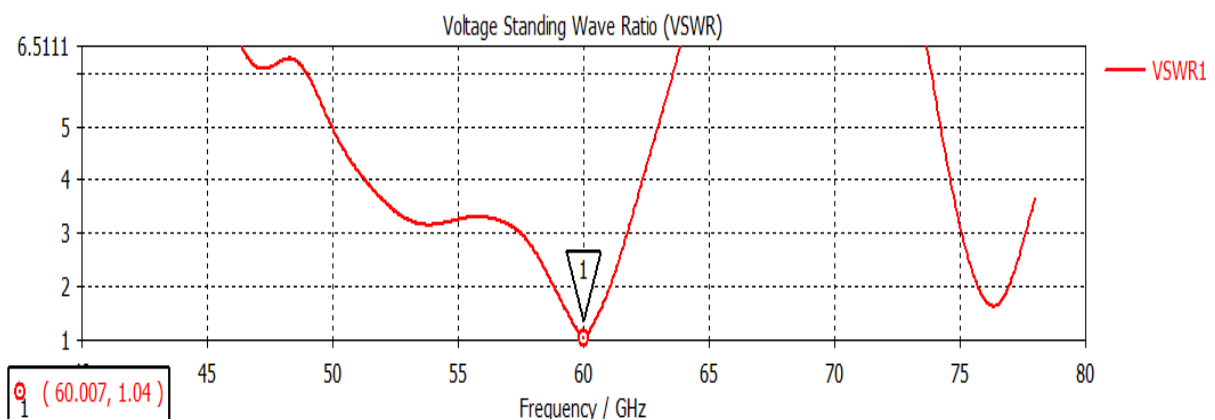


Figure 67: Voltage standing wave Ratio

For the normal microstrip array we have a voltage standing ratio of around 1.04. VSWR indicates the amount of mismatch between an antenna and the feed line connecting to it. We should always aim to make our VSWR as close to 1 as possible for best results.

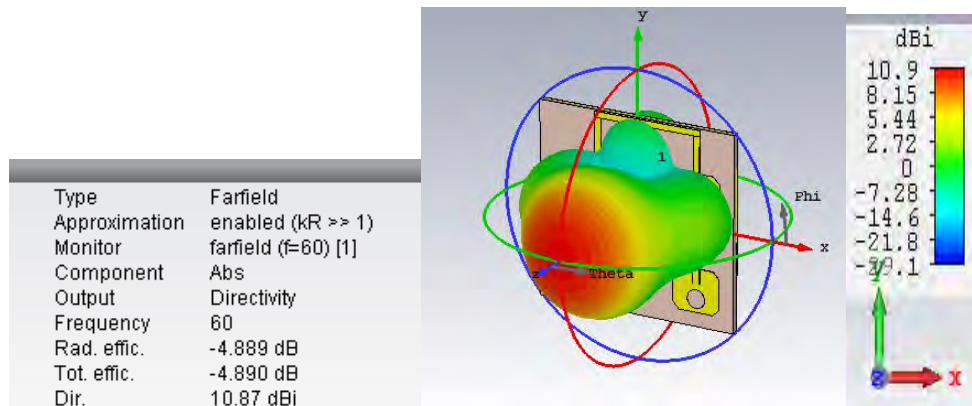


Figure 68: Directivity of a 2x2 microstrip array antenna

Our reference microstrip array antenna has a Directivity of 10.87 dBi. It refers to the fact that how directive our antenna is. An omnidirectional antenna has a directivity of 0 as it radiates equally in all directions.

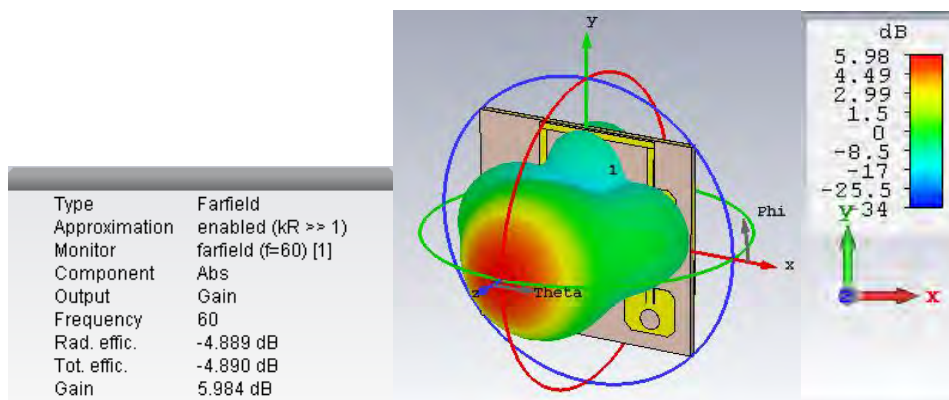


Figure 69: Gain of Directivity of a 2x2 microstrip array antenna

The reference antenna has a gain of 5.98 dB. The higher the gain of the antenna the better.

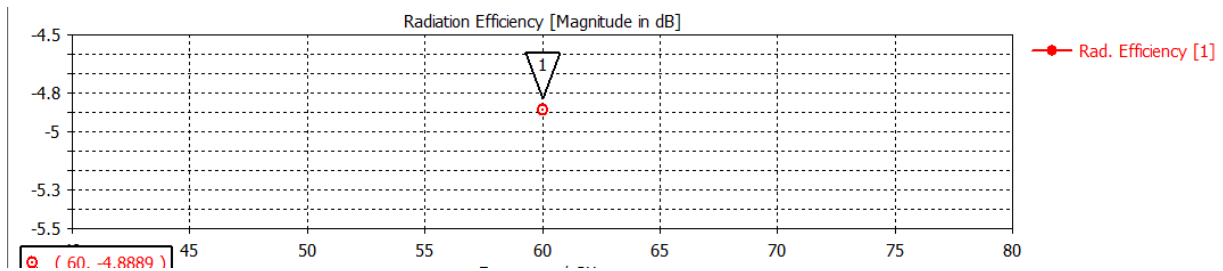


Figure 70: Radiation Efficiency of a 2x2 microstrip array antenna

The radiation efficiency of our reference antenna is -4.8889 dB which corresponds to a percentage of 56.96%.

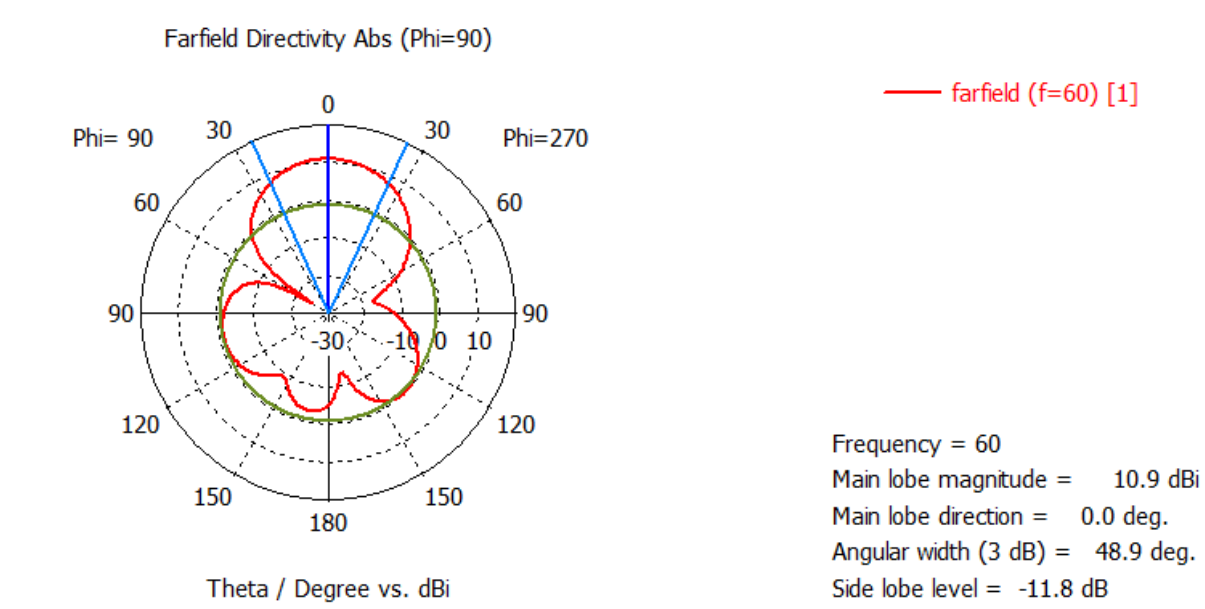


Figure 71: Polar plot of key antenna array

The key array design corresponds to a side lobe level of -11.4 db. A more negative value corresponds to drawing more power away from the main lobe. A side lobe level of below -30 dB is considered unacceptable for most antennas

8.2.1 COMPARISON BETWEEN ARRAY PARAMETERS

Table 6: Comparison between Arrays

Antennas	S-parameters (dB)	VSWR	Directivity (dBi)	Gain (dB)	Side lobe level(dB)	Radiation Efficiency (%)
60 GHz Microstrip antenna 2x2 array	-19	1.204	10.65	6.609	-11.6	57
60 GHz Key antenna 2x2 array	-34.468	1.04	10.87	5.98	-11.4	56.96

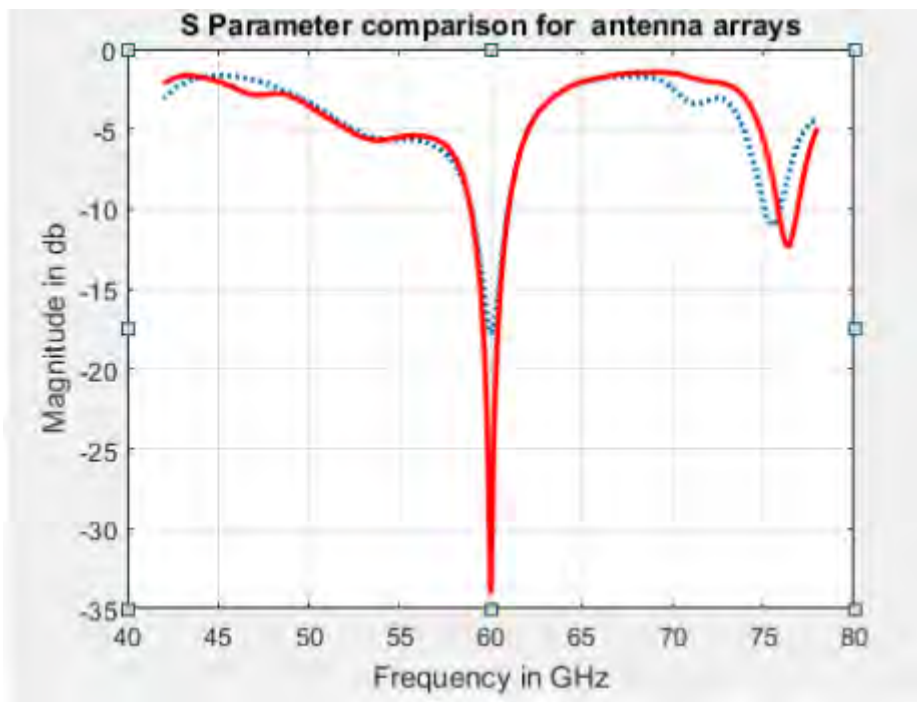


Figure 72: S parameter comparison for antenna arrays

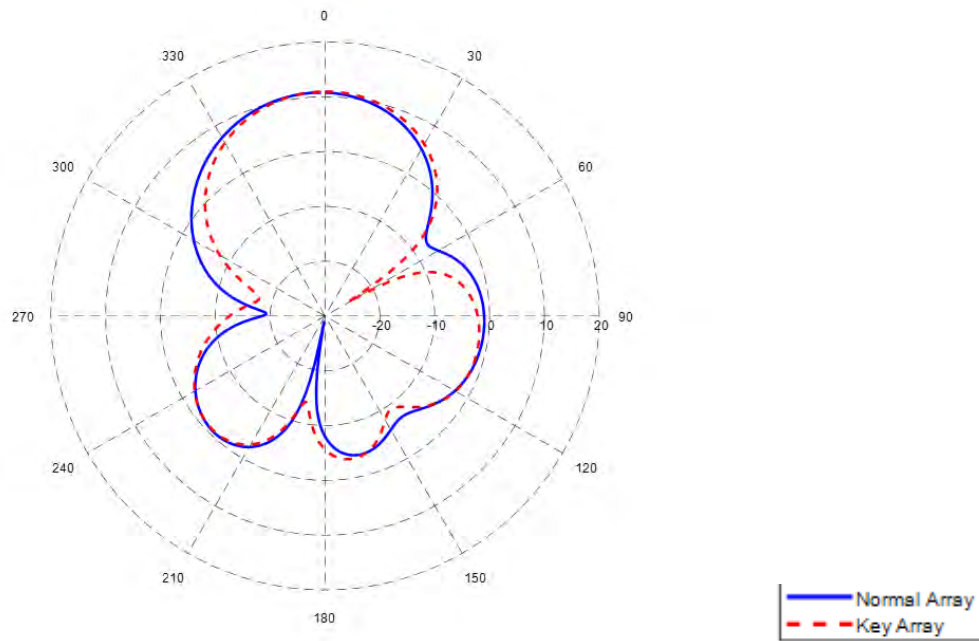


Figure 73: Polar plot comparison of antenna array

After conducting our simulations and comparing the results as in the table above we can come to the following conclusions. In terms of S-11 parameters we can see that our key antenna array offer far superior results (-34.468dB versus -19dB) indicating that our array reflects less of the incoming power in comparison to a normal microstrip array. If we look to the VSWR ratio for both the key antenna array also shows far better performance, 1.04 pointing to the fact it has a better match whereas the normal array VSWR of 1.204 indicates a greater mismatch. Moving on to the directivity our key antenna array offers a directivity of 10.87dBi versus a normal array which offers 10.65dBi therefore our antenna excels at providing better results for one of the most important parameters for any antenna. Additionally, the key antenna array also has much lower side lobe levels so less power is radiated in unwanted directions. Finally, when we come to the efficiency we can see that both antenna arrays perform at almost identical radiation efficiency. The only parameter where the reference antenna holds an advantage over our key antenna array is in gain where the microstrip antenna array has a gain 6.609dB versus ours which is 5.98dB. However, in order to achieve the above improved parameters we had to make some sacrifices when it comes to the gain and in the future we hope to modify and improve future design in order to bridge the gap between the gains of the two array by improving the gain of our antenna.

8.3 COMPARISON OF DIFFERENT SUBSTRATES

8.3.1 ROGERS RT 5880

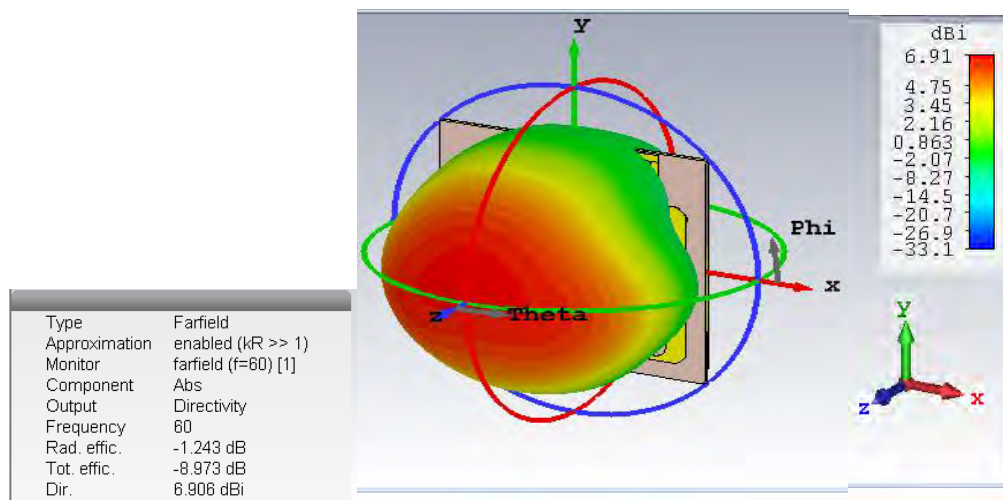


Figure 74: 3d farfield directivity pattern for RT 5880

For our Rogers substrate we have a directivity of 6.91 dB which is pretty good considering other substrates and it has a radiation efficiency of -1.243 dB and a total -8.973 dB.

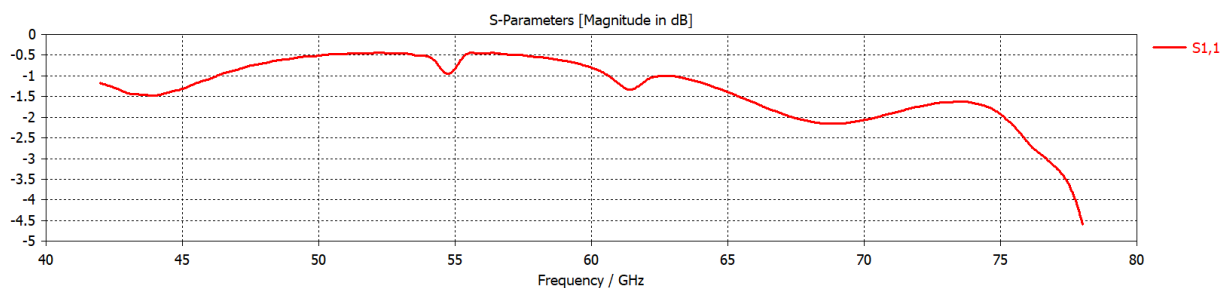


Figure 75: S Parameters for Rogers RT 5880

Here the S parameters for our Rogers substrate is less than -1 db, which signifies that it has a very poor return loss so its not very much feasible to use this substrate.

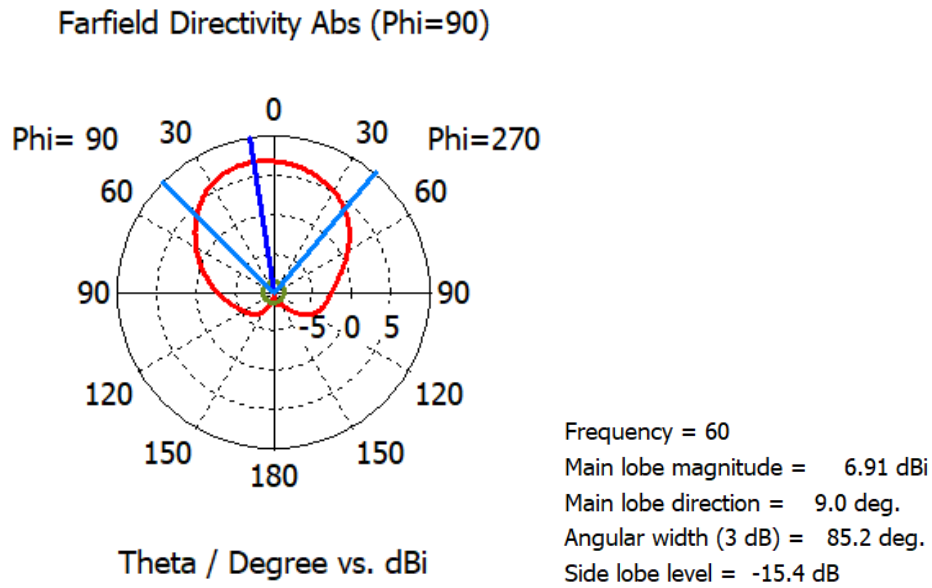


Figure 76: Polar plot for RT 5880

From the above simulation we can see that the main lobe has a magnitude of around 6.91 dBi and the side lobe level is also considerably high -15.4 dBi.

8.3.2 ARLON AD 270

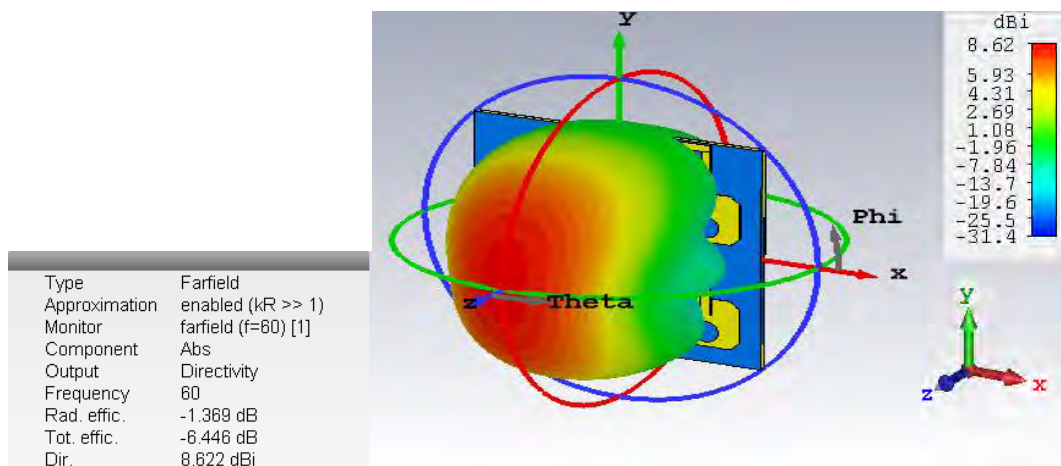


Figure 77: 3d Farfield directivity pattern for AD 270

For our Arlon substrate we have a directivity of 8.62 dB which is tremendous compared to other substrates and it has a radiation efficiency of -1.369 dB and a total -6.446 dB

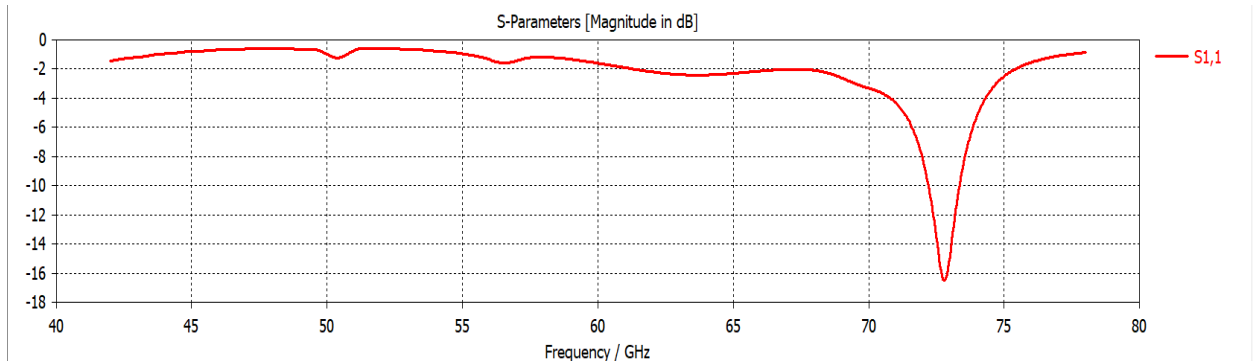


Figure 78: S parameters for AD 270

Here the S parameters for our Arlon substrate is only -2 db at our desired frequency , which signifies that it has a very poor return loss so its not very much feasible to use this substrate either.

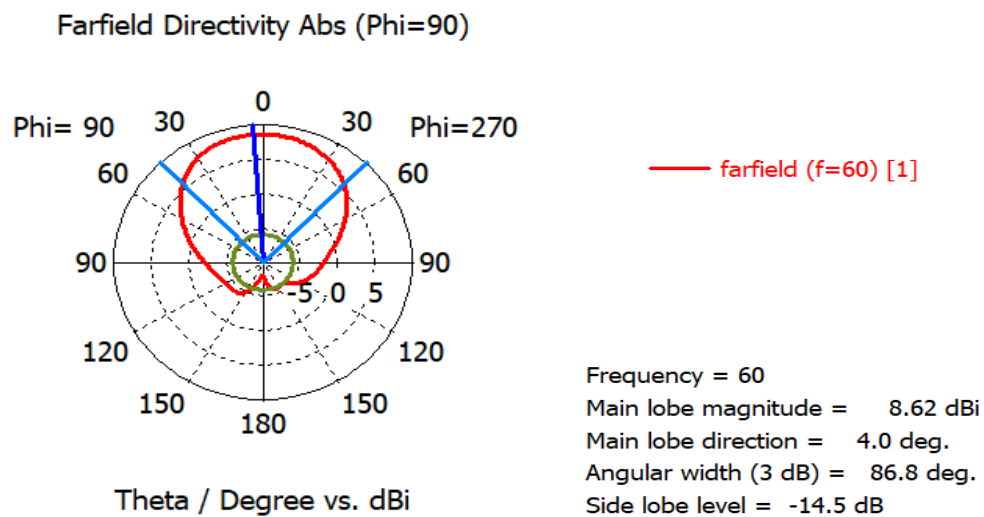


Figure 79: Polar Plot of AD 270

From the above simulation we can see that the main lobe has a magnitude of around 8.62dBi and the side lobe level is also considerably high -14.5dBi.

8.3.3 COMPARISON BETWEEN RESULTS

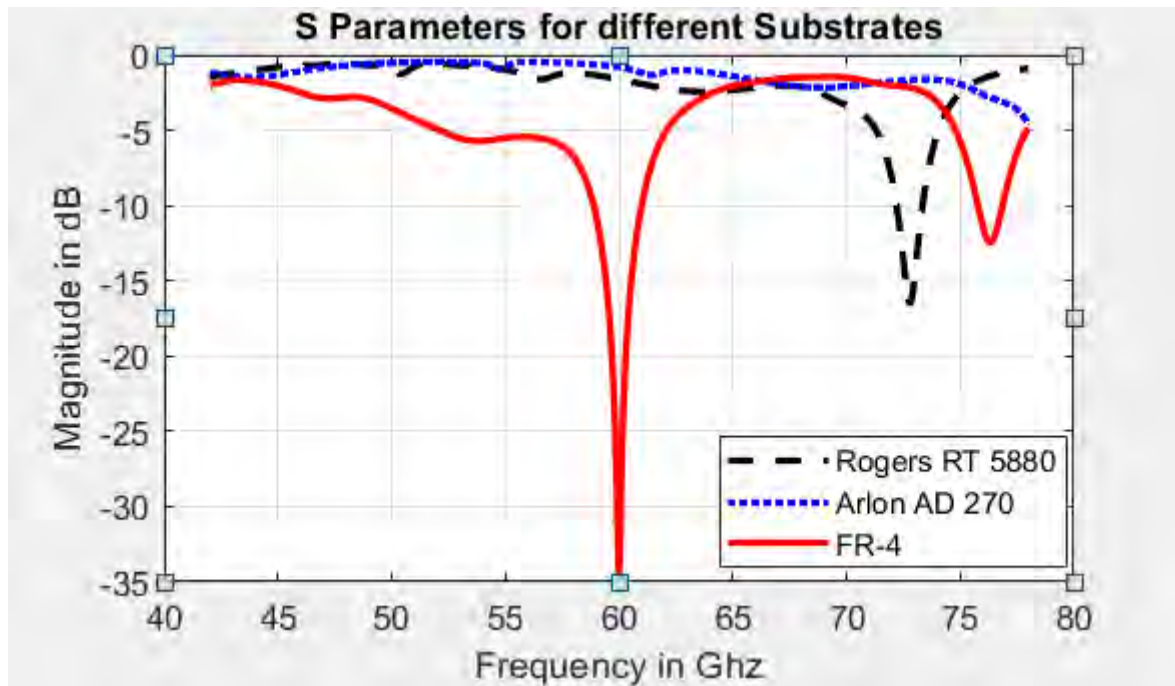


Figure 80: S parameter comparison for different Substrates

Table 7: Comparison between different substrates

Materials	S Parameters	Directivity	Radiation Efficiency	Total Efficiency	Side lobe level
FR-4	-34.468	10.87	-4.89	-4.89	-11.4
ARLON	-2	8.62	-1.37	-6.44	-14.5
Rogers	-1	6.91	-1.24	-8.97	-15.4

After simulating and comparing different substrates we were able to find out the 3 that yielded the best results. Among them FR-4 was the substrate that yielded the best return loss and the greatest directivity. It also corresponded to the best side lobe level among the three so that is why for our thesis simulation we opted to use the FR-4 to yield the best results.

8.4 COMPARAING RESULTS OF DIFFERENT ELEMENTAL SPACING

One of the other key factors that affect an antennas overall performance and out is the elemental spacing of the individual antenna elements. Larger elemental spacing usually results in higher directivity however antenna engineers often keep the spacing less than $\lambda/2$ so as to prevent the occurrence of grating lobes [66]. However given that the maximum possible spacing that is allowed between antenna elements is between $\lambda/2$ and λ while the directivity of the array does increase it results as a value greater than λ result in side lobes so large that their magnitude. From our trial and error sessions with our custom key shaped antenna array for spacing's of 0.6λ to 1.0λ we have found that 0.6λ to provide the best overall results for our array as we explain them below.

8.4.1 ANTENNA ARRAY WITH 0.6λ ELEMENTAL SPACING

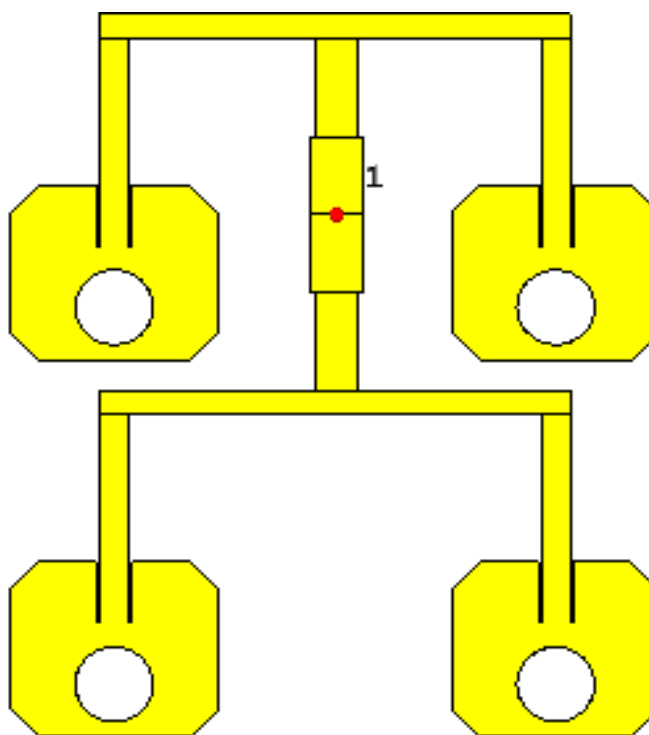


Figure 81: Key Antenna array with 0.6λ Elemental Spacing

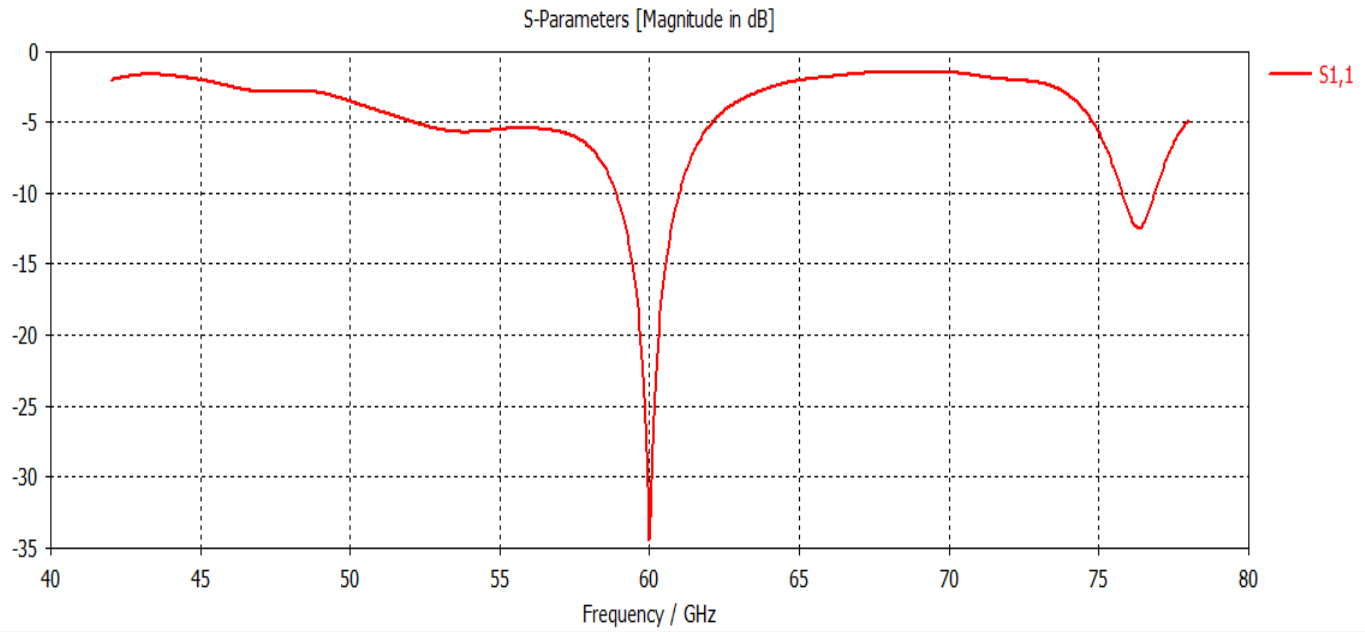


Figure 82: S₁₁ parameter for 0.6λ elemental spacing

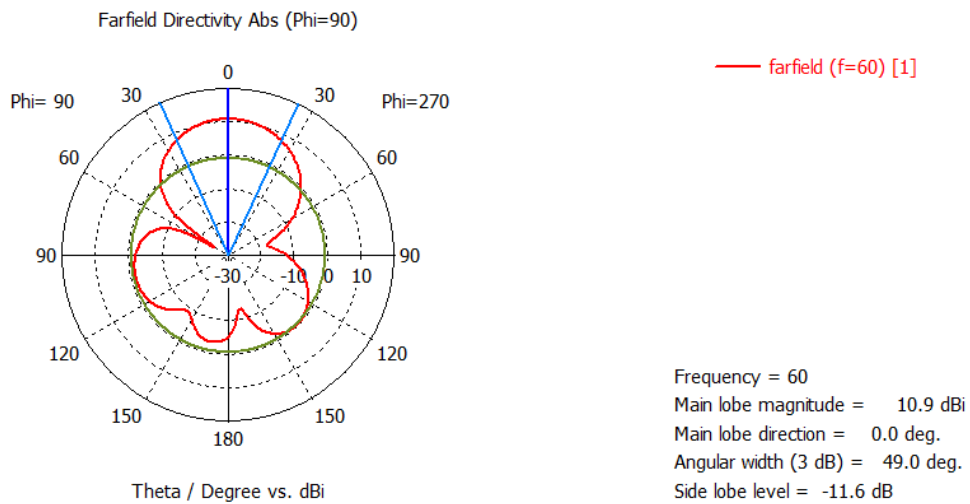


Figure 83: Polar plot for 0.6λ elemental spacing

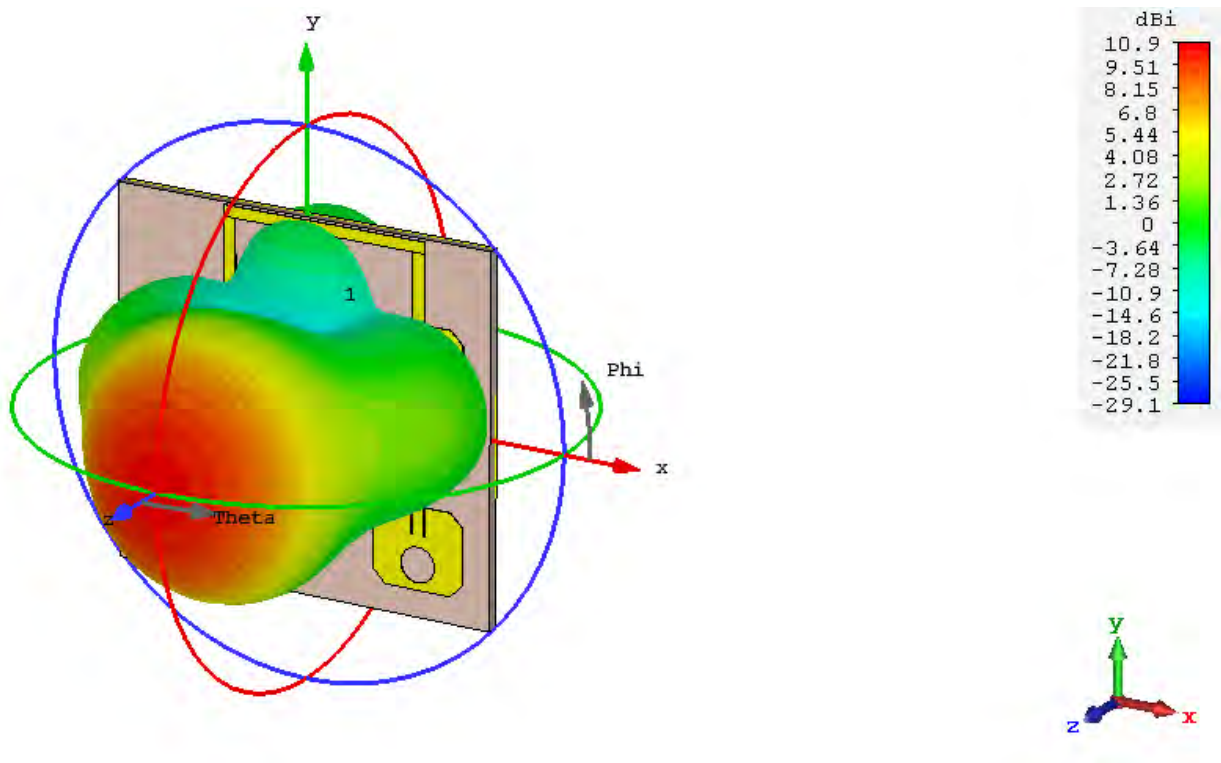


Figure 84: 3d farfield directivity pattern for 0.6λ elemental spacing

For elemental spacing of 0.6λ we can see that the reflection coefficient is about -34.46 dB with directivity of 10.9 dBi with angular width of 49.0 degree and a side lobe level of -11.6 dB while the radiation efficiency is -4.889 dB and the total efficiency is -4.890 dB.

8.4.2 ANTENNA ARRAY WITH 0.7λ ELEMENTAL SPACING

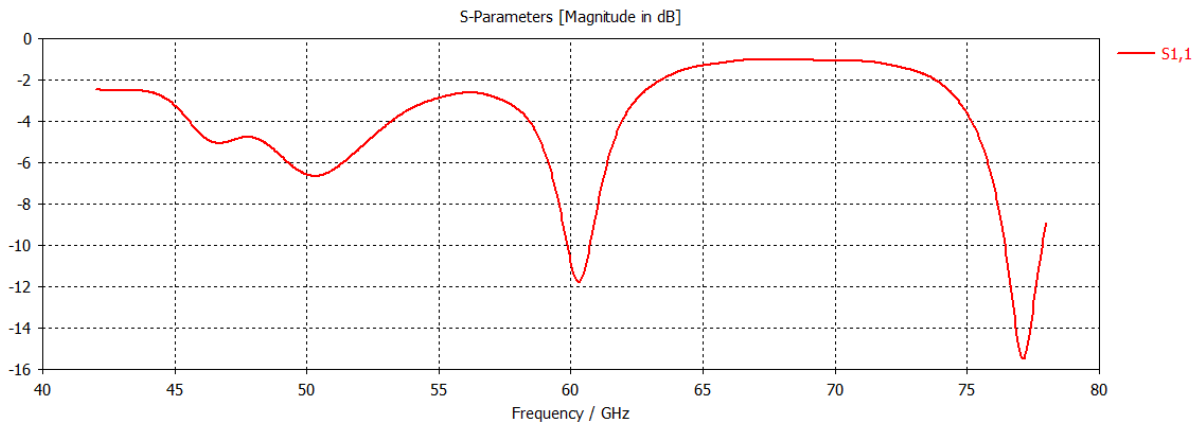


Figure 85: S11 parameter for 0.7λ elemental spacing

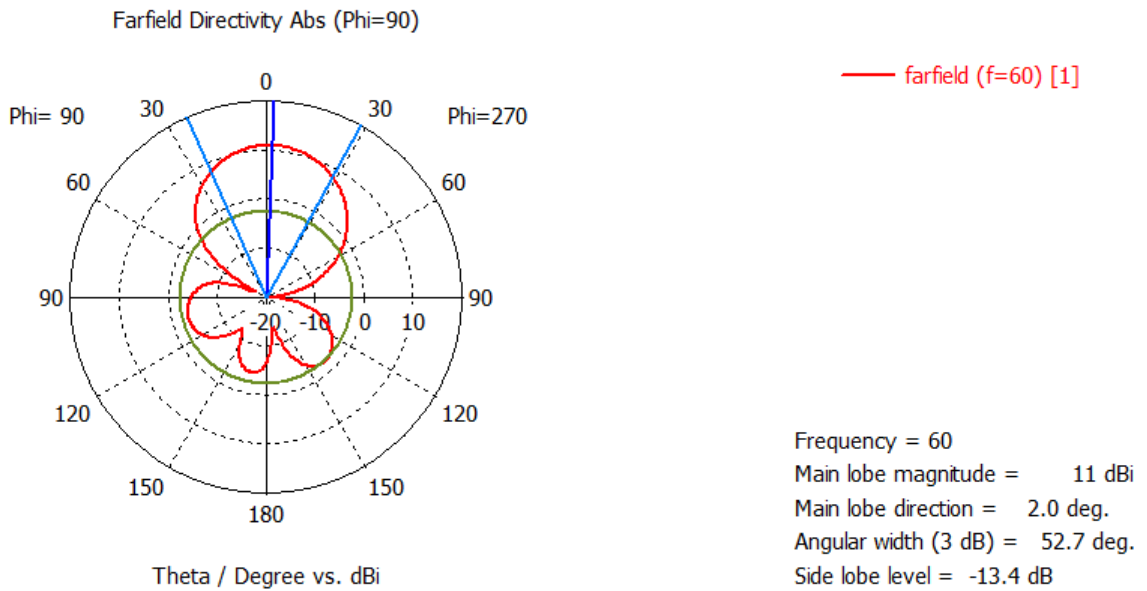


Figure 86: Polar plot for 0.7λ elemental spacing

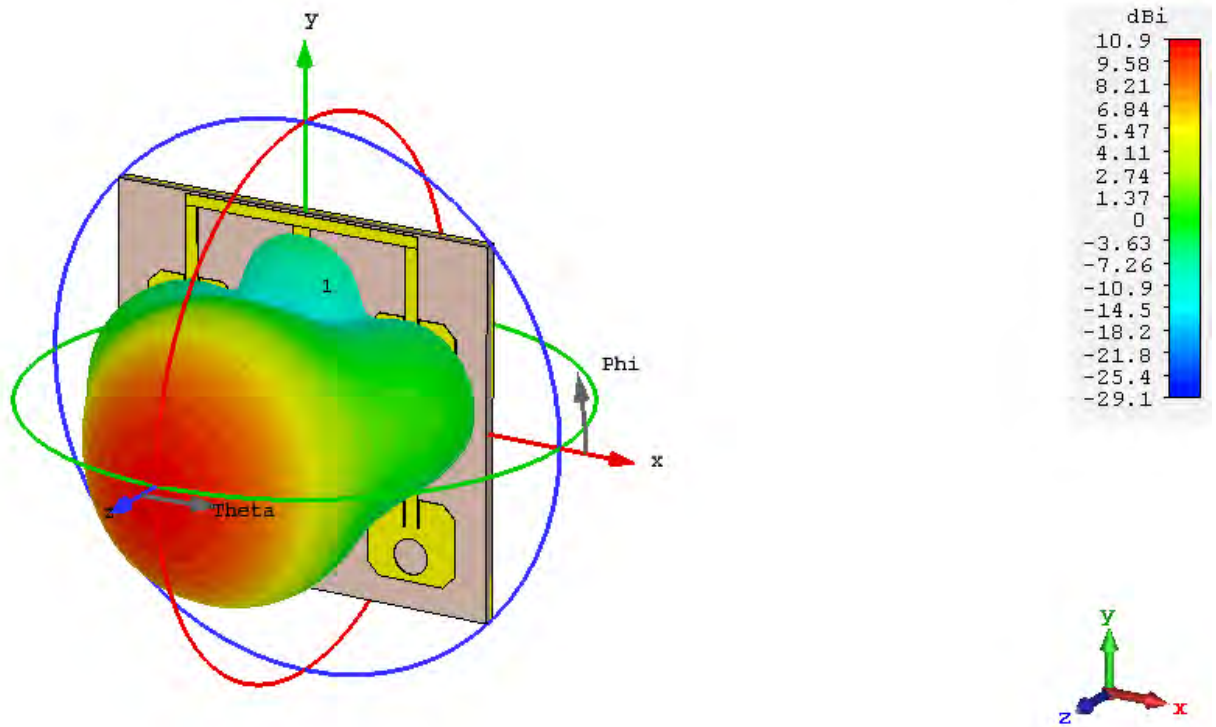


Figure 87: 3d farfield directive pattern for 0.7λ elemental spacing

For elemental spacing of 0.7λ we can see that the reflection coefficient is about -10.85 dB with directivity of 11.0dBi with angular width of 52.7 degree and a side lobe level of -13.6dB while the radiation efficiency is -4.631dB and the total efficiency is -5.003 dB.

8.4.3 ANTENNA ARRAY WITH 0.8λ ELEMENTAL SPACING

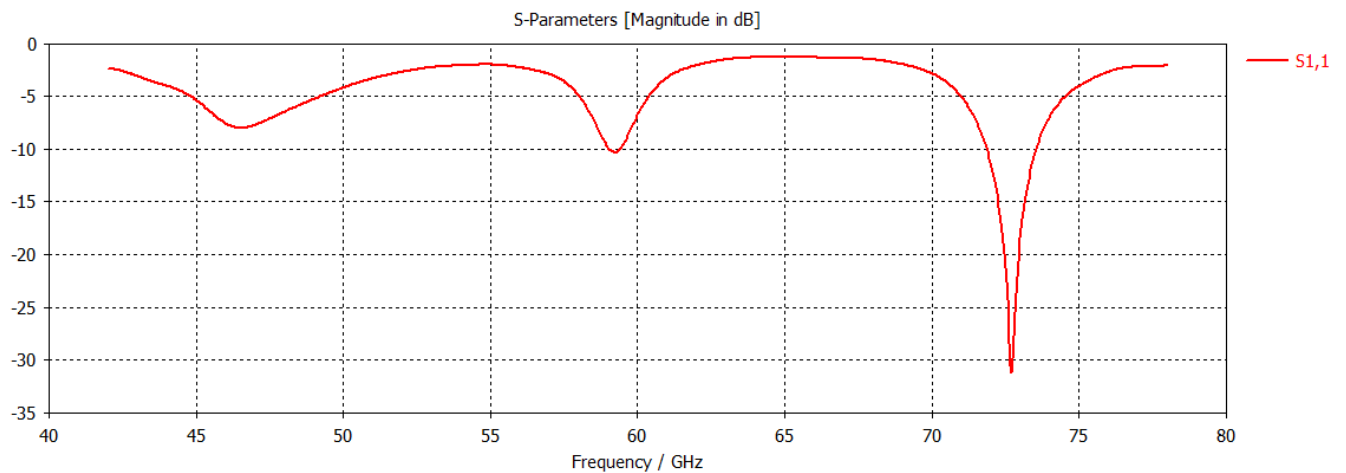


Figure 88: S11 parameter for 0.8λ elemental spacing

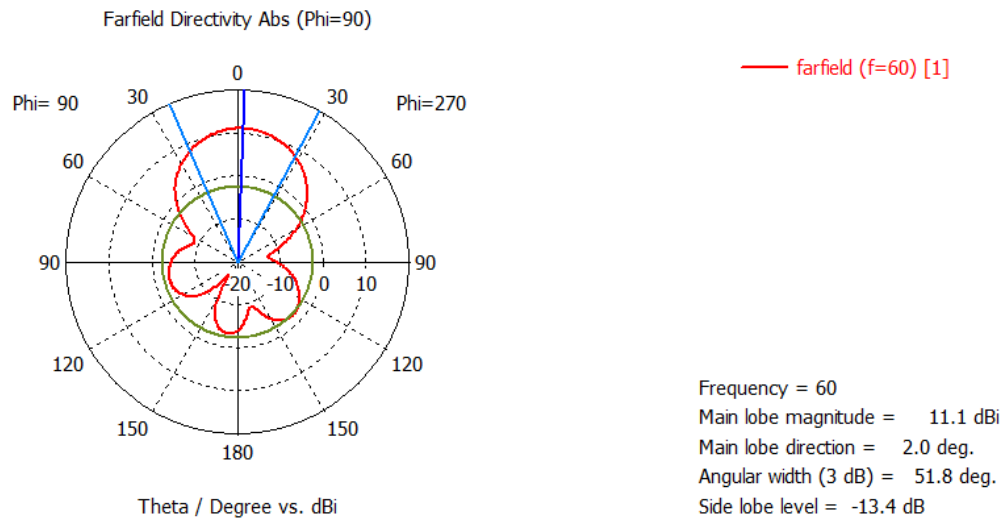


Figure 89: Polar plot for 0.8λ elemental spacing

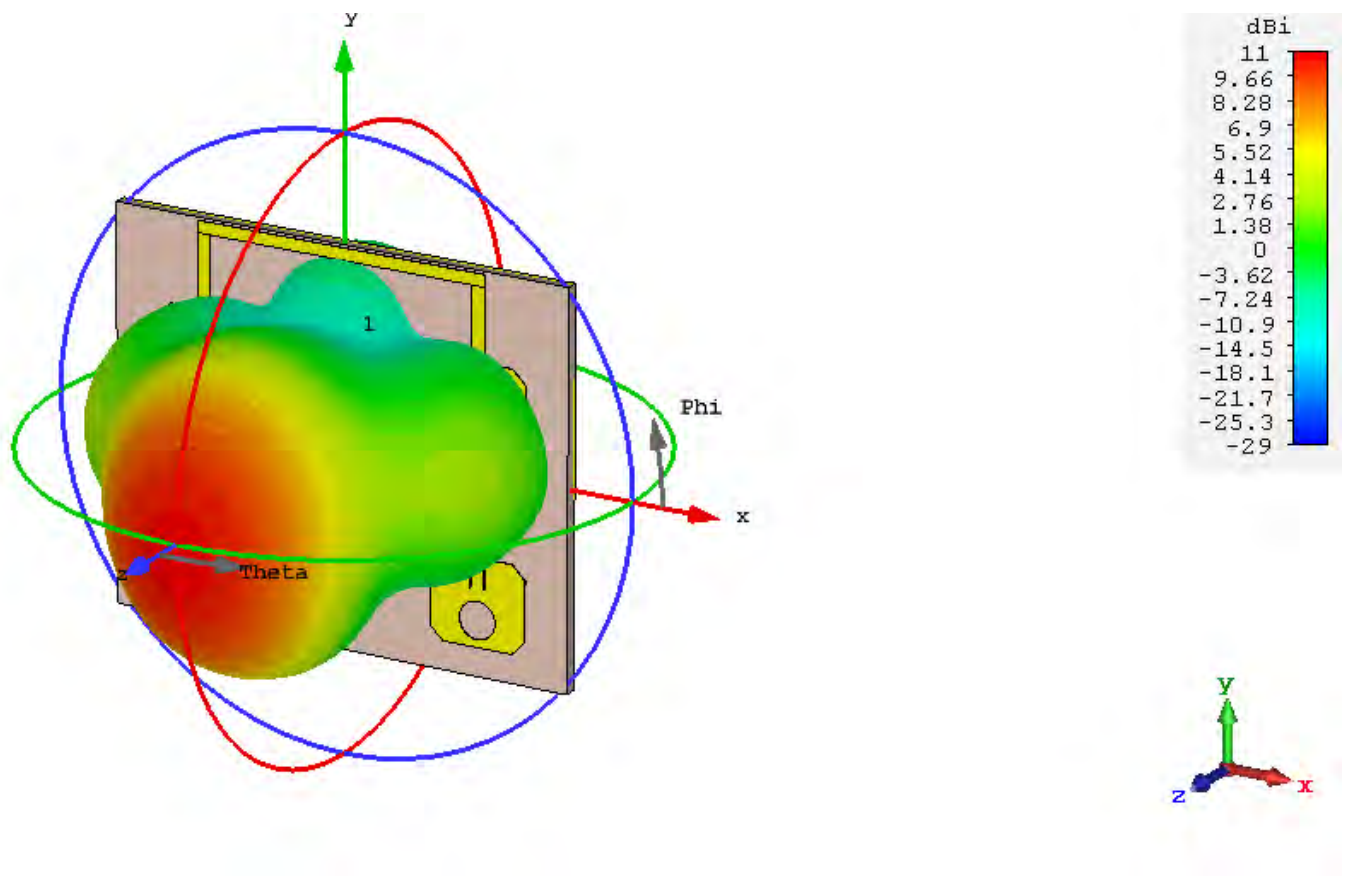


Fig:90 3d farfield directivity pattern for 0.8λ elemental spacing

For elemental spacing of 0.8λ we can see that the reflection coefficient is about -6.8 dB with directivity of 11.1 dBi with angular width of 51.8 degree and a side lobe level of -13.4 dB while the radiation efficiency is -5.107 dB and the total efficiency is -6.104 dB.

8.4.4 ANTENNA ARRAY WITH 1λ ELEMENTAL SPACING

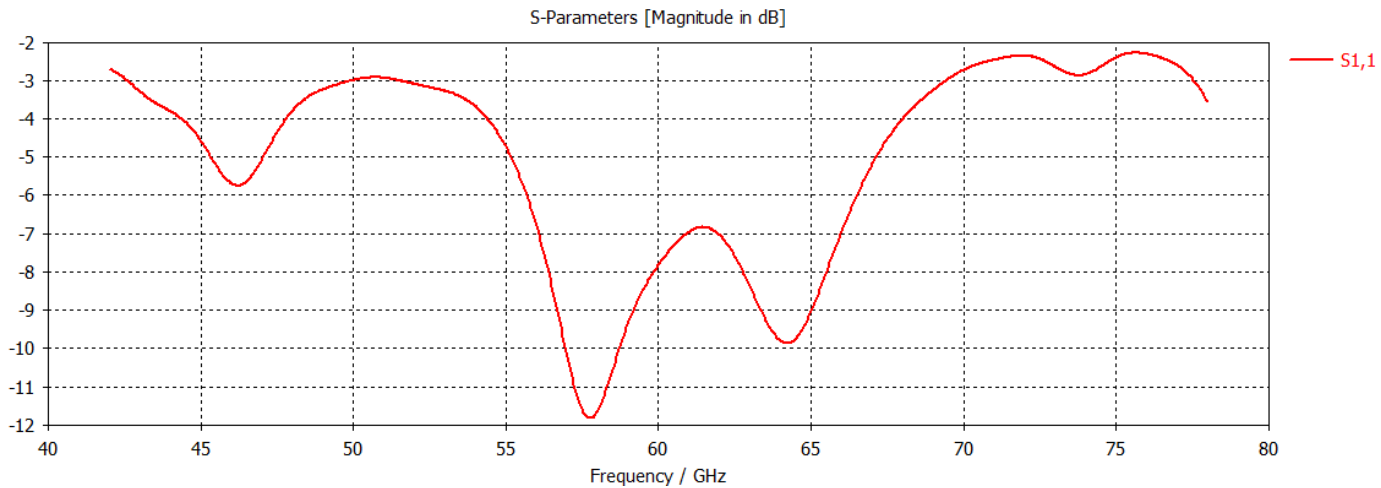


Figure 91: S₁₁ parameter for 1λ elemental spacing

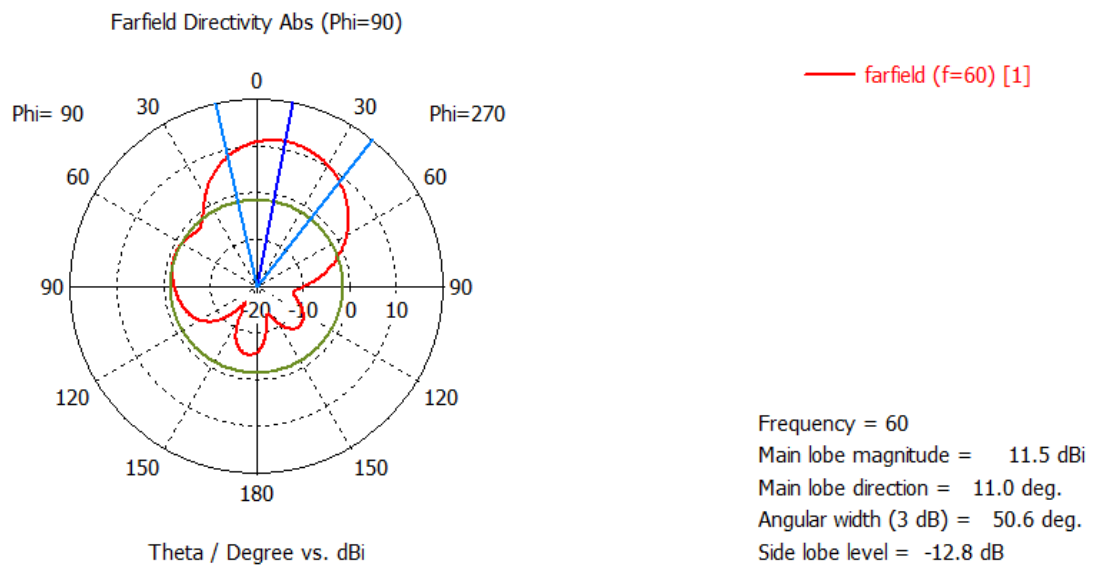


Figure 92: Polar plot for 1λ elemental spacing

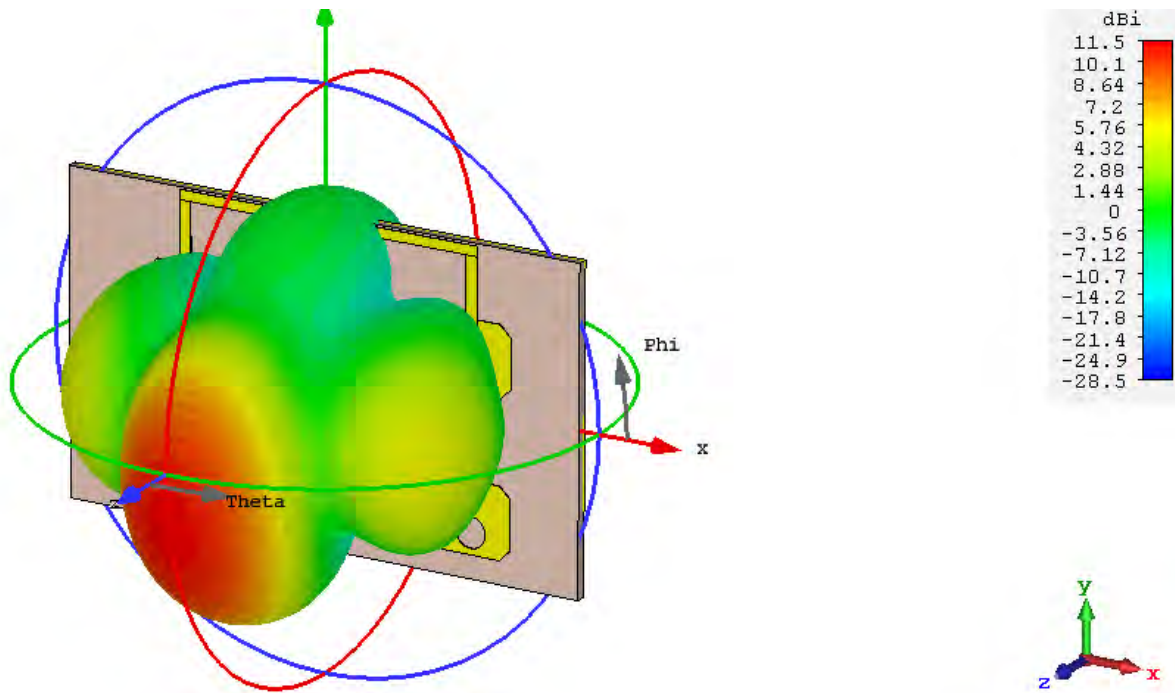


Figure 93: 3d farfield directivity pattern for 1λ elemental spacing

For elemental spacing of 1.0λ we can see that the reflection coefficient is about -7.8dB with directivity of 10.5dBi with angular width of 50.6 degree and a side lobe level of -12.8dB while the radiation efficiency is -5.102dB and the total efficiency is -5.887 dB.

8.4.5 COMPARISON BETWEEN RESULT VALUES

Table 8: Comparison between Different element spacing

Elemental Spacing	S-parameters(dB)	Directivity (dBi)	Angular width(3dB)	Side lobe level(dB)	Radiation Efficiency(dB)	Total Efficiency (dB)
$0.6\lambda(3\text{mm})$	-34.46	10.9	49.0	-11.6	-4.889	-4.890
$0.7\lambda(3.5\text{mm})$	-10.85	11.0	52.7	-13.4	-4.631	-5.003
$0.8\lambda(4\text{mm})$	-6.8	11.1	51.8	-13.4	-5.107	-6.104

$1.0\lambda(5\text{mm})$	-7.8	11.5	50.6	-12.8	-5.102	-5.887
--------------------------	------	------	------	-------	--------	--------

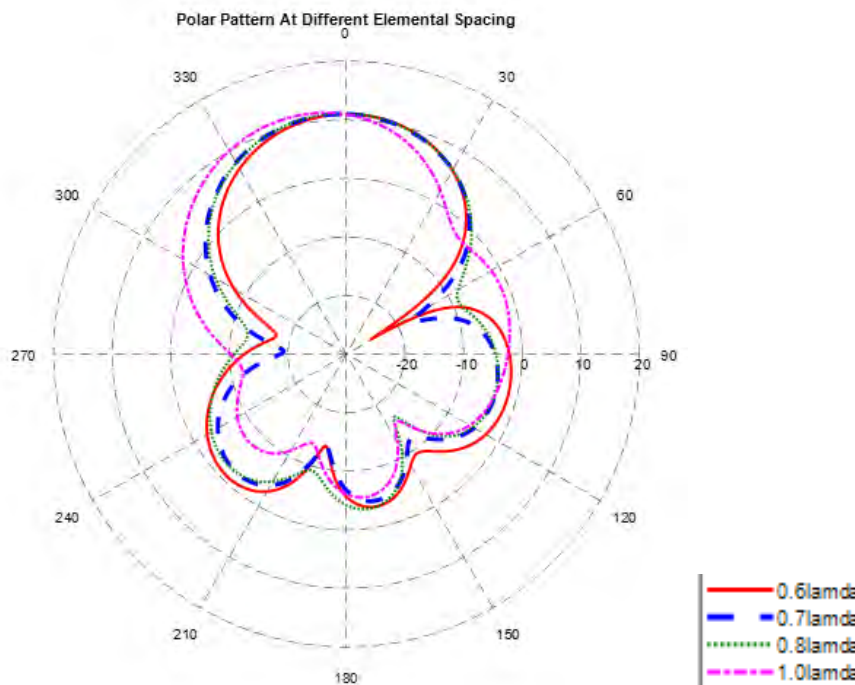


Figure 94: Polar Plot of arrays at different elemental spacing

From the above experimental results and data obtain we can see a general trend if we closely observe the table. As antenna elemental spacing increases so does the directivity however our s_{11} parameters fall which affects our efficiency and at below 0.8λ their efficiency becomes unacceptable as they fall below the minimum standards. Following up with that, the side lobe level can also be seen to be increasing which is undesired, as they will draw away the power of from the main lobe. Lastly, we can observe that the radiation efficiency and total efficiency of our antenna array also decreasing with increased spacing with the odd exception of elemental spacing at 0.7λ but however the tradeoff is the poor s_{11} parameters as well as worse total efficiency. If we also turn our attention to the 3D patterns we can observe that with the elemental spacing becoming larger and larger our antenna radiation pattern is going further and further away from our expected and desired pattern of a 2×2 planar array .So comparing these overall results we can come to the conclusion that for the best overall results elemental spacing of 0.6λ would yield the overall best performance and best results.

8.5 ARRAY BEAMSTEERING

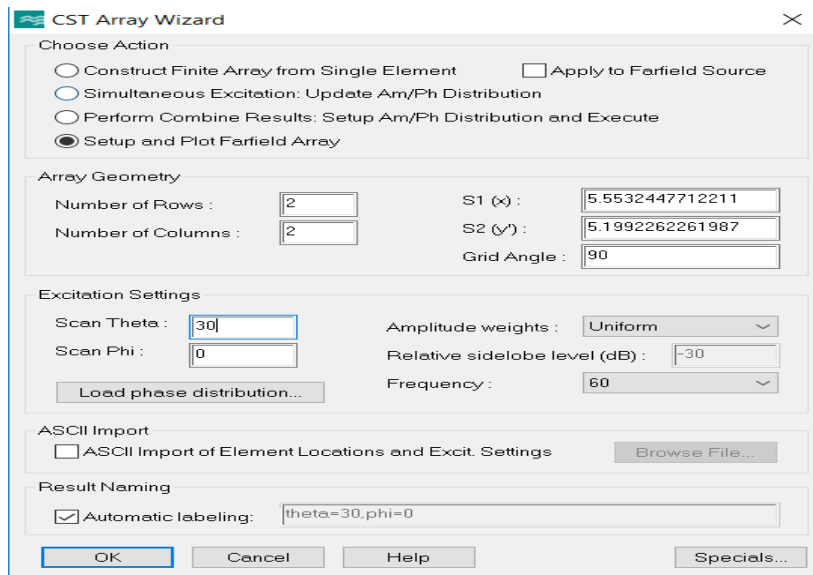


Figure 95: Key shaped antenna of 16 elements steered at 30 degrees

Here we are going to simulate our key shaped antenna for a scan angle of 30 degrees for 2 rows and 2 columns of our main 2x2 antenna. So the total number of patches in the array will be 16. Our scan angle will be in the theta domain and the phi angle will remain zero.

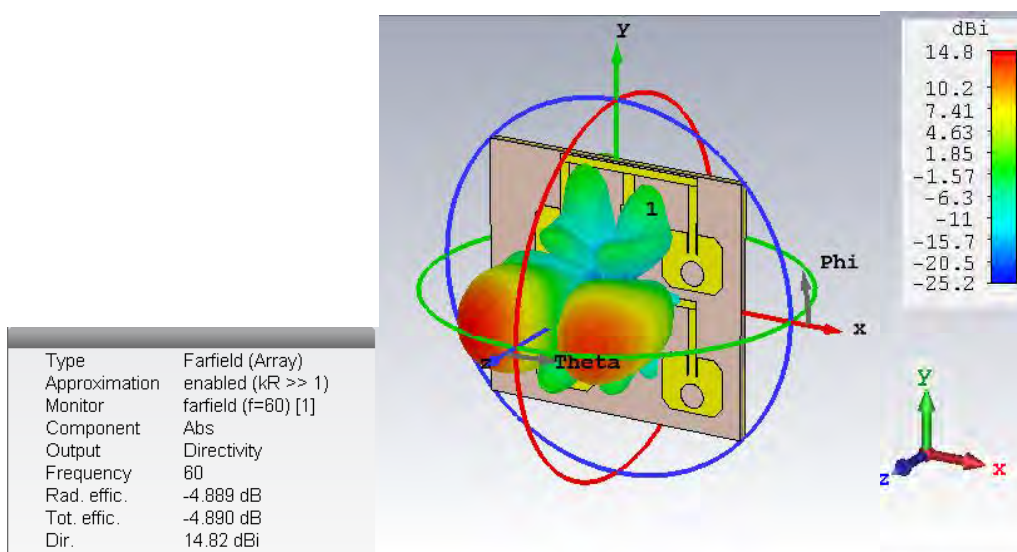


Figure 96: Farfield plot of a 2x2 key antenna with 16 patches steered at 30 degrees

From the above farfield pattern we can see that the directivity of the antenna array when steered at 30 degrees is 14.82

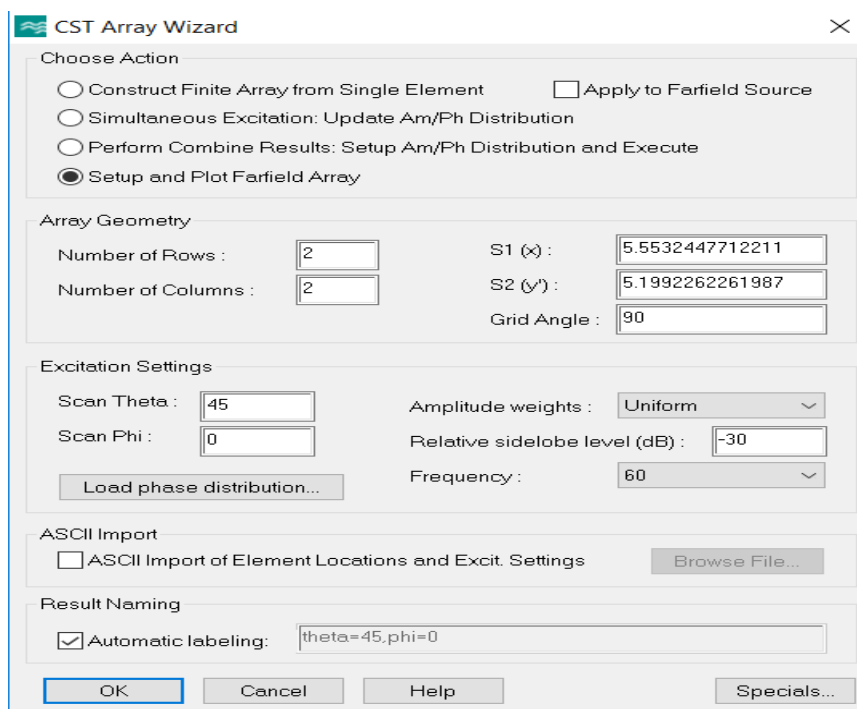


Figure 97: Key shaped antenna of 16 elements steered at 45 degrees

Here we are going to simulate our key shaped antenna for a scan angle of 45 degrees for 2 rows and 2 columns of our main 2x2 antenna. So the total number of patches in the array will be 16. Our scan angle will be in the theta domain and the phi angle will remain zero.

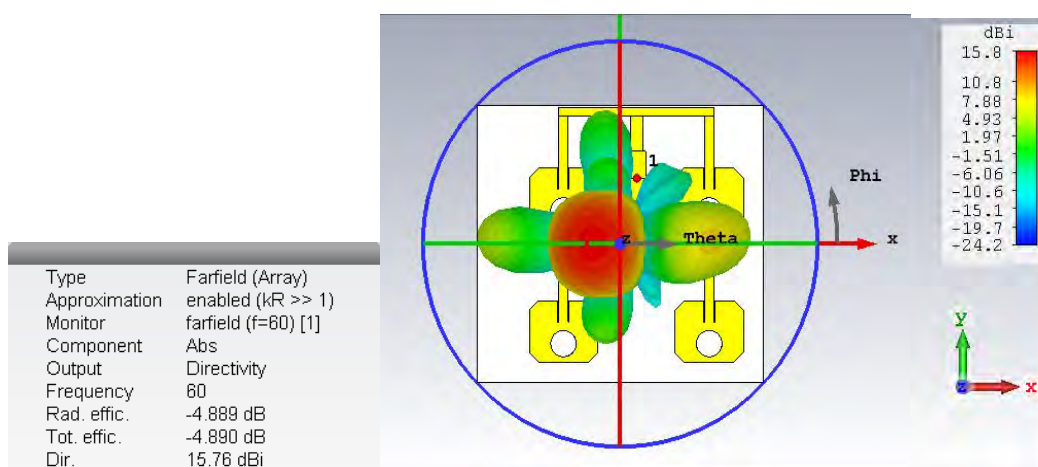


Fig 98: 3D directivity pattern steered at 45°

From the above farfield pattern we can see that the directivity of the antenna array when steered at 45 degrees is 15.76dBi

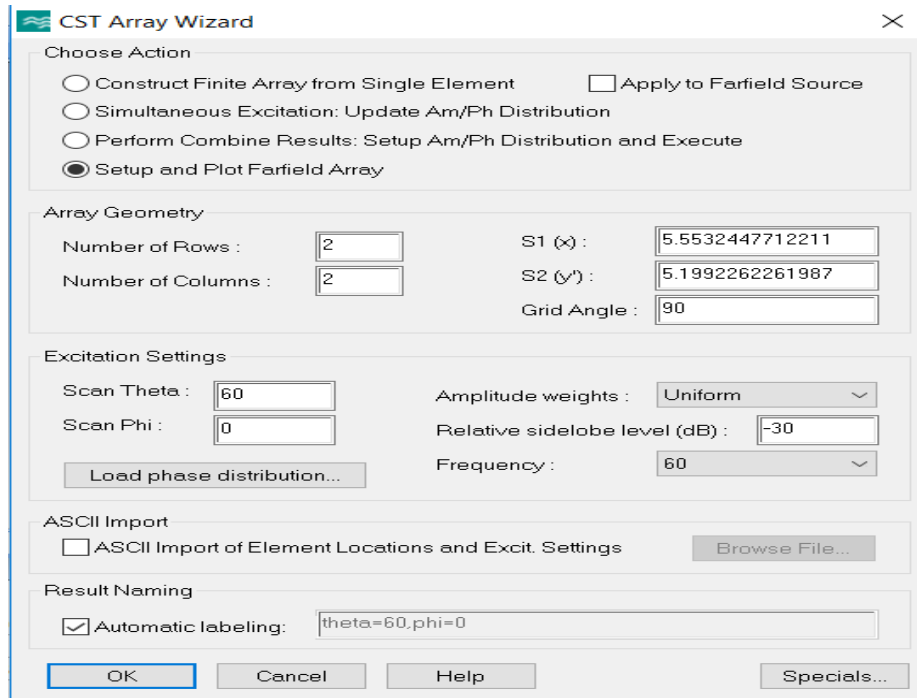


Figure 99: Key shaped antenna of 16 elements steered at 60 degrees

Here we are going to simulate our key shaped antenna for a scan angle of 60 degrees for 2 rows and 2 columns of our main 2x2 antenna. So the total number of patches in the array will be 16. Our scan angle will be in the theta domain and the phi angle will remain zero.

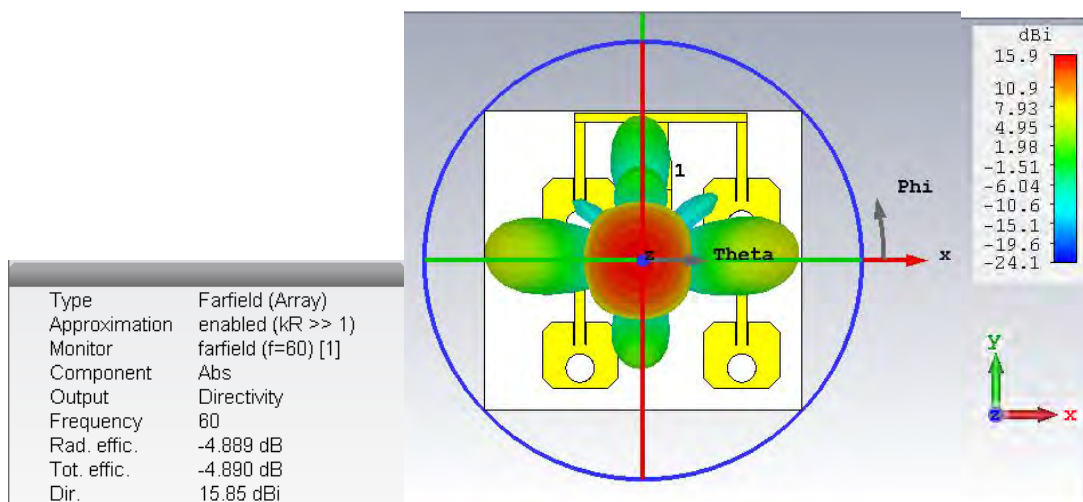


Figure 100: Farfield plot of a 2x2 key antenna with 16 patches steered at 60 degrees

From the above farfield pattern we can see that the directivity of the antenna array when steered at 60 degrees is 15.85dBi

CST Array Wizard

Choose Action

- Construct Finite Array from Single Element Apply to Farfield Source
- Simultaneous Excitation: Update Am/Ph Distribution
- Perform Combine Results: Setup Am/Ph Distribution and Execute
- Setup and Plot Farfield Array

Array Geometry

Number of Rows : S1 (x) :

Number of Columns : S2 (y) :

Grid Angle :

Excitation Settings

Scan Theta : Amplitude weights :

Scan Phi : Relative sidelobe level (dB) :

Frequency :

ASCII Import

ASCII Import of Element Locations and Excit. Settings

Result Naming

Automatic labeling:

Figure 101: Key shaped antenna of 16 elements steered at 75 degrees

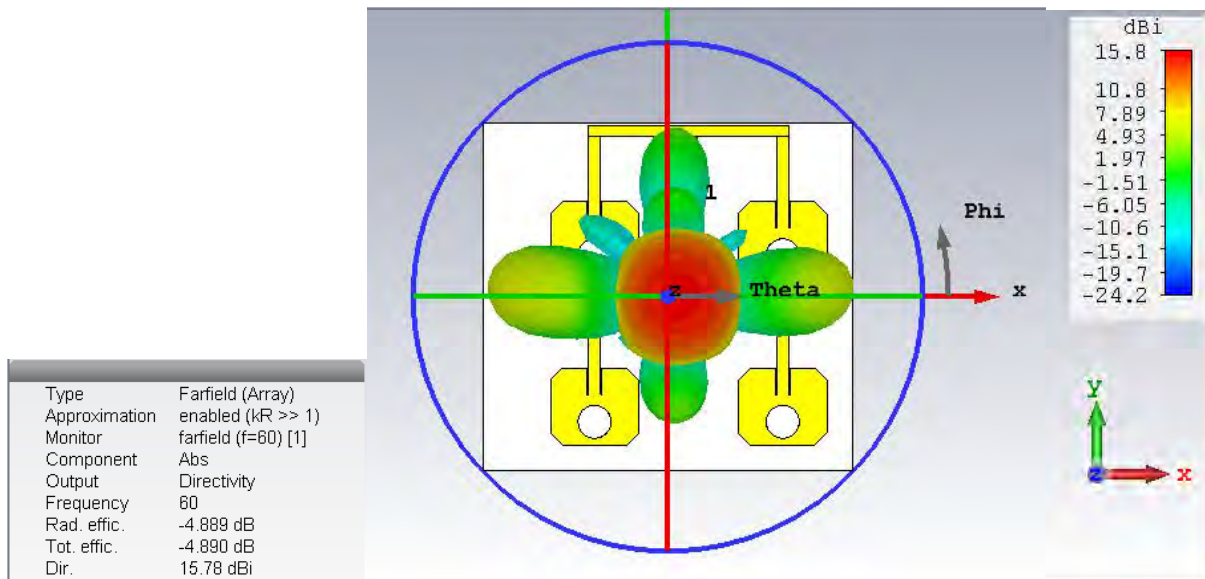


Figure 102: Farfield plot of a 2x2 key antenna with 16 patches steered at 75 degrees

From the above farfield pattern we can see that the directivity of the antenna array when steered at 75 degrees is 15.78dBi

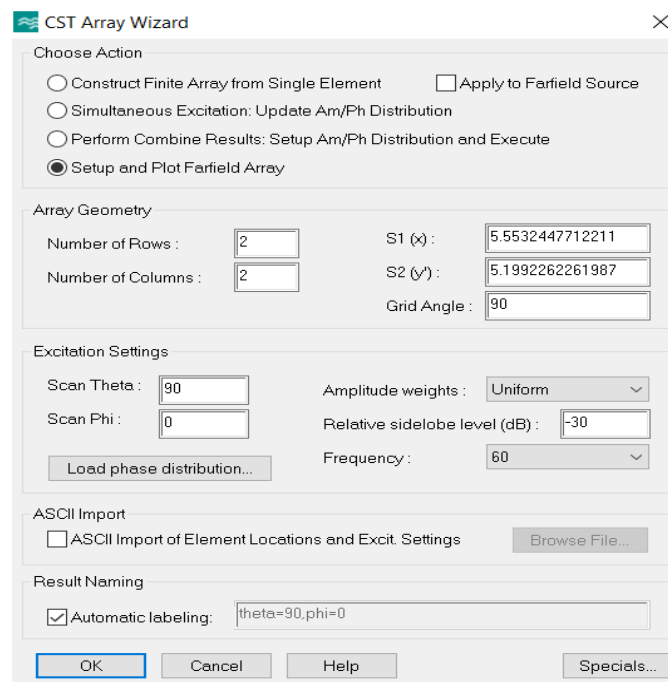


Figure 103: Key shaped antenna of 16 elements steered at 90 degrees

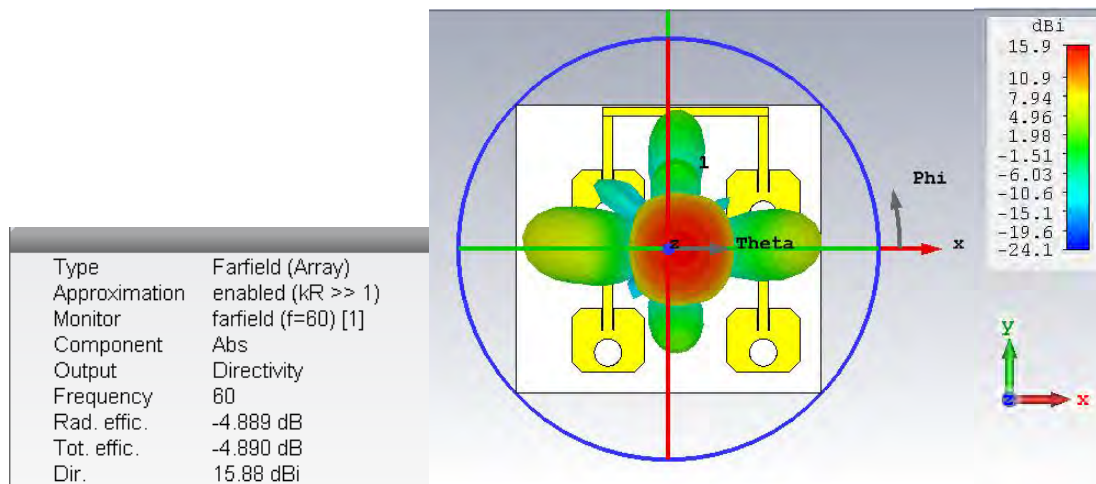


Figure 104: Farfield plot of a 2x2 key antenna with 16 patches steered at 90 degrees

From the above farfield pattern we can see that the directivity of the antenna array when steered at 75 degrees is 15.88dBi

Table 9: Beamsteering vs Directivity comparison

Beamsteering Angle(degrees)	Directivity(dBi)
30	14.82
45	15.76
60	15.85
75	15.78
90	15.88

So as we can see a following pattern from the analysis of beamsteering that what happens to the directivity when we change the angle of the main beam to be steered at a particular direction.

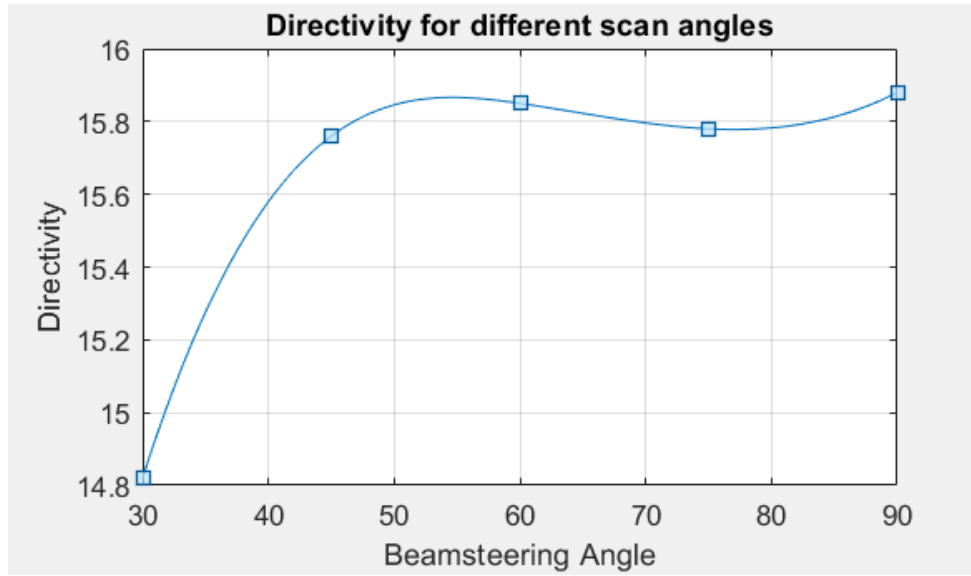


Figure 105: Beamsteering at different Scan Angles

CHAPTER 9

Future Scope and Conclusion

9.1 FUTURE SCOPE

In this paper we built a 2X2 array and analysed its performance. In future we can try to make an array of more elements and compare its radiation efficiency, total efficiency, s parameters and directivity and VSWR to find out whether it gives a better performance. Furthermore, we will try to increase the radiation efficiency of our 2X2 array. We can also improve the gain of the antenna through means of a better design with relatively larger dimensions. Other means of increasing gain include the conventional way of increasing substrate height as well as exploring the realm of stacking substrates of different materials. In addition to that we can also decrease the side lobes by decreasing the antenna elemental spacing so in the future we will conduct more simulation until we find a more optimized array spacing. Apart from these we can also try out more designs with different shapes and size of slots to see which design gives the optimum results.

9.2 CONCLUSION

In our work, we have constructed a conducive mmWave frequency phased array antenna specially designed for the purpose of tracking. Microstrip patch antennas were initially used to create the preliminary array. Our intention was to design the phased array antenna for application at 60 GHz. The 60 GHz mmWave frequency band was specifically chosen since it offers about 7 GHz (57-64 GHz) unlicensed spectrum. It is known to support high-speed (up to 7 Gbps) wireless connectivity, as standardized by IEEE 802.11 ad. Additionally, as of late a lot of works have used the 60 GHz band to trace human activity and other small objects. [67] However, we were largely interested in using the 60 GHz mmWave for tracking and detecting larger items namely vehicles. This design could also be utilized to track airplanes and aircrafts.

For reference, a 2x2 array made from rectangular microstrip patch antenna was created. However, later we were able to improvise our design and a key-shaped microstrip patch design was developed for each element of the 2x2 array. This exact shape is also very symbolic to our overall application. The key-shape gives an implication to the use we were indicating towards, that is tracking. It would prove to be especially innovative to be able to fit our antenna array into a key for the vehicle to be later used for detecting the vehicle. However, what is most noteworthy in our case is that this improved design has attributed to a lot of enhancements. Where the original rectangular microstrip array provided a return loss of -19 dB this new design gives -34.468 dB. Not only that, the VSWR ratio given by our design is closer to one than the reference design. Better directivity and reduced side lobes also signify a few more improvements that were possible. However, it is only in terms of gain where our design shows to fall behind the reference array. But it proved to be particularly difficult for us to modify this, since doing that would cost us the other substantial improvements that were made. Therefore, for now we have concluded to having a slightly lower gain. Nevertheless, in the future, different techniques may be utilized to experiment on increasing the gain without creating any significant losses to other parameters. Then for the next part we experimented with different spacing values between the antenna elements. We were able to conclude that an elemental spacing of 0.6λ produces the most attractive results. Ultimately, this design was then used to demonstrate the beam steering required for our application. For our thesis, we have used the built-in application in the CST software to exhibit this navigation. We were able to effectively steer the radiation pattern of the antenna to an angle of 30 and 45 as well as 60 and 75. Practically, phase shifters would be required to carry out this demonstration.

Overall, our proposed design has shown better-quality performance with effective beam steering. However, that is not to say further improvements cannot be made. More evolvments can be brought to our design that could prove to provide superior results performance-wise. Hopefully, in the future, we would be able to carry out work and help to improve our results.

References

1. Retrieved from Wikipedia: [https://en.wikipedia.org/wiki/Antenna_\(radio\)](https://en.wikipedia.org/wiki/Antenna_(radio)), (2014)
2. I. Poole, (n.d.). Retrieved from Radio Electronics: <https://www.radio-electronics.com/info/antennas/dipole/dipole.php>
3. A review paper on various communication strategies used in Wireless networks. (2018). *International Journal of Recent Trends in Engineering and Research*, 4(4), 433-437. doi:10.23883/ijrter.2018.4257.lk5jh
4. Bevelacqua, P. Welcome to Antenna-Theory.com! Retrieved from <http://www.antenna-theory.com/>, 2017.
5. Straw, R. Dean, Ed. (2000). *The ARRL Antenna Book*, 19th Ed. USA: American Radio Relay League. p. 19.15.
6. C. A. Balanis, “Antenna theory: analysis and design. Hoboken”, NJ: Wiley Interscience, 2005.
7. R. C. Johnson, H. A. Ecker, and J. S. Hollis, “Determination of farfield antenna patterns from near-field measurements” *Proceedings of the IEEE*, vol. 61, no. 12, pp. 1668-1694, Dec. 1973.
8. C. Poole and I. Darwazeh, “Microwave Active Circuit Analysis and Design”, USA Elsevier Academic Press, 2016.
9. Johnson, D. (2018 Jun 26) 5G Beam-Steering Antennas: More Accurate, Less Power Hungry retrieved from <https://spectrum.ieee.org/tech-talk/telecom/wireless/5g-beamsteering-antennas-more-accurate-less-power-hungry>
10. T. S. Rappaport et al., “Millimeter Wave Mobile Communications for 5G Cellular: It Will Work!” *IEEE Access*, vol.1, May 2013, pp. 335–449
11. K. Zheng et al., “10 Gb/s HetsNets with Millimeter-Wave Communications: Access and Networking — Challenges and Protocols,” *IEEE Commun. Mag.*, vol. 53, no. 1, Jan. 2015, pp. 222–31.
12. S. Rangan, T. Rappaport, and E. Erkip, “Millimeter Wave Cellular Wireless Networks: Potentials and Challenges,” *Proc. IEEE*, vol. 102, no. 3, Mar. 2014, pp. 366–85.

13. S. Hur et al., "Millimeter Wave Beamforming for Wireless Backhaul and Access in Small Cell Networks," *IEEE Trans. Commun.*, vol. 61, no. 10, Oct. 2013, pp. 4391–4403.
14. T. Bai, R. Vaze, and R. W. Heath, "Analysis of Blockage Effects on Urban Cellular Networks," *IEEE Trans. Wireless Commun.*, vol. 13, no. 9, Sept. 2014, pp. 5070–83
15. T. S. Rappaport et al., "Broadband Millimeter-Wave Propagation Measurements and Models using Adaptive-Beam Antennas for Outdoor Urban Cellular Communications," *IEEE Trans. Antennas Propagat.*, vol. 61, no. 4, Apr. 2013, pp. 1850–59
16. Cheng-Xiang Wang; Haider, F.; Xiqi Gao; Xiao-Hu You; Yang Yang; Dongfeng Yuan; Aggoune, H.; Haas, H.; Fletcher, S.; Hepsaydir, E., "Cellular architecture and key technologies for 5G wireless communication networks," *Communications Magazine, IEEE* , vol.52, no.2, pp.122,130, February 2014.
17. A. Valdes-Garcia, A. Natarajan, D. X. Liu, M. Sanduleanu, X. X. Gu, M. Ferriss, B. Parker, C. Baks, J. O. Plouchart, H. Ainspan, B. Sadhu, M. Islam and S. Reynolds, "A fully-integrated dual-polarization 16-element W-band phased-array transceiver in SiGe BiCMOS," *IEEE Radio Frequency Integrated Circuits Symposium (RFIC)*, Seattle, USA, pp. 375-378, June 2013
18. B. Sadhu, Y. Tousi, J. Hallin, S. Sahl, S. Reynolds, Ö. Renström, K. Sjögren, O. Haapalahti, N. Mazor, B. Bokinge, G. Weibull, H. Bengtsson, A. Carlinger, E. Westesson, J. E. Thillberg, L. Rexberg, M. Yeck, X. X. Gu, D. Friedman and A. Valdes-Garcia, "A 28GHz 32-element phased-array transceiver IC with concurrent dual polarized beams and 1.4 degree beam-steering resolution for 5G communication," *IEEE International Solid-State Circuits Conference (ISSCC)*, San Francisco, USA, pp. 128-129, Feb. 2017.
19. P. Chen, W. Hong, H. Zhang, J. X. Chen, H. J. Tang and Z. Chen, "Virtual Phase Shifter Array and Its Application on Ku Band Mobile Satellite Reception," *IEEE Trans. on Antennas and Propagat.*, vol.63, no. 4, 2015, pp. 1408-1416
20. Wonbin Hong, Kwang-Hyun Baek, Youngju Lee, Yoongeon Kim, and Seung-Tae Ko, "Study and Prototyping of Practically Large-Scale mmWave Antenna Systems for 5G Cellular Devices", *IEEE Antennas and Propag. Maga.*, vol. 52, no. 9, pp. 63-69, Sep. 2014.

21. T.G. Pelham, D. Reyes, M. Beach, E. Mellios, M. Rumney ,” Non-Intrusive Characterization of 60GHz Antenna Array, using Packet Measurements”,EuCap 2018
22. A. A. Sharatol Ahmad Shah, N. H. Abd Rahman, M. T. Ali, N. F. Fauzi and A. A. Ab Aziz, “Beam Scanning of Phased Array Antenna using Phase Modification Method for Satellite Application,” 2016 IEEE Asia-Pacific Conference on Applied Electromagnetics (APACE) 11 - 13 December 2016 at Langkawi, Kedah, Malaysia.
23. Joana S. Silva, Eduardo B. Lima, Jorge R. Costa, and Carlos A. Fernandes, “Ground Terminal Antenna for Ka-Band Satellite Communication,” Proc. 7th Eur. Conference on Antennas and Propag. (EuCAP), Gothenburg, Sweden, pp. 1613-1616, April 2013.
24. I. Kaplan, I. Marinov, A. Gal, V. Peshlov, M.Gachev, V. Boyanov, and B. Marinov, “Electronically Beam Steerable Antennas for Broadband Satellite Communications,” Proc. 8th Eur. Conf. Antenna and Propag. (EuCAP), The Hague, The Netherlands, pp. 2450-2454, April 2014.
25. Y. -B. Jung, Alexander V. Shishlov, and S. -O. Park, “Cassegrain Antenna with Hybrid Beam Steering Scheme for Mobile Satellite Communication,” IEEE Transactions on Antennas Propagation, vol. 57, no. 5, pp. 1367-1372, May 2009
26. G. Buttazzoni, A. Cuttin and R. Vescovo,” Design Procedures for Rectangular Patch Antennas,”EuCap 2018
27. Y. Y. Yoshimura, “A microstripline slot antenna,” IEEE Trans. Microw. Theory Techn., vol. 20, no. 11, pp. 760–762, 1972.
28. C. F. Zhou, and S. W. Cheung “A Wideband CP Antenna Using $1-\lambda$ Resonant Mode with Single Feeding,” IEEE Trans. Antennas Propag.,vol. 65, no. 8, 2017
29. S. Yun, D. Kim, and S. Nam, “Bandwidth enhancement of cavity backed slot antenna using a via-hole above the slot,” IEEE Antennas and Wireless Propaga. Lett. , vol. 11, pp. 1092-1095, 2012.
30. Paul Czeresko III, Nowrin H. Chamok, Mohammad Ali,” Fabric Based Beam Steering Wearable Antenna Array”, EuCap 2018
31. Y. Ouyang and W.J. Chappell, “High Frequency Properties of Electro-Textiles for Wearable Antenna Applications,” IEEE Trans.Antennas Propagat., pp. 381-389. Feb. 2008.
32. C. Hertleer, H. Rogier, L. Vallozzi, and L. Van Langenhove, “A textile antenna for off-body communication integrated into protectiveclothing for firefighters,” IEEE Trans. Antennas Propagat., pp. 919–925, Apr. 2009.

33. S. Zhu and R. Langley, "Dual-Band Wearable Textile Antenna on an EBG Substrate," *IEEE Trans. Antennas Propagat.*, vol. 57, no. 4, pp.926–935, Apr 2009.
Antennas and Wireless Propagation Letters, vol. 15, pp. 504–507, 2016.
34. I. Syrytsin, S. Zhang, G. Pedersen, K. Zhao, T. Bolin, and Z. Ying, "Statistical investigation of the user effects on mobile terminal antennas for 5g applications," *IEEE Transactions on Antennas and Propagation*, vol. PP, no. 99, pp. 1–1, 2017.
35. K. Zhao, J. Helander, D. Sjoberg, S. He, T. Bolin, and Z. Ying, "User Body Effect on Phased Array in User Equipment for 5G mm Wave Communication System," *IEEE Antennas and Wireless Propagation Letters*, vol. PP, no. 99, p. 1, 2016.
36. R. Schulpen¹, U. Johannsen, S.C. Pires, A.B. Smolders , "Design of a Phased-Array Antenna for 5G Base Station Applications in the 3.4-3.8 GHz Band," *EuCAP 2018*.
37. Igor Syrytsin, Shuai Zhang, Gert Frølund Pedersen, "Finger Ring Phased Antenna Array for 5G IoT and Sensor Networks at 28 GHz," *EuCap 2018*
38. J. L. Volakis, "Antenna engineering handbook.," New York: McGraw-Hill, 2007.
39. R.Garg, P. Bhartia, I. Bahl, and A. Ittipiboon, "Microstrip antenna design handbook," Artech House: London, 2001.
40. James J., and P.S. Hall (Eds), "Handbook of microstrip antenna", Peter Peregrinus, London, UK, 1989.
41. H. Werfelli, K. Tayari, M. Chaoui, M. Lahiani, H. Ghariani, "Design of Rectangular Microstrip Patch Antenna", 2nd International Conference on Advanced Technologies for Signal and Image Processing – ATSIP'2016, March 2016.
42. Retrieved from: <http://shodhganga.inflibnet.ac.in/bitstream/10603/48026/9/09-chapter%203.pdf>
43. Capacitor ESR, Dissipation Factor, Loss Tangent and Q. (n.d.). Retrieved from <https://www.radio-electronics.com/info/formulae/capacitance/esr-df-loss-tangent-q-tutorial-basics.php>
44. G9 G10 FR4 Glass Epoxy Sheet. (n.d.). Retrieved from <http://www.eplastics.com/G9-G10-FR4-glass-epoxy-sheet>
45. RT/duroid® 5880 Laminates. (n.d.). Retrieved from <http://www.rogerscorp.com/acs/products/32/rt-duroid-5880-laminates.aspx>
46. Prospector, U. (n.d.). Arlon® AD270 Datasheet. Retrieved from <https://plastics.ulprospector.com/datasheet/e120261/aron-ad270>

47. Khan, A., & Nema, R. (2012). Analysis of Five Different Dielectric Substrates on Microstrip Patch Antenna. *International Journal of Computer Applications*, 55(14), 40-47. doi:10.5120/8826-2905
48. Visser, H. J. (2006). *Array and phased array antenna basics*. Chichester: Wiley.
49. Mailloux, R. J. (1994). *Phased array antenna handbook* (3rd Ed.). Boston; London: Artech House.
50. Huang, Y., & Boyle, K. (2008). *Antennas: From theory to practice*. Chichester: J. Wiley & Sons
51. S. Koul and B. Bhat, "Microwave and Millimeter Wave Phase Shifters," Volume I, Boston, MA: Artech House, 1991.
52. Yu Yue, B. Yan, and R. Xu, "A Millimeter-Wave 4-bit digital phase shifter," 2005 Asia-Pacific Microwave Conference Proceedings, vol. 2, Dec. 2005.
53. Microwaves101.com, Microwaves101, Retrieved from: <http://www.microwaves101.com/>, July 2017
54. R. J. Mailloux, "Phase Array Antenna Handbook" New York: Artech House Inc., 1994.
55. S. Koul and B. Bhat, "Microwave and Millimeter Wave Phase Shifters," Volume II, Boston, MA: Artech House, 1991.
56. M. T. Qureshi, V. Desmaris, M. Geurts and J. van de Sluis, "Passive Reciprocal high-pass/low-pass 4-bit phase shifter at 2.45 GHz," 2014 44th European Microwave Conference, Rome, 2014, pp. 1076-1078.
57. B.-W. Min and G. M. Rebeiz, "Single-ended and differential Ka-band BiCMOS phased array front-ends," *IEEE J. Solid-State Circuits*, vol. 43, no. 10, pp. 2239–2250, Oct. 2008.
58. T. Edwards, "Foundations for Microstrip Circuit Design," New York: Wiley, 1992.
59. F. Xiong, R. R. Romanofsky, "Study of Behavior of Digital Modulations for Beam Steerable Reflectarray Antennas," *IEEE Trans. A&P*, vol. 53, pp. 1083-1097, 2005.
60. B. L. Smith, and M.-H. Carpentier, Eds., *The Microwave Engineering Handbook Volume 2—Microwave Components*, London, U.K.: Chapman & Hall, 1993, pp. 231–237
61. I. Uchendu and J. Kelly, "Survey of beam steering techniques available for millimeter wave applications," *Progress in Electromagnetics Research B*, vol. 68, pp. 35–54, 2016.

62. C.-W. Baek, S. Song, C. Cheon, Y.-K. Kim, and Y. Kwon, "2-D Mechanical Beam Steering Antenna Fabricated Using MEMS Technology," 2001 IEEE MTT-S Inter. Microwave Symp. Dig., Vol. 1, pp. 211–214, Phoenix, Arizona, May 20–25, 2001.
63. M. Nikfalazar, M. Sazegar, A. Mehmood, A. Wiens, A. Friederich, H. Maune, J. R. Binder, R. Jakoby, "Two-dimensional beam-steering phased-array antenna with compact tunable phase shifter based on BST thick films," IEEE Antennas Wireless Propag. Lett., vol. 16, pp. 586–588, 2017.
64. M. Longbrake, "True time-delay beamsteering for radar," in Proceedings of the IEEE National Aerospace and Electronics Conference (NAECON '12), pp. 246–249, 2012.
65. J. Ehmouda, Z. Briqech, A. Amer, "Steered microstrip phased array antennas," World Academy of Science, Engineering and Technology, Vol. 49, 319-323, 2009
66. Moernaut, G.J.K, & Orban,D. ,The basics of antenna arrays, retrieved from <http://orbanmicrowave.com/the-basics-of-antenna-arrays/>
67. Y. Zeng, P. H. Pathak, Z. Yang, and P. Mohapatra, "Poster Abstract: Human Tracking and Activity Monitoring Using 60 GHz mmWave," ACM/IEEE International Conference on Information Processing in Sensor Networks (IPSN), April 2016, pp. 1-2.
68. R.Bhalla and L.Shafai.(2002).“Resonance behaviour of a single U slot and dual U slot antenna”,IEEE Antennas and Propagation.